Formin-2 function in growth cone motility and substrate attachment

A thesis

Submitted in partial fulfillment of the requirements

for the Degree of

Doctor of Philosophy

Abhishek Sahasrabudhe

20083011

Indian Institute of Science Education and Research (IISER), Pune

2015

CERTIFICATE

Certified that the work incorporated in the thesis entitled **"Formin-2 function in growth cone motility and substrate attachment"**, submitted by Mr. Abhishek Sahasrabudhe was carried out by the candidate, under my supervision. The work presented here or any part of it has not been included in any other thesis submitted previously for the award of any degree or diploma from any other University or Institution.

Date:

Dr. Aurnab Ghose

Supervisor

DECLARATION

I declare that this written submission represents my ideas in my own words and where others' ideas have been included; I have adequately cited and referenced the original sources. I also declare that I have adhered to all principles of academic honesty and integrity and have not misrepresented or fabricated or falsified any idea/data/fact/source in my submission. I understand that violation of the above will be cause for disciplinary action by the Institute and can also evoke penal action from the sources that have not been properly cited or from whom proper permission has not been taken when needed.

Date:

Abhishek Sahasrabudhe

20083011

ACKNOWLEDGMENTS

I would like to thank my thesis supervisor Dr. Aurnab Ghose for giving me the opportunity to work with him. Interactions and discussions with him over the years have indeed shaped my analytical thinking, scientific approach to experiments and writing skills. Being only the second student in the lab, setting up the lab and seeing the lab grow was an exciting experience.

I thank the members of my research advisory committee and Prof. LS Shashidhara for their valuable suggestions and inputs during the meetings and even outside the meetings.

I truly thank all my past and present colleagues from Ghose lab for their support, encouragement and discussions. I would begin by thanking Anurag, who helped me in settling down in the lab and helped with the initial experiments. Sampada, Ketakee, Tanushree, Mahekta, Prashanth and Ajesh were great team members and helped me at various times for my experiments and discussions. A special mention to Ketakee, who experimentally validated some of the predictions that came out of this work. I am sure these experiments will form a solid body of work for her own PhD thesis in the near future. Thanks to all the summer trainees and project students that were involved in the work.

Life outside the lab was as enjoyable and eventful as the one inside. The road to my PhD started with Rini, Payal, Kanika, Vimal, Aniruddh, Mithila, Ameya, Harsha, Anurag and JP and I am thankful to them for making this a pleasant journey. The heated discussions that turned in to arguments with Harsha and JP taught me how to be patient during discussions. Kanika and Vimal made the dinner times delightful with the 'interrupted' discussions about physics, biology and beyond. Rini with her jokes and coffee always kept the air around us full of energy. All of you made it possible to forget the worries in the lab and start fresh every morning.

I am extremely grateful to the lab manager, instrument and chemical in-charges, and all the support staff at IISER without whom working in the lab would have been chaotic. I thank IISER for providing the infrastructure to carry out my research and a scientifically stimulating environment. It was a pleasure to be a part of a new and sprouting institute. I thank CSIR for my fellowship. The work would not have been possible without the generous project funding from DBT.

I extend my heartfelt thanks to my parents and my brother who always supported me and believed in me. Without their support this journey would not have been possible. Aasma, thanks for being there with me to share my frustrations and joys of PhD.

Table of contents

Table of figures

List of tables

1 SYNOPSIS

Formin-2 function in growth cone motility and substrate attachment

Name of the student	:	ABHISHEK SAHASRABUDHE
Registration Number	:	20083011
Name of the Thesis Advisor	:	Dr. Aurnab Ghose
Date of Registration	:	4th August 2008

Indian Institute of Science Education and Research (IISER), Pune, India.

Introduction:

A key process in embryonic development is the establishment of precise neuronal connectivity. This stereotyped neuronal circuitry forms the basis for neural function and results from a highly regulated process of path finding by the neuronal extensions (axons and dendrites) towards their synaptic targets. The critical component of the axon's journey to its destination is the specialized motile structure at its tip, the 'growth cone'. Numerous substrate-bound and diffusible chemotropic guidance cues in the environment guide the growth cone to its target tissue. The receptors on the growth cone membrane interact with the extracellular cues providing spatiotemporally resolved information about the environment. This information is integrated and interpreted by the intracellular signaling machinery and transmitted to the effector system to generate an appropriate response. This can range from an alteration of growth rate to directional movement towards (attraction) or away (repulsion) from the guidance cue.

The growth cone is the specialized, motile tip of growing neuronal processes that explores the external space for guidance cues and brings about directional motility. The growth cone consists of two types of protrusive structures with distinct morphologies—flat, sheet-like extensions called lamellipodia and long, finger-like filopodia. These structures not only differ in their morphologies but also in their underlying sub-cellular actin architecture. The lamellipodia are produced by the protrusive activities of a dense meshwork of cross-linked actin while long bundles of filamentous actin (F-actin) generate filopodial structures. Unlike other motile cells, filopodial extensions dominate growth cone motility. The filopodia are highly dynamic, undergo bouts of extension and retraction, making them ideally suited for interrogating the environment. It has been demonstrated that the filopodia form the key sensory modality in growth cones and bear the necessary guidance receptors (Bentley and Toroian-Raymond, 1986; Dent et al., 2007; Gomez and Letourneau, 1994; Zheng et al., 1996).

The actin cytoskeleton underlying the leading edge is primarily responsible for the protrusion and retraction of the growth cone. Growth cones treated with cytochalasin, which prevents actin polymerization, show loss of directionality, slow translocation rates and altered morphology (Forscher and Smith, 1988; Marsh and Letourneau, 1984). Low magnitude forces exerted by the growing MTs are thought to bring about the residual motility in such growth cones. The growth of actin filaments form the mechanical basis of actin driven protrusions (filopodia and lamellipodia) (Suter and Miller, 2011). The dynamic balance between barbed end polymerization on one hand and depolymerization and retrograde flow on the other, determine extension or retraction of filopodia and lamellipodia (Gungabissoon and Bamburg, 2003). The length of the actin filaments is controlled by the activities of elongation factors and capping proteins. Capping proteins provide a check on the length of the filament while elongation factors

like the Ena/VASP family counteract capping and promote elongation (Reinhard et al., 1992). The ability to generate long filaments is of particular importance to filopodia dominated structures like growth cones. In accordance with this, members of this family are found to localize to filopodial tips and regulate filopodia formation and guidance.

The formation of new actin filaments by nucleation of globular actin (G-actin) monomers is not spontaneous and requires other proteins to facilitate the reaction. These proteins, referred to as actin nucleators, along with accessory nucleation promoting factors (NPFs) regulate key aspects of actin dynamics. In non-neuronal cells, Arp2/3 along with an accessory factor N-WASP are the major actin nucleators, which generates the branched meshwork of actin filaments at the leading edge of the cell. The minimal region of Arp2/3 required for actin nucleation has a WASP homology domain (WH2) which binds to the actin monomers (Goley et al., 2004). The role of Arp2/3 and N-WASP in neuronal cells is debatable since its removal does not have a drastic effect on the growth cone morphology or motility (Korobova and Svitkina, 2008; Steffen et al., 2006; Strasser et al., 2004).

Formins, another class of actin nucleators, use a very different mechanism of F-actin formation. Several formins have an inactive autoinhibited conformation due to the intramolecular interactions which can be relieved upon Rho-GTPase binding. Upon activation, formins nucleate actin filaments using their formin homology (FH1 and FH2) domains. Working as dimers, these proteins processively add actin monomers to the barbed end of the filament (Romero et al., 2004). Thus they form straight, unbranched actin bundles similar to those found in the filopodia. Experiments in *Dictyostelium* have implicated a formin, dDia2 in filopodia formation (Schirenbeck et al., 2005b). Another formin family member dDAAM is shown to be important for filopodia formation in *Drosophila* embryonic neurons (Matusek et al., 2008). Apart from

their nucleation activity, formins also act as elongation factors (Bartolini et al., 2008). Being associated with the barbed end of the filament, formins could potentially counteract the activity of capping proteins.

Objective:

Formin based actin dynamics provide an alternate mechanism for the maintenance of growth cone morphology, motility and guidance given their involvement in a process like filopodia formation which in turn is responsible for efficient guidance as mentioned earlier. Previous unpublished work in the lab suggested the possible involvement of a particular formin family member Cappuccino (Capu) in the process of axon guidance at the midline in *Drosophila* embryos.

This formed the basis for our study where we investigated the contribution of the vertebrate homologue of Capu, Formin-2 (Fmn2) in the process of axon guidance at the midline and its role in maintenance of growth cone shape and motility. Capu was identified as a gene required for cytoplasmic streaming in the *Drosophila* oocyte and establishment of polarity in the early embryo (Emmons et al., 1995). The vertebrate homologue of Capu was later shown to be enriched in the central nervous system of developing mouse embryo (Leader and Leder, 2000). But surprisingly Fmn2 knockout mice did not exhibit any apparent gross nervous system defects; however detailed analysis for nervous system defects has not yet been reported. Fmn2 knockout females were found to exhibit recurrent pregnancy loss and sub-fertility (Leader et al., 2002). Subsequent studies focused on the role of Fmn2 in spindle positioning, oocyte maturation and fertility (Dumont et al., 2007; Kwon et al., 2011; Pfender et al., 2011; Schuh and Ellenberg, 2008). A study which undertook QTL analysis in humans showed that Fmn2 could be involved in neurobehavioral phenotypes (Mozhui et al., 2008). The involvement of Fmn2 in behavior

became stronger in the last few years as Fmn2 was shown to be involved in age-dependant memory impairment in mice, dendritic spine morphology and intellectual capabilities in humans (Law et al., 2014; Mozhui et al., 2008; Peleg et al., 2010). These recent findings have begun to underscore the importance of Fmn2 in the development and function of the nervous system.

Major findings in the study:

Efficient growth cone motility results in formation of precise neuronal connections which are important for the survival of the organism. We took a cell biological approach to understand the role of Fmn2 in the process of growth cone motility. Using primary neurons from the developing chick embryo we analyzed the effect of morpholino mediated Fmn2 depletion on growth cone morphology and motility *in vitro* and *in ovo* in the developing spinal cord of chick embryos.

Fmn2 is enriched in the developing spinal cord

Using quantitative real time PCR, the Fmn2 transcript was found to be enriched in the spinal cords of developing chick embryos. An earlier report had already demonstrated the enrichment in the central nervous system in developing mouse embryos (Leader and Leder, 2000). In our analysis we find that Fmn2 is differentially enriched in the spinal cords and brain. The levels of Fmn2 transcript detected in the spinal tissue are 4-times higher than in the brain. We used cultured spinal neurons for the *in vitro* studies regarding the growth cone morphology and motility.

Fmn2 localizes to the filopodial actin bundles

Using a custom designed antibody against chick Fmn2 it was found that Fmn2 decorated the actin bundles that formed the core of the filopodial shaft. Occasionally, Fmn2 signal was found at the tip of a presumably newly forming filopodia suggesting a role in either formation of

new filopodia or elongation of the existing filopodia. Secondary staining for GFP in growth cones transfected with Fmn2-GFP supported the observations from the antibody staining where Fmn2 was found to colabel the actin bundles.

Fmn2 is needed for maintenance of growth cone morphology

Fmn2 morphant growth cones showed a reduction in the total spread area as opposed to the control growth cones treated with non-specific morpholino. Depletion of Fmn2 from the neurons also resulted in reduced filopodial lengths and the number of filopodia per growth cone when compared to control growth cones. Thus Fmn2 seems to control in part the overall morphology of the growth cone and suggested a role for Fmn2 in either the generation of new filopodia or elongation and/or stabilization of the existing filopodia. This does not rule out the contribution from other actin nucleators in the process of generation and maintenance of the filopodia and growth cone morphology.

Fmn2 is needed for efficient growth cone motility

Growth cones with reduced levels of Fmn2 exhibited compromised motility. These growth cones translocated slower than the control growth cones and hence showed lower displacement than the control growth cones. Slow rates of motility could have potential implications in the process of axon path finding by the growth cone as the temporal coordination with the guidance cues could be disrupted and thus lead to mistimed information about the environment. Fmn2 depletion resulted in compromised persistent directionality of the growth cones i.e. the growth cone took a more meandering path to reach its final point rather than a straighter. We hypothesized that this could have implications in growth cone guidance, as the ability to maintain the directionality is critical during the process of axon path finding.

Fmn2 affects focal adhesions in the growth cone

We used Focal Adhesion Kinase autophosphorylation (pFAK-Y397) as a marker for assessing the early stages of focal contact formation and stabilization in the growth cones. Overall levels of pFAK in the growth cone were reduced after Fmn2 depletion suggesting a compromised substrate attachment. This could also have subsequent implication in the processes like focal contact maturation and stabilization which are essential for efficient migration.

Analysis of the pFAK traces along individual filopodia revealed that there are significant differences in the terminal point contacts along the filopodia between the control group and Fmn2 morphant group. pFAK levels in the Fmn2 morphant growth cones are seen to drop substantially closer to the tip of the filopodium where the new point contacts are expected to assemble. Given the limitations of the smaller size of point contacts and difficulty in analyzing individual point contacts, we moved to a non-neuronal system where focal adhesions form the equivalents of the point contacts in the growth cone. Focal adhesions owing to their large size proved better for the understanding of the adhesion dynamics on Fmn2 depletion.

Fmn2 depletion affects actin ordering inside the growth cone

Using anisotropy measurements on phalloidin stained growth cones; we found that the ordering of F-actin inside the growth cone is affected. It was seen that the anisotropy per unit area of the growth cone increased when Fmn2 was knocked down suggesting increased disorder in the F-actin composition. To better understand the mode of change in which the actin ordering was disturbed, we used FRAP analysis on bundled actin in NIH3T3 cells to show that the turnover rate of the actin monomers at the F-actin bundles is reduced following Fmn2 depletion.

Fmn2 is need for stabilization of the focal adhesions in non-neuronal cells

We used NIH3T3 cells to analyze the effect of Fmn2 depletion on focal adhesions. Fmn2 was knocked down using siRNA and the focal adhesion parameters were analyzed. It was found that reduced levels of Fmn2 did not change the number of the focal adhesions in the cell but resulted in significant reduction of the area of individual focal adhesions when compared to the control cells. Live imaging of focal adhesions revealed that the focal adhesions disassembled faster when Fmn2 levels were reduced. The assembly rate for individual focal adhesion in the as seen by deposition of Paxillin at the focal adhesions remained comparable with the controls but the focal adhesions in Fmn2 depleted cells spent considerably lower times in the assembly phase. In other words, the focal adhesions in Fmn2 depleted cells spent more time disassembling than assembling. Together, the smaller assembly phase and higher disassembly rate of the focal adhesions results in smaller focal adhesions upon Fmn2 knockdown.

Fmn2 is involved in stress fiber turnover

Stress fibers in the non-neuronal cells form bridges between two distant focal adhesions as in the case of ventral stress fibers. These are actomyosin bundles and the contractility along the stress fibers is responsible for maturation of the focal adhesions (Chang and Kumar, 2013a; Lavelin et al., 2013; Oakes et al., 2012b). FRAP on the stress fibers using mGFP-βactin showed slower recovery rates in case of Fmn2 siRNA treated cells. This shows that Fmn2 is involved in the turnover of actin monomers at the stress fibers.

Depletion of Fmn2 slows down the commissural axons in ovo

At stage 26 in the development of chick embryos, the commissural axons have completed the midline crossing and follow a rostral trajectory post-crossing (Stoeckli and Landmesser,

1995). A sub-population of commissural axons express a cell surface marker, Axonin-I. Axonin-I positive axons move towards the midline in response to Ng-CAM/Nr-CAM present at the midline (Fitzli et al., 2000). After midline crossing the Axonin-I levels are down regulated. The mechanism of down regulation of Axonin-I is not clearly understood but it is speculated that since the midline choice point of Ng-CAM/Nr-CAM is reached, Axonin-I is no longer needed for the guidance and hence is down regulated.

Unilateral electroporations of Fmn2 morpholino in the developing spinal cord lumen of chick embryos, it was seen that Fmn2 morphant embryos failed to down regulate Axonin-I levels at the commissural neurons. While the control group showed down regulation of Axonin-I in the commissural neurons, the Fmn2 morphant embryos still maintained high Axonin-I levels in the commissural neurons. When the Fmn2 morphant embryos were analyzed at stage 28/29 the Axonin-I levels were seen to drop as seen in the control embryos as well.

The effect on commissural neurons was confirmed by analyzing open-book preperations of the spinal cords in which the commissural neuron population was marked using mCherry driven by a commissural neuron specific enhancer Atoh1 (Helms and Johnson, 1998). Control group showed characteristic rostral sigmoid trajectories for the Atoh1 expressing neurons but majority of the Fmn2 morphant commissural neurons failed to cross the midline.

Discussion:

The importance of filopodia in growth cone motility and guidance has been well established in the literature (Chacón et al., 2012; Dent et al., 2007; Gomez and Letourneau, 1994; Gomez et al., 2001; Zheng et al., 1996). In this study we characterize the role of Fmn2 in growth cone filopodia, growth cone motility and in commissural axon guidance. Depletion of Fmn2 from the growth cones results in shorter filopodia thus providing a functional basis to the

localization seen along the filopodial actin bundles. Although no drastic change was seen in filopodial numbers upon Fmn2 depletion, Fmn2 could be detected at the tips of some of the filopodia suggesting a potential role in filopodia generation and/or elongation. Thus a small subset of filopodia could be generated by Fmn2 activity at the leading edge of the growth cone while in a different or the same subset Fmn2 could be the elongator of already existing filopodia.

The protrusive force for the growth cone to migrate is provided by the actin polymerization at the leading edge and any disturbance in this polymerization could have potential effects on the motility rates. Loss of Fmn2 from the growth cone decreases the rate of migration of the growth cones thus suggesting that Fmn2 is actively responsible for adding actin bulk below the cell membrane which in turn is provides the protrusive force needed to push the membrane and achieve a net forward motion.

Fmn2 depletion results in the reduction of pFAK-397 levels in the growth cone suggesting compromised substrate attachment. As seen from the analysis of focal adhesions in non-neuronal cells, Fmn2 is seen to be important in the stabilization of focal adhesions. One of the ways in which Fmn2 can affect the stability of focal adhesions is via stress fiber mediated tension development at the focal adhesions. Tension development along the stress fibers is seen to be important in focal adhesion stabilization (Chang and Kumar, 2013b; Oakes et al., 2012b). Reduced actin turnover at the stress fibers in the FRAP experiment after Fmn2 knockdown reveals a functional role for Fmn2 at the stress fibers. Tension induced focal adhesion maturation leads to sustained pFAK activation (Chen et al., 2013). Thus, the destabilization of focal adhesions is an indirect effect of compromised stress fiber integrity which in turn leads to failure of necessary tension generation needed for focal adhesion maturation. Although stress fibers have not been reported in growth cones in any of the previously published studies, their presence

or presence of functionally similar actin structure can be speculated. Even in the absence of the stress fiber like template the highly contractile actomyosin mesh in the central region of the growth cone could provide the tension required for stabilization of substrate attachments via the croslinking of actin filaments to the integrins. Similar to stress fibers, these structures would contribute to tension development and serve as mediators for physical crosstalk between distant focal adhesions within a growth cone.

In case of commissural neurons, the sustained expression of Axonin-I in Fmn2 morphant embryos could be an effect of delayed signaling events at the midline resulting from slower growth rates of the axons. The midline signaling events are required for Axonin-I down regulation. Due to the temporal offset as a result of slower growth, the Axonin-I downregulation is hampered. Using an independent strategy of enhancer driven labeling of the commissural neurons, it was found that a majority of the Atoh1 positive commissural axon population failed to cross the midline. Both these techniques provide complementary evidence for the requirement of Fmn2 for midline crossing by the commissural neurons.

Our study characterizes a previously neglected cellular role of Fmn2 in growth cone motility and substrate attachment during early neuronal development. Given the redundancy in the formin family, it is possible that each family member plays a subtle role during development enabling the cell to fine tune the actin cytoskeletal response to a particular process in a context dependent manner. But the same redundancy could form a compensatory salvage mechanism to deal with the loss of a family member and thus the subtle phenotypes could eventually be corrected at a gross morphological level. Indeed, $Fmn2^{-/-}$ mice do not show gross morphological differences in the nervous system organization (Leader et al., 2002). But careful studies carried out recently revealed a role for Fmn2 in processes like age-dependent memory loss (Peleg et al.,

2010). Recent reports in humans suggest a role of Fmn2 in dendritic spin morphology and intellectual disability (Law et al., 2014).

References:

Abe, Y., Chen, W., Huang, W., Nishino, M. and Li, Y.-P. (2006). CNBP regulates forebrain formation at organogenesis stage in chick embryos. *Dev. Biol.* **295**, 116–27.

Applewhite, D. A., Barzik, M., Kojima, S., Svitkina, T. M., Gertler, F. B. and Borisy, G. G. (2007). Ena / VASP Proteins Have an Anti-Capping Independent Function in Filopodia Formation □. *Mol. Biol. Cell* **18**, 2579–2591.

Arthur, W. T. and Burridge, K. (2001). RhoA inactivation by p190RhoGAP regulates cell spreading and migration by promoting membrane protrusion and polarity. *Mol. Biol. Cell* **12**, 2711–2720.

Avraham, O., Zisman, S., Hadas, Y., Vald, L. and Klar, A. (2010). Deciphering Axonal Pathways of Genetically Defined Groups of Neurons in the Chick Neural Tube Utilizing in ovo Electroporation. *J. Vis. Exp.* **39**, e1792.

Baeriswyl, T. and Stoeckli, E. T. (2008). Axonin-1/TAG-1 is required for pathfinding of granule cell axons in the developing cerebellum. *Neural Dev.* **3**,.

Balaban, N. Q., Schwarz, U. S., Riveline, D., Goichberg, P., Tzur, G., Sabanay, I., Mahalu, D., Safran, S., Bershadsky, A., Addadi, L., et al. (2001). Force and focal adhesion assembly : a close relationship studied using elastic micropatterned substrates. *Nat. Cell Biol.* **3**, 466–472.

Ballestrem, C., Erez, N., Kirchner, J., Kam, Z., Bershadsky, A. and Geiger, B. (2006). Molecular mapping of tyrosine-phosphorylated proteins in focal adhesions using fluorescence resonance energy transfer. *J. Cell Sci.* **119**, 866–875.

Bartolini, F., Moseley, J. B., Schmoranzer, J., Cassimeris, L., Goode, B. L. and Gundersen, G. G. (2008). The formin mDia2 stabilizes microtubules independently of its actin nucleation activity. *J. Cell Biol.* **181**, 523–36.

Barzik, M., Mcclain, L. M., Gupton, S. L., Gertler, F. B. and Ginsberg, M. H. (2014). Ena / VASP regulates mDia2-initiated filopodial length , dynamics , and function. *Mol. Biol. Cell* **25**, 2604–2619.

Bentley, D. and Toroian-Raymond, a (1986). Disoriented pathfinding by pioneer neurone growth cones deprived of filopodia by cytochalasin treatment. *Nature* **323**, 712–715.

Bor, B., Vizcarra, C. L., Phillips, M. L. and Quinlan, M. E. (2012a). Autoinhibition of the formin Cappuccino in the absence of canonical autoinhibitory domains. *Mol. Biol. Cell* **23**, 3801–13.

Bor, B., Vizcarra, C. L., Phillips, M. L. and Quinlan, M. E. (2012b). Autoinhibition of the formin Cappuccino in the absence of canonical autoinhibitory domains. *Mol. Biol. Cell* **23**, 3801–13.

Bornschlögl, T. (2013). How filopodia pull: What we know about the mechanics and dynamics of filopodia. *Cytoskeleton* **70**, 590–603.

Bornschlögl, T., Romero, S., Vestergaard, C. L., Joanny, J.-F., Van Nhieu, G. T. and Bassereau, P. (2013). Filopodial retraction force is generated by cortical actin dynamics and controlled by reversible tethering at the tip. *Proc. Natl. Acad. Sci. U. S. A.* **110**, 18928–33.

Burridge, K. and Wittchen, E. S. (2013). The tension mounts: stress fibers as force-generating mechanotransducers. *J. Cell Biol.* **200**, 9–19.

Campellone, K. G. and Welch, M. D. (2010). A nucleator arms race: cellular control of actin assembly. *Nat. Rev. Mol. Cell Biol.* **11**, 237–51.

Chacón, M. R., Navarro, A. I., Cuesto, G., del Pino, I., Scott, R., Morales, M. and Rico, B. (2012). Focal adhesion kinase regulates actin nucleation and neuronal filopodia formation during axonal growth. *Development* **139**, 3200–10.

Chang, C.-W. and Kumar, S. (2013a). Vinculin tension distributions of individual stress fibers within cell-matrix adhesions. *J. Cell Sci.* **126**, 3021–30.

Chang, C.-W. and Kumar, S. (2013b). Vinculin tension distributions of individual stress fibers within cell-matrix adhesions. *J. Cell Sci.* **126**, 3021–30.

Chen, S. and Hamm, H. E. (2006). DEP domains: More than just membrane anchors. *Dev. Cell* **11**, 436–8.

Chen, Y., Pasapera, A. M., Koretsky, A. P. and Waterman, C. M. (2013). Orientation-speci fi c responses to sustained uniaxial stretching in focal adhesion growth and turnover.

Chesarone, M. a and Goode, B. L. (2009). Actin nucleation and elongation factors: mechanisms and interplay. *Curr. Opin. Cell Biol.* **21**, 28–37.

Chesarone, M., Gould, C. J., Moseley, J. B. and Goode, B. L. (2009). Displacement of Formins from Growing Barbed Ends by Bud14 Is Critical for Actin Cable Architecture and Function. *Dev. Cell* **16**, 292–302.

Chesarone, M. a, DuPage, A. G. and Goode, B. L. (2010). Unleashing formins to remodel the actin and microtubule cytoskeletons. *Nat. Rev. Mol. Cell Biol.* **11**, 62–74.

Chilton, J. K. (2006). Molecular mechanisms of axon guidance. *Dev. Biol.* **292**, 13–24.

Colombelli, J., Besser, a., Kress, H., Reynaud, E. G., Girard, P., Caussinus, E., Haselmann, U., Small, J. V., Schwarz, U. S. and Stelzer, E. H. K. (2009). Mechanosensing in actin stress fibers revealed by a close correlation between force and protein localization. *J. Cell Sci.* **122**, 1928–1928.

Cramer, L. P., Siebert, M. and Mitchison, T. J. (1997). Identification of novel graded polarity actin filament bundles in locomoting heart fibroblasts: Implications for the generation of motile force. *J. Cell Biol.* **136**, 1287–1305.

Del Rio, A., Perez-Jimenez, R., Liu, R., Roca-Cusachs, P., Fernandez, J. M. and Sheetz, M. P. (2009). Stretching single talin rod molecules activates vinculin binding. *Science* **323**, 638–641.

Dent, E. W. and Gertler, F. B. (2003). Cytoskeletal Dynamics and Transport in Growth Cone Motility and Axon Guidance. *Neuron* **40**, 209–227.

Dent, E. W., Kwiatkowski, A. V, Mebane, L. M., Philippar, U., Barzik, M., Rubinson, D. A., Gupton, S., Van Veen, J. E., Furman, C., Zhang, J., et al. (2007). Filopodia are required for cortical neurite initiation. *Nat. Cell Biol.* **9**, 1347–59.

Dent, E. W., Gupton, S. L. and Gertler, F. B. (2011). The growth cone cytoskeleton in axon outgrowth and guidance. *Cold Spring Harb. Perspect. Biol.* **3**,.

Dettenhofer, M., Zhou, F. and Leder, P. (2008). Formin 1-isoform IV deficient cells exhibit defects in cell spreading and focal adhesion formation. *PLoS One* **3**, e2497.

Dumont, J., Million, K., Sunderland, K., Rassinier, P., Lim, H., Leader, B. and Verlhac, M.-H. (2007). Formin-2 is required for spindle migration and for the late steps of cytokinesis in mouse oocytes. *Dev. Biol.* **301**, 254–65.

Emmons, S., Phan, H., Calley, J., Chen, W., James, B. and Manseau, L. (1995). Cappuccino, a Drosophila maternal effect gene required for polarity of the egg and embryo, is related to the vertebrate limb deformity locus. *Genes Dev.* **9**, 2482–2494.

Ezratty, E. J., Partridge, M. a and Gundersen, G. G. (2005). Microtubule-induced focal adhesion disassembly is mediated by dynamin and focal adhesion kinase. *Nat. Cell Biol.* **7**, 581–90.

Faix, J. (2008). Filopodia formation induced by active mDia2 / Drf3. *J. Microsc.* **231**, 506–517.

Fitzli, D., Stoeckli, E. T., Kunz, S., Siribour, K., Rader, C., Kunz, B., Kozlov, S. V, Buchstaller, a, Lane, R. P., Suter, D. M., et al. (2000). A direct interaction of axonin-1 with NgCAM-related cell adhesion molecule (NrCAM) results in guidance, but not growth of commissural axons. *J. Cell Biol.* **149**, 951–68.

Forscher, P. and Smith, S. J. (1988). Actions of cytochalasins on the organization of actin filaments and microtubules in a neuronal growth cone. *J. Cell Biol.* **107**, 1505–16.

Galbraith, C. G., Yamada, K. M. and Sheetz, M. P. (2002). The relationship between force and focal complex development. *J. Cell Biol.* **159**, 695–705.

Gardel, M. L., Schneider, I. C., Aratyn-Schaus, Y. and Waterman, C. M. (2010). Mechanical integration of actin and adhesion dynamics in cell migration. *Annu. Rev. Cell Dev. Biol.* **26**, 315–33.

Geiger, B. and Bershadsky, a (2001). Assembly and mechanosensory function of focal contacts. *Curr. Opin. Cell Biol.* **13**, 584–92.

Geiger, B., Spatz, J. P. and Bershadsky, A. D. (2009). Environmental sensing through focal adhesions. *Nat. Rev. Mol. Cell Biol.* **10**, 21–33.

Gilestro, G. F. (2008). Redundant mechanisms for regulation of midline crossing in Drosophila. *PLoS One* **3**, e3798.

Girao, H., Geli, M. I. and Idrissi, F. Z. (2008). Actin in the endocytic pathway: From yeast to mammals. *FEBS Lett.* **582**, 2112–2119.

Goh, W. I. and Ahmed, S. (2012). mDia1-3 in mammalian filopodia. *Commun. Integr. Biol.* **5**, 340–344.

Goh, W. I., Sudhaharan, T., Lim, K. B., Sem, K. P., Lau, C. L. and Ahmed, S. (2011). Rif-mDia1 interaction is involved in filopodium formation independent of Cdc42 and Rac effectors. *J. Biol. Chem.* **286**, 13681–94.

Goley, E. D. and Welch, M. D. (2006). The ARP2/3 complex: an actin nucleator comes of age. *Nat. Rev. Mol. Cell Biol.* **7**, 713–26.

Goley, E. D., Rodenbusch, S. E., Martin, A. C. and Welch, M. D. (2004). Critical conformational changes in the Arp2/3 complex are induced by nucleotide and nucleation promoting factor. *Mol. Cell* **16**, 269–79.

Gomez, T. M. and Letourneau, P. C. (1994). Filopodia Initiate Choices Made by Sensory Neuron Growth Cones at Laminin / Fibronectin Borders in vitro. *J. Neurosci.* **7414**, 5959–5972.

Gomez, T. M., Roche, F. K. and Letourneau, P. C. (1996). Chick sensory neuronal growth cones distinguish fibronectin from laminin by making substratum contacts that resemble focal contacts. *J. Neurobiol.* **29**, 18–34.

Gomez, T. M., Robles, E., Poo, M. and Spitzer, N. C. (2001). Filopodial calcium transients promote substrate-dependent growth cone turning. *Science (80-.).* **291**, 1983–1987.

Gonçalves-Pimentel, C., Gombos, R., Mihály, J., Sánchez-Soriano, N. and Prokop, A. (2011). Dissecting regulatory networks of filopodia formation in a Drosophila growth cone model. *PLoS One* **6**, e18340.

Grabham, P. W. and Goldberg, D. J. (1997). Nerve growth factor stimulates the accumulation of beta1 integrin at the tips of filopodia in the growth cones of sympathetic neurons. *J. Neurosci.* **17**, 5455–5465.

Grashoff, C., Hoffman, B. D., Brenner, M. D. and Zhou, R. (2010). Measuring mechanical tension across vinculin reveals regulation of focal adhesion dynamics. *Nature* **466**, 263–266.

Gungabissoon, R. A. and Bamburg, J. R. (2003). Regulation of Growth Cone Actin Dynamics by ADF / Cofilin 1. *J. Histochem. Cytochem.* **51**, 411–420.

Gupton, S. L., Eisenmann, K., Alberts, A. S. and Waterman-Storer, C. M. (2007a). mDia2 regulates actin and focal adhesion dynamics and organization in the lamella for efficient epithelial cell migration. *J. Cell Sci.* **120**, 3475–87.

Gupton, S. L., Eisenmann, K., Alberts, A. S. and Waterman-Storer, C. M. (2007b). mDia2 regulates actin and focal adhesion dynamics and organization in the lamella for efficient epithelial cell migration. *J. Cell Sci.* **120**, 3475–87.

Helms, A. W. and Johnson, J. E. (1998). Progenitors of dorsal commissural interneurons are defined by MATH1 expression. *Development* **928**, 919–928.

Higgs, H. N. and Peterson, K. J. (2005). Phylogenetic analysis of the formin homology 2 domain. *Mol. Biol. Cell* **16**, 1–13.

Holinstat, M., Knezevic, N., Broman, M., Samarel, A. M., Malik, A. B. and Mehta, D. (2006). Suppression of RhoA activity by focal adhesion kinase-induced activation of p190RhoGAP: Role in regulation of endothelial permeability. *J. Biol. Chem.* **281**, 2296–2305.

Homem, C. C. F., Peifer, M. and Hill, C. (2009). Exploring the Roles of Diaphanous and Enabled Activity in Shaping the Balance between Filopodia and Lamellipodia. *Mol. Biol. Cell* **20**, 5138–5155.

Hotulainen, P. and Lappalainen, P. (2006). Stress fibers are generated by two distinct actin assembly mechanisms in motile cells. *J. Cell Biol.* **173**, 383–94.

Humphries, J. D., Wang, P., Streuli, C., Geiger, B., Humphries, M. J. and Ballestrem, C. (2007). Vinculin controls focal adhesion formation by direct interactions with talin and actin. *J. Cell Biol.* **179**, 1043–1057.

Ilić, D., Furuta, Y., Kanazawa, S., Takeda, N., Sobue, K., Nakatsuji, N., Nomura, S., Fujimoto, J., Okada, M. and Yamamoto, T. (1995). Reduced cell motility and enhanced focal adhesion contact formation in cells from FAK-deficient mice. *Nature* **377**, 539–544.

Iskratsch, T., Yu, C.-H., Mathur, A., Liu, S., Stévenin, V., Dwyer, J., Hone, J., Ehler, E. and Sheetz, M. (2013). FHOD1 Is Needed for Directed Forces and Adhesion Maturation during Cell Spreading and Migration. *Dev. Cell* **27**, 545–59.

Iyer, K. V., Pulford, S., Mogilner, a. and Shivashankar, G. V. (2012). Mechanical activation of cells induces chromatin remodeling preceding MKL nuclear transport. *Biophys. J.* **103**, 1416–1428.

Johnston, S. a, Bramble, J. P., Yeung, C. L., Mendes, P. M. and Machesky, L. M. (2008). Arp2/3 complex activity in filopodia of spreading cells. *BMC Cell Biol.* **9**, 65.

Kalil, K., Li, L. and Hutchins, B. I. (2011). Signaling Mechanisms in Cortical Axon Growth, Guidance, and Branching. *Front. Neuroanat.* **5**, 1–15.

Kanchanawong, P., Shtengel, G., Pasapera, A. M., Ramko, E. B., Davidson, M. W., Hess, H. F. and Waterman, C. M. (2010). Nanoscale architecture of integrin-based cell adhesions. *Nature* **468**, 580–4.

Kaprielian, Z., Imondi, R. and Runko, E. (2000). Axon guidance at the midline of the developing CNS. *Anat. Rec.* **261**, 176–97.

Kaprielian, Z., Runko, E. and Imondi, R. (2001). Axon Guidance at the Midline Choice Point. *Dev. Dyn.* **221**, 154–181.

Koka, S., Neudauer, C. L., Li, X., Lewis, R. E., McCarthy, J. B. and Westendorf, J. J. (2003). The formin-homology-domain-containing protein FHOD1 enhances cell migration. *J. Cell Sci.* **116**, 1745–1755.

Korobova, F. and Svitkina, T. (2008). Arp2 / 3 Complex Is Important for Filopodia Formation , Growth Cone Motility , and Neuritogenesis in Neuronal Cells. *Mol. Biol. Cell* **19**, 1561–1574.

Kos, R., Tucker, R. P., Hall, R., Duong, T. D. and Erickson, C. a (2003). Methods for introducing morpholinos into the chicken embryo. *Dev. Dyn.* **226**, 470–7.

Kuo, J.-C., Han, X., Hsiao, C.-T., Yates, J. R. and Waterman, C. M. (2011). Analysis of the myosin-II-responsive focal adhesion proteome reveals a role for β-Pix in negative regulation of focal adhesion maturation. *Nat. Cell Biol.* **13**, 383–93.

Kwon, S., Shin, H. and Lim, H. J. (2011). Dynamic interaction of formin proteins and cytoskeleton in mouse oocytes during meiotic maturation. *Mol. Hum. Reprod.* **17**, 317–327.

Lai, F. P. L., Szczodrak, M., Block, J., Faix, J., Breitsprecher, D., Mannherz, H. G., Stradal, T. E. B., Dunn, G. a, Small, J. V. and Rottner, K. (2008). Arp2/3 complex interactions and actin network turnover in lamellipodia. *EMBO J.* **27**, 982–992.

Lammers, M., Rose, R., Scrima, A. and Wittinghofer, A. (2005). The regulation of mDia1 by autoinhibition and its release by Rho*GTP. *EMBO J.* **24**, 4176–4187.

Lavelin, I., Wolfenson, H., Patla, I., Henis, Y. I., Medalia, O., Volberg, T., Livne, A., Kam, Z. and Geiger, B. (2013). Differential effect of actomyosin relaxation on the dynamic properties of focal adhesion proteins. *PLoS One* **8**, e73549.

Law, R., Dixon-Salazar, T., Jerber, J., Cai, N., Abbasi, A. a, Zaki, M. S., Mittal, K., Gabriel, S. B., Rafiq, M. A., Khan, V., et al. (2014). Biallelic Truncating Mutations in FMN2, Encoding the Actin-Regulatory Protein Formin 2, Cause Nonsyndromic Autosomal-Recessive Intellectual Disability. *Am. J. Hum. Genet.* **95**, 721–8.

Le Clainche, C. and Carlier, M.-F. (2008). Regulation of actin assembly associated with protrusion and adhesion in cell migration. *Physiol. Rev.* **88**, 489–513.

Leader, B. and Leder, P. (2000). Formin-2 , a novel formin homology protein of the cappuccino subfamily , is highly expressed in the developing and adult central nervous system. *Mech. Dev.* **93**, 221–231.

Leader, B., Lim, H., Carabatsos, M. J., Harrington, A., Ecsedy, J., Pellman, D., Maas, R. and Leder, P. (2002). Formin-2, polyploidy, hypofertility and positioning of the meiotic spindle in mouse oocytes. *Nat. Cell Biol.* **4**, 921–8.

Lebrand, C., Dent, E. W., Strasser, G. A., Lanier, L. M., Krause, M., Svitkina, T. M., Borisy, G. G. and Gertler, F. B. (2004). Critical Role of Ena / VASP Proteins for Filopodia Formation in Neurons and in Function Downstream of Netrin-1. *Neuron* **42**, 37–49.

Li, F. and Higgs, H. N. (2003). The Mouse Formin mDia1 Is a Potent Actin Nucleation Factor Regulated by Autoinhibition. *Curr. Biol.* **13**, 1335–1340.

Lowery, L. A. and Van Vactor, D. (2009). The trip of the tip: understanding the growth cone machinery. *Nat. Rev. Mol. Cell Biol.* **10**, 332–43.

Lu, J., Meng, W., Poy, F., Maiti, S., Goode, B. L. and Eck, M. J. (2007). Structure of the FH2 Domain of Daam1: Implications for Formin Regulation of Actin Assembly. *J. Mol. Biol.* **369**, 1258–1269.

Machaidze, G., Sokoll, A., Shimada, A., Lustig, A., Mazur, A., Wittinghofer, A., Aebi, U. and Mannherz, H. G. (2010). Actin filament bundling and different nucleating effects of mouse Diaphanous-related formin FH2 domains on actin/ADF and actin/cofilin complexes. *J. Mol. Biol.* **403**, 529–45.

Mallavarapu, A. and Mitchison, T. (1999). Regulated actin cytoskeleton assembly at filopodium tips controls their extension and retraction. *J. Cell Biol.* **146**, 1097–1106.

Marsh, L. and Letourneau, P. C. (1984). Growth of Neurites without Filopodial or Lamellipodial Activity in the Presence of Cytochalasin B. *J. Cell Biol.* **99**, 2041–2047.

Marshall, B. T., Long, M., Piper, J. W., Yago, T., McEver, R. P. and Zhu, C. (2003). Direct observation of catch bonds involving cell-adhesion molecules. *Nature* **423**, 190–193.

Matusek, T., Gombos, R., Szécsényi, A., Sánchez-Soriano, N., Czibula, A., Pataki, C., Gedai, A., Prokop, A., Raskó, I. and Mihály, J. (2008). Formin proteins of the DAAM subfamily play a role during axon growth. *J. Neurosci.* **28**, 13310–9.

Mellor, H. (2005). The Rho Family GTPase Rif Induces Filopodia through mDia2. *Curr. Biol.* **15**, 129–133.

Mellor, H. (2010). The role of formins in filopodia formation. *Biochim. Biophys. Acta* **1803**, 191–200.

Mende, M., Christophorou, N. a D. and Streit, A. (2008). Specific and effective gene knock-down in early chick embryos using morpholinos but not pRFPRNAi vectors. *Mech. Dev.* **125**, 947–62.

Milev, P., Maurel, P., Ha, M., Margolis, K. and Margolis, R. U. (1996). TAG-1 / Axonin-1 Is a High-affinity Ligand of Neurocan , Phosphacan / Protein-tyrosine Phosphatase- / , and N-CAM *. *Biochemistry* **271**, 15716–15723.

Montanez, E., Ussar, S., Schifferer, M., Bösl, M., Zent, R., Moser, M. and Fässler, R. (2008). Kindlin-2 controls bidirectional signaling of integrins. *Genes Dev.* **22**, 1325–1330.

Montaville, P., Jégou, A., Pernier, J., Compper, C., Guichard, B., Mogessie, B., Schuh, M., Romet-Lemonne, G. and Carlier, M. F. (2014). Spire and Formin 2 Synergize and Antagonize in Regulating Actin Assembly in Meiosis by a Ping-Pong Mechanism. *PLoS Biol.* **12**, 1–20.

Moore, S. W., Zhang, X., Lynch, C. D. and Sheetz, M. P. (2012). Netrin-1 attracts axons through FAK-dependent mechanotransduction. *J. Neurosci.* **32**, 11574–11585.

Moser, M., Nieswandt, B., Ussar, S., Pozgajova, M. and Fässler, R. (2008). Kindlin-3 is essential for integrin activation and platelet aggregation. *Nat. Med.* **14**, 325–330.

Mozhui, K., Ciobanu, D. C., Schikorski, T., Wang, X., Lu, L. and Williams, R. W. (2008). Dissection of a QTL hotspot on mouse distal chromosome 1 that modulates neurobehavioral phenotypes and gene expression. *PLoS Genet.* **4**, e1000260.

Myers, J. P. and Gomez, T. M. (2011). Focal Adhesion Kinase Promotes Integrin Adhesion Dynamics Necessary for Chemotropic Turning of Nerve Growth Cones. *J. Neurosci.* **31**, 13585–13595.

Nakamura, H., Katahira, T., Sato, T., Watanabe, Y. and Funahashi, J. I. (2004). Gain- and loss-of-function in chick embryos by electroporation. *Mech. Dev.* **121**, 1137–1143.

Nalbant, P. (2014). FHOD1 regulates stress fiber organization by controlling transversal arc and dorsal fiber dynamics. *J. Cell Sci.*

Nayal, A., Webb, D. J. and Horwitz, A. F. (2004). Talin: An emerging focal point of adhesion dynamics. *Curr. Opin. Cell Biol.* **16**, 94–98.

O'Donnell, M., Chance, R. K. and Bashaw, G. J. (2009). Axon growth and guidance: receptor regulation and signal transduction. *Annu. Rev. Neurosci.* **32**, 383–412.

Oakes, P. W., Beckham, Y., Stricker, J. and Gardel, M. L. (2012a). Tension is required but not sufficient for focal adhesion maturation without a stress fiber template. *J. Cell Biol.* **196**, 363–74.

Oakes, P. W., Beckham, Y., Stricker, J. and Gardel, M. L. (2012b). Tension is required but not sufficient for focal adhesion maturation without a stress fiber template. *J. Cell Biol.* **196**, 363–74.

Otomo, T., Tomchick, D. R., Otomo, C., Panchal, S. C., Machius, M. and Rosen, M. K. (2005). Structural basis of actin filament nucleation and processive capping by a formin homology 2 domain. *Nature* **433**, 488–494.

Paul, A. and Pollard, T. (2008). The Role of the FH1 Domain and Profilin in Formin-Mediated Actin-Filament Elongation and Nucleation. *Curr. Biol.* **18**, 9–19.

Pekarik, V., Bourikas, D., Miglino, N., Joset, P., Preiswerk, S. and Stoeckli, E. T. (2003). Screening for gene function in chicken embryo using RNAi and electroporation. *Nat. Biotechnol.* **21**, 93–6.

Peleg, S., Sananbenesi, F., Zovoilis, A., Burkhardt, S., Bahari-Javan, S., Agis-Balboa, R. C., Cota, P., Wittnam, J. L., Gogol-Doering, A., Opitz, L., et al. (2010). Altered histone acetylation is associated with age-dependent memory impairment in mice. *Science* **328**, 753–6.

Pellegrin, S. and Mellor, H. (2007). Actin stress fibres. *J. Cell Sci.* **120**, 3491–9.

Perrin, F. E. and Stoeckli, E. T. (2000). Use of Lipophilic Dyes in Studies of Axonal Pathfinding In Vivo. *Microsc. Res. Tech.* **48**, 25–31.

Peterson, L. J., Rajfur, Z., Maddox, A. S., Freel, C. D., Chen, Y., Edlund, M., Otey, C. and Burridge, K. (2004). Simultaneous Stretching and Contraction of Stress Fibers In Vivo. **15**, 3497–3508.

Pfender, S., Kuznetsov, V., Pleiser, S., Kerkhoff, E. and Schuh, M. (2011). Spire-type actin nucleators cooperate with Formin-2 to drive asymmetric oocyte division. *Curr. Biol.* **21**, 955–60.

Pollard, T. D. and Cooper, J. a (2009). Actin, a central player in cell shape and movement. *Science* **326**, 1208–12.

Polleux, F., Ince-Dunn, G. and Ghosh, A. (2007). Transcriptional regulation of vertebrate axon guidance and synapse formation. *Nat. Rev. Neurosci.* **8**, 331–340.

Ponti, a, Machacek, M., Gupton, S. L., Waterman-Storer, C. M. and Danuser, G. (2004). Two distinct actin networks drive the protrusion of migrating cells. *Science* **305**, 1782–1786.

Prosser, D. C., Drivas, T. G., Maldonado-Báez, L. and Wendland, B. (2011). Existence of a novel clathrin-independent endocytic pathway in yeast that depends on Rho1 and formin. *J. Cell Biol.* **195**, 657–671.

Quinlan, M. E., Hilgert, S., Bedrossian, A., Mullins, R. D. and Kerkhoff, E. (2007). Regulatory interactions between two actin nucleators, Spire and Cappuccino. *J. Cell Biol.* **179**, 117–28.

Rao, M., Baraban, J. H., Rajaii, F. and Sockanathan, S. (2004). In vivo comparative study of RNAi methodologies by in ovo electroporation in the chick embryo. *Dev. Dyn.* **231**, 592–600.

Reinhard, M., Halbrugge, M., Scheer, U., Wiegand, C., Jockusch, B. M. and Walter, U. (1992). The 46/50 kDa phosphoprotein VASP purified from human platelets is a novel protein associated with actin filaments and focal contacts. *EMBO J.* **11**, 2063–2070.

Renaudin, a, Lehmann, M., Girault, J. and McKerracher, L. (1999). Organization of point contacts in neuronal growth cones. *J. Neurosci. Res.* **55**, 458–471.

Robles, E. and Gomez, T. M. (2006). Focal adhesion kinase signaling at sites of integrin-mediated adhesion controls axon pathfinding. *Nat. Neurosci.* **9**, 1274–83.

Roca-Cusachs, P., del Rio, A., Puklin-Faucher, E., Gauthier, N. C., Biais, N. and Sheetz, M. P. (2013). Integrin-dependent force transmission to the extracellular matrix by α-actinin triggers adhesion maturation. *Proc. Natl. Acad. Sci. U. S. A.* **110**, E1361–70.

Romero, S., Clainche, C. Le, Didry, D., Egile, C., Pantaloni, D. and Carlier, M. (2004). Formin Is a Processive Motor that Requires Profilin to Accelerate Actin Assembly and Associated ATP Hydrolysis. *Cell* **119**, 419–429.

Rosales-nieves, A. E., Johndrow, J. E., Keller, L. C., Magie, C. R., Pinto-Santini, D. M. and Parkhurst, S. M. (2006). Coordination of microtubule and microfilament dynamics by Drosophila Rho1, Spire and Cappuccino. *Nat. Cell Biol.* **8**, 367–376.

Rose, R., Weyand, M., Lammers, M., Ishizaki, T., Ahmadian, M. R. and Wittinghofer, a (2005). Structural and mechanistic insights into the interaction between Rho and mammalian Dia. *Nature* **435**, 513–518.

Schirenbeck, A., Arasada, R., Bretschneider, T., Schleicher, M. and Faix, J. (2005a). Formins and VASPs may co-operate in the formation of filopodia. *Biochem. Soc. Trans.* **33**, 1256–1259.

Schirenbeck, A., Bretschneider, T., Arasada, R., Schleicher, M. and Faix, J. (2005b). The Diaphanous-related formin dDia2 is required for the formation and maintenance of filopodia. *Nat. Cell Biol.* **7**, 619–25.

Schönichen, A., Alexander, M., Gasteier, J. E., Cuesta, F. E., Fackler, O. T. and Geyer, M. (2006). Biochemical characterization of the diaphanous autoregulatory interaction in the formin homology protein FHOD1. *J. Biol. Chem.* **281**, 5084–5093.

Schönichen, A., Mannherz, H. G., Behrmann, E., Antonina, J. and Geyer, M. (2013). FHOD1 is a combined actin filament capping and bundling factor that selectively associates with actin arcs and stress fibers Accepted manuscript Journal of Cell Science * Corresponding authors : Accepted manuscript.

Schuh, M. (2011). An actin-dependent mechanism for long-range vesicle transport. *Nat. Cell Biol.* **13**, 1–7.

Schuh, M. and Ellenberg, J. (2008). A new model for asymmetric spindle positioning in mouse oocytes. *Curr. Biol.* **18**, 1986–92.

Shi, Q. and Boettiger, D. (2003). A Novel Mode for Integrin-mediated Signaling : Tethering Is Required for Phosphorylation of FAK Y397. *Mol. Biol. Cell* **14**, 4306–4315.

Steffen, A., Faix, J., Resch, G. P., Linkner, J., Wehland, J., Small, J. V., Rottner, K. and Stradal, T. E. B. (2006). Filopodia Formation in the Absence of Functional WAVE- and Arp2 / 3-Complexes. *Mol. Biol. Cell* **17**, 2581–2591.

Stern, C. D. (2005). The chick: A great model system becomes even greater. *Dev. Cell* **8**, 9–17.

Stoeckli, E. T. and Landmesser, L. T. (1995). Axonin-1, Nr-CAM, and Ng-CAM Play Different Roles in the In Vivo Guidance of Chick Commissural Neurons. *Neuron* **14**, 1165–1179.

Strasser, G. a, Rahim, N. A., VanderWaal, K. E., Gertler, F. B. and Lanier, L. M. (2004). Arp2/3 is a negative regulator of growth cone translocation. *Neuron* **43**, 81–94.

Suter, D. M. and Forscher, P. (2001). Transmission of growth cone traction force through apCAM – cytoskeletal linkages is regulated by Src family tyrosine kinase activity. *J. Cell Biol.* **155**, 427–438.

Suter, D. M. and Miller, K. E. (2011). The emerging role of forces in axonal elongation. *Prog. Neurobiol.* **94**, 91–101.

Tomar, A., Lim, S., Lim, Y., Schlaepfer, D. D., Tomar, A., Lim, S., Lim, Y. and Schlaepfer, D. D. (2009). A FAK-p120RasGAP-p190RhoGAP complex regulates polarity in migrating cells A FAK-p120RasGAP-p190RhoGAP complex regulates polarity in migrating cells. *J. Cell Sci.* 1852–1862.

Wallar, B. J., Stropich, B. N., Schoenherr, J. a., Holman, H. a., Kitchen, S. M. and Alberts, A. S. (2006). The basic region of the diaphanous-autoregulatory domain (DAD) is required for autoregulatory interactions with the diaphanous-related formin inhibitory domain. *J. Biol. Chem.* **281**, 4300–4307.

Watanabe, S., Ando, Y., Yasuda, S., Hosoya, H., Watanabe, N., Ishizaki, T. and Narumiya, and S. (2008). mDia2 Induces the Actin Scaffold for the Contractile Ring and Stabilizes Its Position during Cytokinesis in NIH 3T3 Cells. *Mol. Biol. Cell* **19**, 2328–2338.

Weston, L., Coutts, A. S. and Thangue, N. B. La (2012). Actin nucleators in the nucleus : an emerging theme.

Winckler, B. and Mellman, I. (2010). Trafficking guidance receptors. *Cold Spring Harb. Perspect. Biol.* **2**, 1–19.

Wolfenson, H., Bershadsky, A., Henis, Y. I. and Geiger, B. (2011). Actomyosin-generated tension controls the molecular kinetics of focal adhesions. *J. Cell Sci.* **124**, 1425–32.

Woo, S., Rowan, D. J. and Gomez, T. M. (2009). Retinotopic mapping requires focal adhesion kinase-mediated regulation of growth cone adhesion. *J. Neurosci.* **29**, 13981–13991.

Xu, Y., Moseley, J. B., Sagot, I., Poy, F., Pellman, D., Goode, B. L. and Eck, M. J. (2004). Crystal structures of a formin homology-2 domain reveal a tethered dimer architecture. *Cell* **116**, 711–723.

Yamada, H., Abe, T., Satoh, a., Okazaki, N., Tago, S., Kobayashi, K., Yoshida, Y., Oda, Y., Watanabe, M., Tomizawa, K., et al. (2013). Stabilization of Actin Bundles by a Dynamin 1/Cortactin Ring Complex Is Necessary for Growth Cone Filopodia. *J. Neurosci.* **33**, 4514–4526.

Yang, C., Czech, L., Gerboth, S., Kojima, S., Scita, G. and Svitkina, T. (2007). Novel roles of formin mDia2 in lamellipodia and filopodia formation in motile cells. *PLoS Biol.* **5**, e317.

Zamir, E., Geiger, B. and Kam, Z. (2008). Quantitative multicolor compositional imaging resolves molecular domains in cell-matrix adhesions. *PLoS One* **3**, e1901.

Zhang, X.-F., Schaefer, A. W., Burnette, D. T., Schoonderwoert, V. T. and Forscher, P. (2003). Rho-Dependent Contractile Responses in the Neuronal Growth Cone Are Independent of Classical Peripheral Retrograde Actin Flow. *Neuron* **40**, 931–944.

Zheng, J. Q., Wan, J. J. and Poo, M. M. (1996). Essential role of filopodia in chemotropic turning of nerve growth cone induced by a glutamate gradient. *J. Neurosci.* **16**, 1140–1149.

Zimerman, B., Volberg, T. and Geiger, B. (2004). Early molecular events in the assembly of the focal adhesion-stress fiber complex during fibroblast spreading. *Cell Motil. Cytoskeleton* **58**, 143–59.

2 INTRODUCTION

2.1 Axon guidance

The achievement of precise neuronal connections forms the basis of a properly functional nervous system. To ensure the correct wiring of the nervous system, a highly precise and coordinated sequence of events must take place. Each neuron during the embryonic development extends an axonal process that travels a large distance through the surrounding embryonic tissue to reach its final destination via a process called 'axon guidance'. To achieve this low error connectivity pattern, the target tissues must express a set of guidance cues that interact with the receptors present on the growing tip of the axon, the 'growth cone'. The guidance cues present in the environment as diffusible or substrate bound ligands are recognized by the receptor's growth cone and an appropriate signaling is elicited depending on the favorability of the cue. Some cues act as attractants and promote the growth cone of the axon towards it via growth cone mediated motility while others are repulsive and act as barriers for the advancing growth cone limiting its entry in their zone of influence.

In bilaterally symmetrical animals, sub-groups of axons cross from one side of the body to the other side. These axons are referred to as the commissural axons and their guidance is controlled by a dedicated signaling network conserved from flies to mammals (Figure 2.1, below). In vertebrates, the commissural neurons reside in the dorsal horn of the spinal cord and their axons travel ventromedially to cross the midline and turn rostrally extending along the longitudinal pathways. Extensive studies over the years have demonstrated the involvement of Netrins, Semaphorins, IgSFCAMs, Slits, and various morphogens in the process of midlne crossing by the commissural axons (Chilton, 2006; Gilestro, 2008; Kalil et al., 2011; Kaprielian et al., 2001; O'Donnell et al., 2009). In vertebrates, a small group of specialized columnar

ependymal cells called the floor plate are located at the ventral midline of the spinal cord and act as intermediate targets for the axons. The axons that cross the midline do not re-enter the midline under wild-type conditions. Thus, the trajectory of a given class of axons which navigates in the vicinity of the midline is determined by the manner in which their growth cones integrate a variety of extracellular guidance signals.

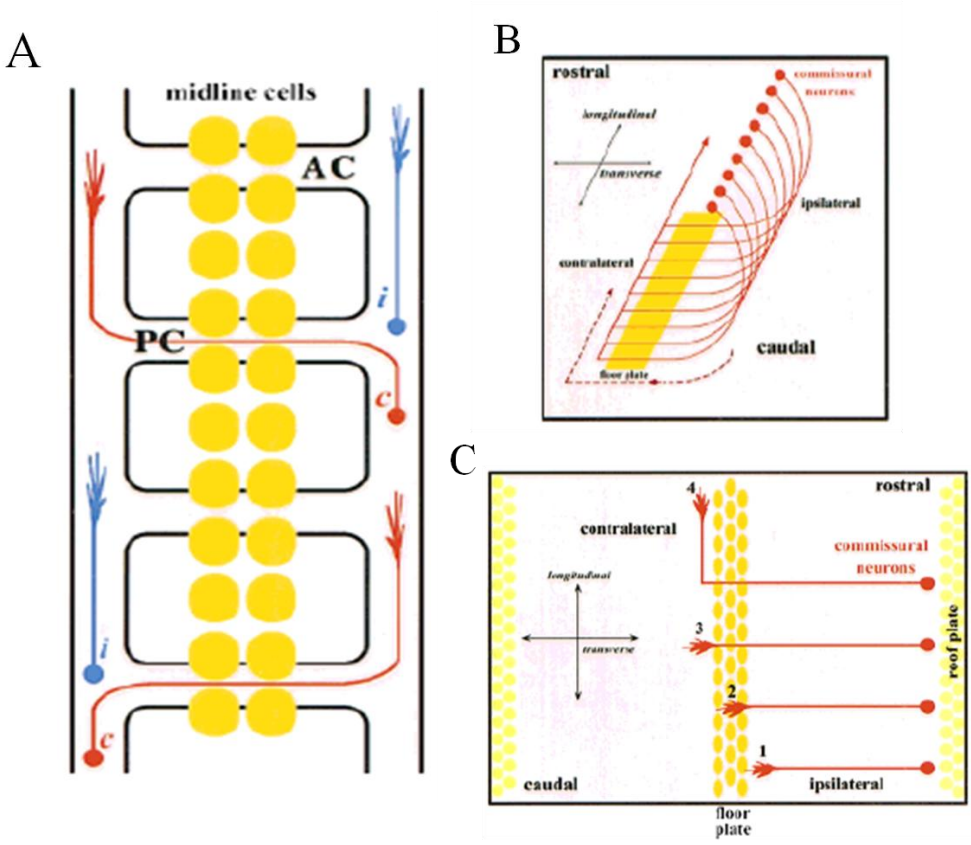

Figure 2.1: Axon guidance at the midline.
A. Schematic representation of the *Drosophila* ventral nerve cord. The midline cells send out signals that are interpreted by the surrounding axons via the growth cones and a decision is made whether to cross the midline through the anterior commissure (AC) or the posterior commissure (PC). Axons post-crossing are referred to as the contralateral projections (c) and the ones that do not cross are called the ipsilateral projections (i). **B.** Schematic representation of vertebrate spinal cord showing the commissural trajectories as seen in a transverse section. **C.** Commissural trajectories in vertebrate spinal cord as seen in an open-book preparation. Adapted from *(Kaprielian et al., 2000)*.

The cells of the floor plate equivalent in *Drosophila* are called the midline cells. They serve a similar function in guiding the axons past the midline and providing trophic support. A

wide variety of mechanisms are in place to ensure the correct presentation and receipt of guidance signals, ranging from spatially and temporally restricted transcriptional regulation (Polleux et al., 2007) of cues and receptors to their specific posttranslational trafficking (O'Donnell et al., 2009) (Figure 2.2, below).

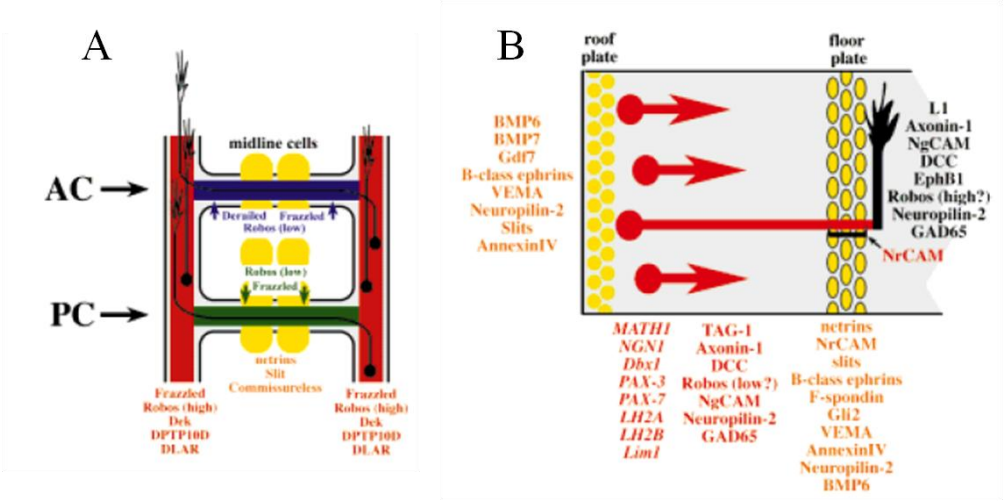

Figure 2.2: Molecules coordinating midline guidance.
Numerous molecules have been described as mediators of midline crossing and the majority of them are conserved between invertebrates and vertebrates. **A.** Drosophila midline, **B.** Open-book representation of vertebrate midline**.** Adapted from *(Kaprielian et al., 2000)*.

2.2 The growth cone structure

The growth cone is the active motile structure at the tip of a growing axon and is responsible for receiving the information about guidance cues and relaying them inside the cell via the receptors expressed on the surface of the growth cone. The growth cone can be compared to a motile cell with some differences. The neuronal growth cone mainly consists of two structures with distinct morphologies, a flat lamellipodium and long finger-like projections ahead of the lamellipodium, the filopodia (Figure 2.3, below). The lamellipodium has a dense meshwork of actin filaments while the filopodia contain long bundles of unbranched actin. Unlike other motile cells, the growth cone motility is dominated by filopodia. Filopodia owing to

their dynamic nature are best suited for interrogating the environment and serve as sites of sensors about the extracellular environment (Gomez et al., 2001). Filopodial protrusions and retractions are mediated by a dynamic balance of barbed-end polymerization and F-actin retrograde flow. At the same time the capping proteins provide a check on the length of the growing filament. For countering the capping activity actin elongation factors are important. The dynamics of the actin machinery at the growth cone dictates the protrusion of the leading edge membrane. Axons devoid of actin polymerization activity can still advance, but with reduced speed, compromised growth cone morphology and substrate selectivity (Marsh and Letourneau, 1984).

The growth cone is divided in to three domains based on the underlying cytoskeletal elements. The peripheral or P-domain contains actin bundles that form the filopodia and actin mesh that forms the lamellipodium. Dynamic exploratory MTs invade the P-domain sliding along the actin bundles. The central or C-domain consists of stable MTs that originate in the axon shaft. Additionally, this domain also contains organelles, vesicles and actin filaments. The region between the P and C-domain is referred to as the transition or T-zone. Here contractile actomyosin structures called actin arcs form a barrier for the entry of MTs in the P-domain.

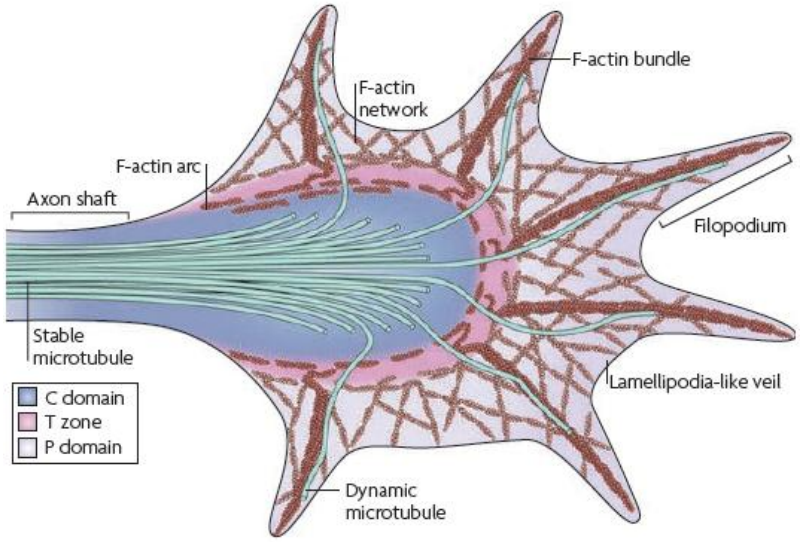

Figure 2.3: Schematic representation of the growth cone cytoskeleton.
The axonal shaft has a core of MTs which splay out in the C-domain of the growth cone and occasionally invade a filopodium. The filopodia consist of bundled unbranched F-actin while the P-domain has a meshwork of branched F-actin. Adapted from *(Lowery and Van Vactor, 2009)*.

2.3 Growth cone actin cytoskeleton in motility and axon guidance

The actin and microtubule components of the growth cone cytoskeleton work together to bring about the growth cone motility in response to a guidance cue. The contribution from the actin cytoskeleton has been extensively studied while the importance of the microtubule component is being recognized recently. Growth cone protrusion and motility is driven primarily by the cyclical polymerization and depolymerization of actin filaments. Actin dynamics are necessary for directed axonal outgrowth, but not necessarily for growth *per se*. Growth cones treated with an actin depolymerization agent like cytochalasin still move but with limited sense of directionality, reduced speeds and do not respond appropriately to guidance cues (Bentley and Toroian-Raymond, 1986; Forscher and Smith, 1988; Marsh and Letourneau, 1984). The free barbed ends of the actin filaments are oriented towards the periphery of the growth cone. Using speckle microscopy it has been seen that there is a steady retrograde flow of actin towards the

center of the growth cone (Zhang et al., 2003). This retrograde movement of actin is a result of myosin-II-driven actin transport and a pushing force that actin exerts on the peripheral membrane as it is polymerizing. The balance between the rate of polymerization and retrograde flow determines if the growth cone extends or withdraws protrusions. If the polymerization rate exceeds retrograde flow, then the growth cone protrudes. If the polymerization rate is balanced with the velocity of retrograde flow, then the membrane remains stationary. When connection to the underlying substratum is increased by tighter coupling between the actin cytoskeleton and transmembrane adhesion receptors, retrograde flow slows and the balance shifts to polymerization-driven protrusion (Suter and Forscher, 2001).

Control over processes like actin nucleation, elongation, depolymerization, bundling, and contraction are important to shape the growth cone and bring about the dynamic responses to a wide range of extracellular cues. Various actin associated proteins participate in the process of growth cone motility by fine tuning the polymerization dynamics of the actin network and integrating the information from the extracellular guidance cues.

Adapted from *(Dent et al., 2011)*

Table 2-1: Actin associated proteins in axon guidance.

Protein Family	**Guidance Assay**	**Potential Guidance Pathways**
Barbed-end Binding Proteins		
Ena/VASP	I (Mm, Dm, Ce)	Netrin and SLIT pathway Dm Ce
DAAM	I (Dm)	Misrouted axons, broken commissures
F-actin Binding/Bundling Proteins		
ERM proteins	C, C-R	Sema Pathway
Unc115/Ablim	I (Ce)	VD DD motor neurons
GAP43	I (MR), C	Retinal, callosal, thalamocortical
Unc-44/Ankryin	I (Ce)	Netrin pathway

ß-Spectrin	I(Dm)	midline defects
Abl	I(Dm)	Slit, EphrinA, and Netrin pathway
Fascin	I(Dm)	Trajectory maintenance
F-actin Severing Proteins		
Cofilin	I (MR, Dm), C, C-R	Netrin, NGF, Semaphorin, BMP, SLIT
F-actin Depolymerizing Proteins		
Mical	I (Dm)	Sema pathway
Monomer Binding Proteins		
CAP	I (Dm)	SLIT pathway
Profilin	I (Dm)	ISNb
Arp2/3+Activating Factors		
WASP/WAVE	I (Dm, Ce)	Netrin, Semaphorin
Arp2/3 subunits	I (Dm, Ce)	Netrin, Semaphorin
F-actin Motor Proteins		
Myosin IIA	C-R	Required for Sema3A/ RGMa collapse
Myosin IIB	C-R	Required for Sema3A retraction
F-actin-Cytoskeletal-Linking Proteins		
Short Stop/ACF7	I (Dm)	Required for repulsion
MAP1B		Netrin
POD1	I (Dm)	ISN, SNa, ISNb neurons

Table key:
(S) Substrate-Stripe, (C) Collagen Gel, (C-R) collapse/retraction, (I) In vivo, (Ce) C. elegans, (Dm) Drosophila, (Dr) zebrafish, (Gg) chicken,(MR) mouse/rat,(Xl) Xenopus, (P) pipet assay, (M) Micro-CALI.

2.4 Actin nucleators and cell motility

Eukaryotic cells move by protruding in front and retracting at the rear end. Protrusion results from the polarized growth of actin filaments at the leading edge of the cell (Figure 2.4, below). The protruding front of the cell (~200nm thick and several micrometers inside the cell) is called the lamellipodium and is composed of polarized arrays of actin filaments. Addition of new

monomers to the actin filaments at the front of the cell leads to protrusive forces that push the cell membrane forward. The newly formed front edge of the cell then attaches to the substrate and a new wave of actin monomer addition is initiated. Behind the highly dynamic lamellipodium is a more stable region, called the lamella, which contributes to cell migration by coupling the actin network to myosin II-mediated contractility and substrate adhesion (Ponti et al., 2004). To initiate actin assembly during cell motility, the cells generate free barbed ends that act as templates for polymerization of actin monomers. The free barbed ends can be generated by uncapping or severing existing filaments or by nucleating from monomers de novo. Actin in cells is dynamic and strongly out of equilibrium. Unlike an equilibrium polymer, whose polymerized state persists once formed, actin undergoes a cycle of polymerization and depolymerization fuelled by a continuing input of chemical energy. This cycle allows the actin cytoskeleton to respond rapidly to changing external stimuli, and causes spontaneous dynamic behaviors. Due to the non-equilibrium state of the actin pool, spontaneous actin assembly is inefficient and the formation of actin dimers and trimeric 'nuclei' is kinetically unfavorable. To overcome this thermodynamic barrier, cells use factors that assist in the nucleation process. For many years, only the actin-related protein 2/3 (ARP2/3) complex, a few of its activators, were known to directly participate in nucleation (Goley and Welch, 2006). However, many more bonafide actin nucleators have been described (Campellone and Welch, 2010; Chesarone and Goode, 2009; Weston et al., 2012) (Figure 2.5, below).

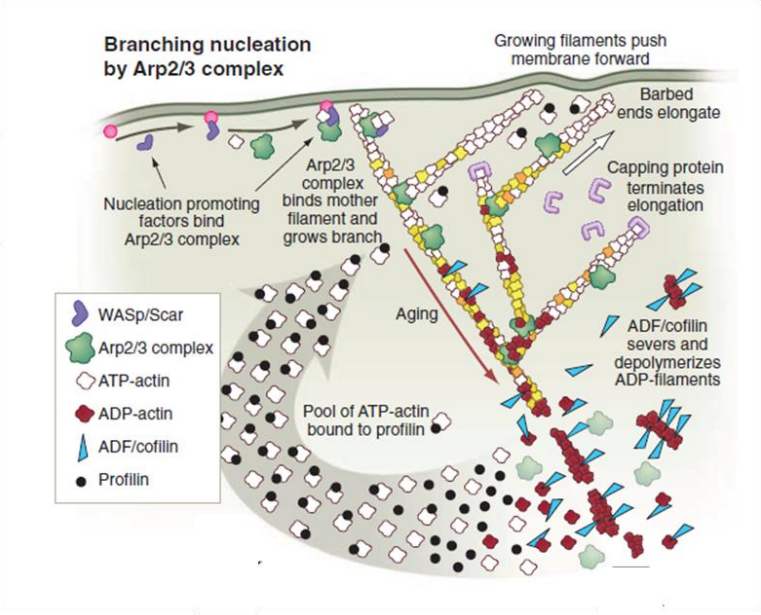

Figure 2.4: Actin cytoskeleton at the leading edge.
A large number of proteins participate in the process of generating the actin filaments to push the membrane forward and also to recycle the old actin cytoskeleton towards the centre of the cell. The actin mesh towards the cell centre is broken down/severed by a special category of proteins like cofilin and the monomers are then supplied to the leading edge by the help of monomer sequestrating proteins like profilin. Adapted from *(Pollard and Cooper, 2009)*.

Arp2/3 remains associated with filament pointed ends, and it is distributed throughout the lamellipodium, but it is incorporated only into the network at the front of the lamellipodium (Lai et al., 2008). *In vitro*, the nucleation-promoting factors of the WASP (Wiskott–Aldrich syndrome protein) family stimulate the ability of the Arp2/3 complex to induce actin polymerization. These factors, which include WASP itself, N-WASP, WAVE1–3, WASH, and WHAMM proteins, all bind to the Arp2/3 complex through a C-terminal acidic domain. WAVE proteins are known to localize to the leading edge and contribute to lamellipodium extension, whereas N-WASP may localize to lamellipodia in some cell types and participate in endocytosis (Campellone and Welch, 2010).

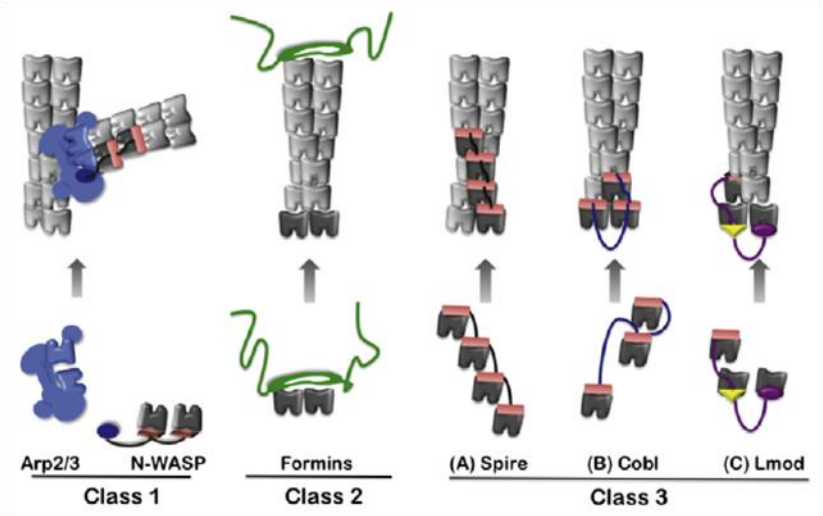

Figure 2.5: Actin nucleation factors.
Schematic representation of different actin nucleators and their mode of nucleation. Arp2/3 generates a branch along an existing actin filament while others form a new unbranched filament. Notice that formins differ from other classes in that they remain attached to the growing/barbed end of the filament. Adapted from *(Chesarone and Goode, 2009)*.

Over the last decade, other actin nucleators have been found to contribute to lamellipodium extension, including several members of the Formin and Spire families (Campellone and Welch, 2010).

2.5 Formins

Apart from Arp2/3 the best characterized family of actin nucleators is the formins. The conserved FH1 and FH2 domain are the defining features of the proteins belonging to this family (Figure 2.6, below). These proteins fall into seven different subclasses based on FH2 sequence divergence: Diaphanous (DIA), formin-related proteins in leukocytes (FRLs), Dishevelled-associated activators of morphogenesis (DAAMs), formin homology domain proteins (FHODs), formins (FMNs), delphilin and inverted formins (INFs) (Higgs and Peterson, 2005).

The FH2 domain on its own is capable of promoting actin nucleation (Chesarone et al., 2010). In contrast to ARP2/3, which caps pointed ends, FH2 domains bind to barbed ends and

act as processive caps on elongating filaments. As a result, they prevent other capping proteins from terminating elongation (Romero et al., 2004) and compete with displacement factors at the barbed end to determine filament length (Chesarone et al., 2009).

Crystallography studies have shown that the proteins work as dimers due to the homodimerization property of the FH2 domains (Lu et al., 2007; Xu et al., 2004). Structural analyses have also demonstrated two possible confirmations of the FH2 dimer. In a closed conformation, both FH2 monomers bind the two terminal actin subunits, blocking further actin incorporation. In an open conformation, actin incorporation is enabled. Two potential open states have been proposed, one in which the FH2 steps towards the barbed end to allow addition of a new actin subunit (Otomo et al., 2005) and another in which actin addition occurs before FH2 stepping (Paul and Pollard, 2008).

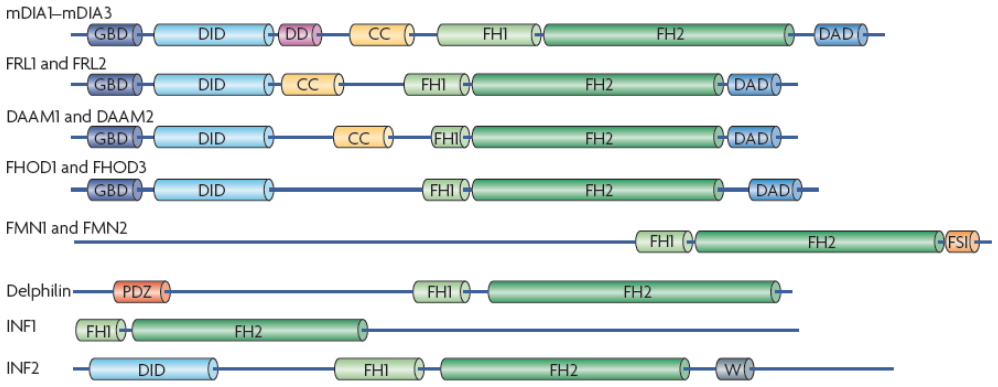

Figure 2.6: Domain organization in formins.
All the formins are categorized based on the presence of the formin homology (FH) domains. The GTPase binding domain (GBD) and the diaphanous autoregulatory domain (DAD) control the transition of the proteins from inactive state to active state. Although not all the formins have these regulatory domains distinctly characterized. Adapted from *(Campellone and Welch, 2010)*.

2.5.1 DRFs

The best-characterized mammalian formins are called the Diaphanous-related formins (DRFs) based on their similarity to *Drosophila* Diaphanous. In mice and other mammals, the

DRFs are commonly named mDIA1 (or DIAPH1), mDIA2 (or DIAPH3) and mDIA3 (or DIAPH2) and are thought to be widely expressed. The DRFs have a modular domain organization that can be divided into three functional regions (Figure 2.7, below). Their N-terminus contains a regulatory sequence, including a GBD and a partially overlapping Diaphanous inhibitory domain (DID) that participates in autoinhibition (Li and Higgs, 2003). These motifs are followed by central coiled-coil and dimerization domains that influence autoregulation. Lastly, the C-terminus encompasses the FH1–FH2 domains and the Diaphanous autoregulatory domain (DAD) that binds the GBD–DID to inhibit the actin polymerizing activity of the FH2 domain (Wallar et al., 2006). This inhibitory interaction is disrupted by the binding of RhoA to the GBD–DID (Lammers et al., 2005) and results in FH2 activation in vitro (Li and Higgs, 2003). Structural comparisons of the GBD–DID bound to either a DAD or to Rho GTPases (Rose et al., 2005) indicate that binding of Rho and DAD is mutually exclusive, and their binding sites in the GBD–DID partially overlap. Importantly, DRF activation on GTPase binding *in vitro* is incomplete, raising the possibility that additional cellular factors are required for full activation.

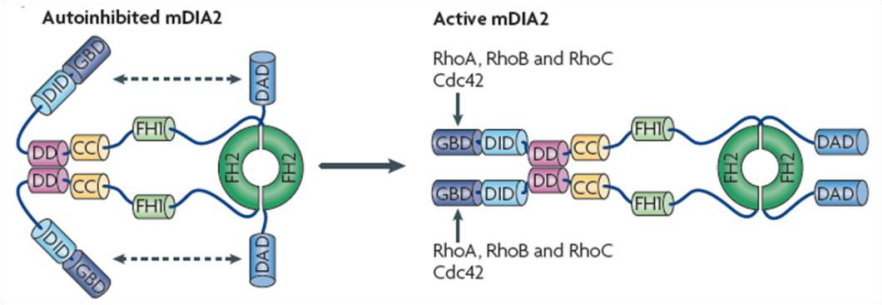

Figure 2.7: Regulation of DRF by autoinhibition.
Dia2 is known to work as a dimer and undergoes autoinhibition. The actin nucleation function is stimulated by binding to Rho family GTPases, such as RhoA, RhoB and RhoC and Cdc42. Adapted from *(Campellone and Welch, 2010)*.

DRF-mediated actin assembly participates in the formation of a variety of cellular structures like stress fibers , dorsal filaments that emerge from focal adhesions at the leading edge of migrating cells (Hotulainen and Lappalainen, 2006) and the contractile ring that forms during cytokinesis (Watanabe et al., 2008). DRFs have also been shown to be involved in filopodia and lamellipodia formation and focal adhesion dynamics (Faix, 2008; Gupton et al., 2007a; Schirenbeck et al., 2005a). Although the mechanism of activation for DRFs is the best described, not all formins share this mechanism.

2.5.2 FMNs

Formin1 (Fmn1) and Formin2 (Fmn2) were the founding members of this sub-class later followed by FH homology domain containing proteins (FHOD1 and FHOD3). Members of this sub-class share similarities with the DRFs in other regions except the N-terminus (Higgs and Peterson, 2005). FHOD1 is involved in stress fiber formation, early cell spreading and substrate attachment (Iskratsch et al., 2013; Nalbant, 2014). Regulation of Fmn1 and Fmn2 are still debated while FHOD1 has been shown to undergo autoinhibition through the interaction between C-terminal DAD and the N-terminus (Koka et al., 2003; Schönichen et al., 2006) mediated by Rac1 association with GBD. Fmn1 isoform IV is characterized for its role in adherens junctions and focal adhesions (Dettenhofer et al., 2008). Though Fmn2 shares a great similarity with Fmn1, the regulation of Fmn2 is still illusive. Fmn2 knockout female mice show abnormal oocyte development with abnormalities in spindle positioning (Dumont et al., 2007; Leader et al., 2002). The oocyte development aspect of Fmn2 has been also demonstrated in Drosophila where an association with Rho has been clearly shown (Rosales-nieves et al., 2006). In spite of this evidence, vertebrate Fmn2 lacks the conventional regulatory domains and is thought to be unique in its mechanism of activation (Bor et al., 2012a). Early studies have shown that Fmn2 is

selectively enriched in the developing central nervous system (Leader and Leder, 2000), but the role of Fmn2 in the nervous system is still poorly understood except a few recent studies linking Fmn2 to dendritic spine morphology and cognitive capabilities (Law et al., 2014; Mozhui et al., 2008; Peleg et al., 2010).

2.6 Summary

The process of axon guidance via the growth cone motility is highly complex and involves multiple receptor ligand combinations. The cell harbors a battery of actin nucleators and actin associated proteins that maintain a fine balance between the polymerized and unpolymerized states of actin. The activity of many of these proteins is coupled to upstream receptors in the signaling cascade governing the growth cone guidance. The dynamic interchange between the two actin states enables the growth cone (or a motile cell) to respond appropriately to the extracellular cues and ultimately navigate its way through the surrounding environment to reach the target.

3 ESTABLISHING THE CHICK EMBRYO SYSTEM

3.1 Introduction

The developing chick embryo has long been used as a model system in developmental biology. Apart from the classical advantages of a model system like low cost maintenance, short life cycle and well defined developmental stages, the chick embryo provides other features like easy access to the embryo because of the viviparous mode of development and the amenability of the embryos for surgical procedures. Over the years we have learnt a lot about tissue morphogenesis and patterning based on studies that used developing chick embryos as a model. Of particular note are the studies involving cross-transplantations between chick and quail embryos which built our understanding of cell fates and tissue interactions (Stern, 2005).

The reason chick embryos failed to feature as a mainstream developmental biology model similar to *Drosophila* or mouse is because of the lack of genetic tractability. Although the chick genome has been sequenced and annotated to a large extent, generating mutants and maintenance of mutant stock is not practically possible. Given this limitation, the gene interaction studies are difficult to undertake in this model system although temporary gene manipulation in selected tissues has been achieved using plasmid based overexpression and siRNA/dsRNA/morpholino mediated knockdowns (Abe et al., 2006; Kos et al., 2003; Mende et al., 2008; Nakamura et al., 2004; Pekarik et al., 2003; Rao et al., 2004).

For cell biological studies where high resolution imaging of cultured neurons is required, the chick embryo system provides many advantages. The neurons from the Dorsal root ganglia

(DRG), spinal cord and cortical areas are easy to culture and owing to their large size are well suited for high resolution imaging.

Thus, due to the ease of procurement and accessibility to the embryo for whole embryo manipulations and ease of culturing primary neurons for cell biological studies, we chose to work with the chick embryos for our studies.

3.2 Results

3.2.1 Labeling the neuronal trajectories by electroporation

Plasmids constructs were injected in the neural tube of Stage HH14/15 embryos and electroporated using a short voltage pulse across the neural tube (Figure 3.1, below). This delivers the plasmid unilaterally to one half of the spinal cord and the other half serves as a control (wild-type) half. The windowed eggs were carefully resealed using a tape and kept back in the incubator at 37 °C. The expression of GFP/DsRed is visualized 48 hours post injection. Since the GFP/DsRed variants used here were cytoplasmic, the entire axon including the cell body was labeled in these experiments. The efficiency of the expression and survival of the embryos post-electroporation depends on multiple factors like the amount and quality of DNA injected, amount of current passing through the embryo, voltage applied, duration of the electrical pulse and the type of promoter/enhancer used in the plasmid construct (Table 3-1, below).

Different promoters and electroporation setting had to be tried before finalizing the right electroporation protocol to achieve efficient DNA delivery in the cells and at the same time maintain high survival rate of the embryos post-electroporation. Conventional promoters like CMV and β-actin were used in the beginning to drive the expression of GFP/DsRed in the spinal cords. Though these promoters are considered strong enough to drive the gene of interest in

different types of eukaryotic cells, they were not found to be as efficient when tested in neuronal cells. For this reason the GFP/DsRed expression achieved using these promoters was very weak. Two parameters had to be changed to achieve higher expression, the amount of DNA injected and the amount of voltage applied across the spinal cord to achieve more delivery of the plasmid in the cells. Both these parameters can be altered only within a specified range. Too much DNA leads to toxicity, and a higher voltage means more damage to the cells and higher embryo mortality. Given these limitations, the CMV and β-actin based plasmids were not used for the study. An enhancer element CAG, resulting from the fusion of CMV and β-actin was found to strongly drive the expression of the GFP/DsRed cassette as compared to the individual promoter elements. In all the subsequent experiments a plasmid backbone containing CAG enhancer element was used to drive the GFP/DsRed cassette (pCAG-GFP/DsRed).

After choosing the right plasmid backbone for over-expression the next step was to standardize the strength of the electrical pulse use to deliver the plasmid inside the cells so as to achieve efficient/optimal expression and maintain high embryo survival. Using the same amount of plasmid DNA (100ng/ul) in each electroporation round, various settings were used to come up with a most efficient combination.

Table 3-1: Various combinations used for standardizing the in ovo electroporations.

Combination	Voltage applied (V)	Number of pulses	Duration of each pulse (ms)	Inter-pulse interval (ms)	Embryo survival	Expression (visual estimate)
1	30	5	100	500	+	++
2	25	5	100	500	+	+++
3	25	3	100	500	+	++
4	20	3	100	500	++	++
5	20	3	50	950	+++	++
6	18	3	50	950	+++	+

7	15	3	50	950	+++	+

For all the subsequent experiments, combination 5 from the above table was used. The expression levels were improved by increasing the concentration of DNA used for the injections.

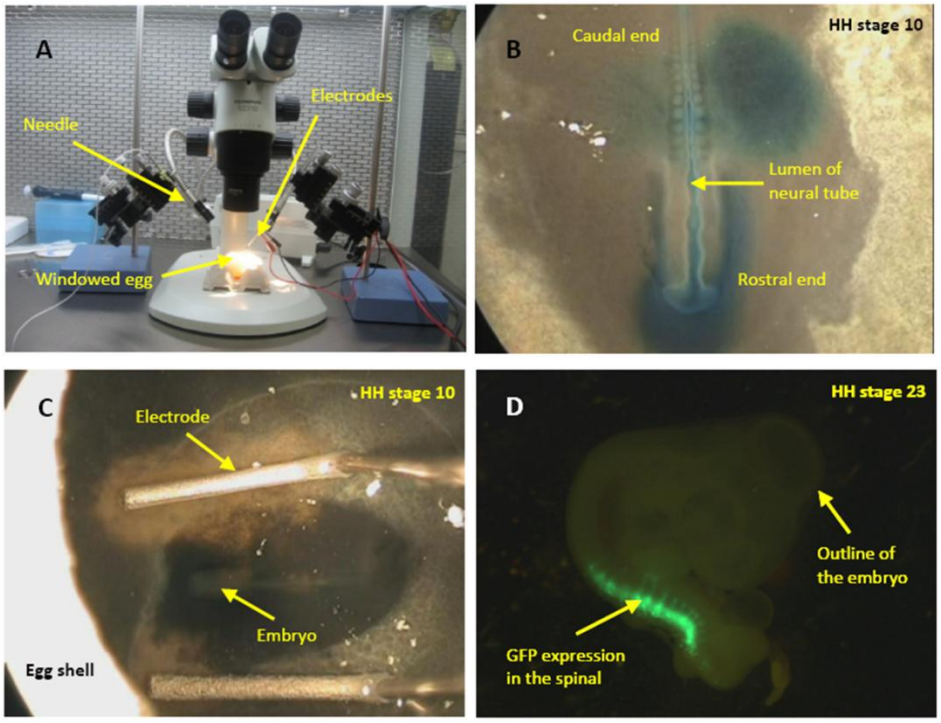

Figure 3.1: *In ovo* electroporation in chick embryo spinal cord.
A. Electroporation setup with the injection needle and electrode assembly, **B.** DNA solution injected in the spinal cord lumen. The DNA solution contains 0.1% fast green dye to allow visualization during injection, **C.** Placement of the electrodes on either side of the embryo for electroporation, **D.** GFP expression as seen after 24-48hrs post electroporation.

Dissected spinal cords were imaged under a confocal microscope to visualize the labeled neurons (Figure 3.2A, below). The expression of the fluorophore was also visualized by fixing and cryosectioning the embryos. After sectioning, the GFP was visualized by using an antibody against GFP as fixation lead to reduced detection of the GFP (Figure 3.2B, below). Different trajectories in the spinal cord were seen following the immunohistochemistry (Figure 3.2C, below).

Though the expression achieved using pCAG-GFP vector was quick (expression was detected as early as 8 hrs post electroporation) and highly efficient, this vector did not allow us to differentiate between sub-populations of neurons with the spinal cord. Unpublished data from our laboratory had suggested requirement of Fmn2 in midline crossing in *Drosophila*. *capu* mutant embryos showed aberrant crossing and breaks in the axon tracts near the midline. Thus, we were particularly interested in the commissural neuron population.

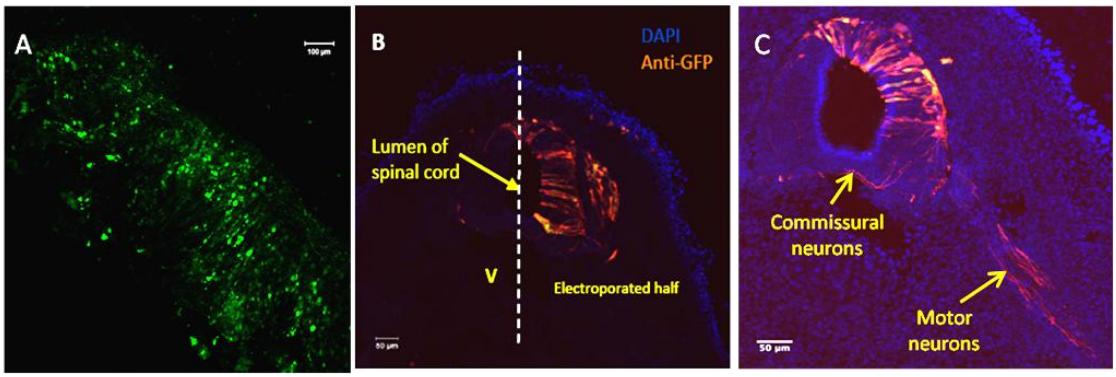

Figure 3.2: Labelling trajectories with GFP using a generic promoter.
A. Entire spinal cord imaged after dissecting it out of the embryo. A sparse distribution of GFP positive cells was seen. **B.** GFP positive cells as visualized after crysectioning and secondary immunostaining for GFP. Only one half of the spinal cord is labelled, **C.** Cryosection of the spinal cord post electroporation and immunostaining for GFP showing neuronal trajectories for commissural and motor neurons.

We used a Cre-Lox based system developed in Dr. Avihu Klar's laboratory at the Hebrew University (Avraham et al., 2010). Using this system, over-expression of the desired DNA cassette could be achieved only in a subset of neurons within the spinal cord; in this case, the commissural inter neurons. This technique uses electroporation of two plasmids simultaneously. One plasmid drives the expression of Cre recombinase under a population specific enhancer while the second plasmid has an in frame mCherry cassette between two LoxP sites followed by an out of frame GFP cassette. When the mCherry cassette is removed by the action of Cre, the GFP cassette is locked in frame thus allowing GFP expression only in the cells that receive both

the plasmids (Figure 3.3, below). We used the plasmids developed in the Klar lab that contained commissural neuron enhancers, EdI1/2 and FoxD3 to drive the Cre that allowed GFP-labeling of specifically the commissural neurons.

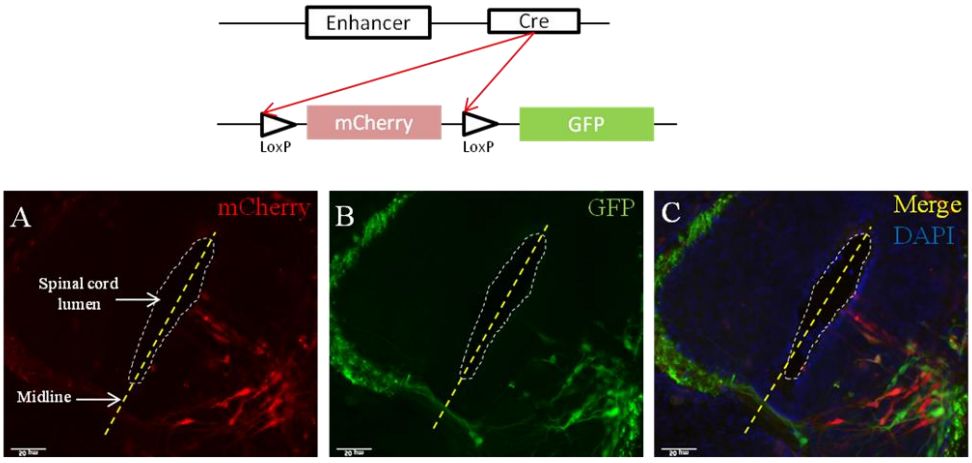

Figure 3.3: Labeling trajectories using specific enhancer.
The enhancer drives the Cre which acts on the LoxP sites and removes the mCherry cassette to bring the GFP cassette in frame. Only those cells that received both the plasmids expressed GFP (along with residual mCherry before LoxP excision). Scale Bar 100µm.

3.2.2 Labeling commissural trajectories using lipophilic dyes

Commissural neuron trajectories could also be labeled using injections of lipophilic dyes like DiI (Perrin and Stoeckli, 2000). The cell bodies of commissural neurons were targeted for injection of DiI solution in chloroform or methanol. The dye travelled the entire axon length in about 2-3 days in fixed open book preparations (Figure 3.4, below). This method was not very efficient and reliable as small deviations from the correct site of injections labeled trajectories other than the commissural neurons and the analysis of the commissural trajectories was thus difficult.

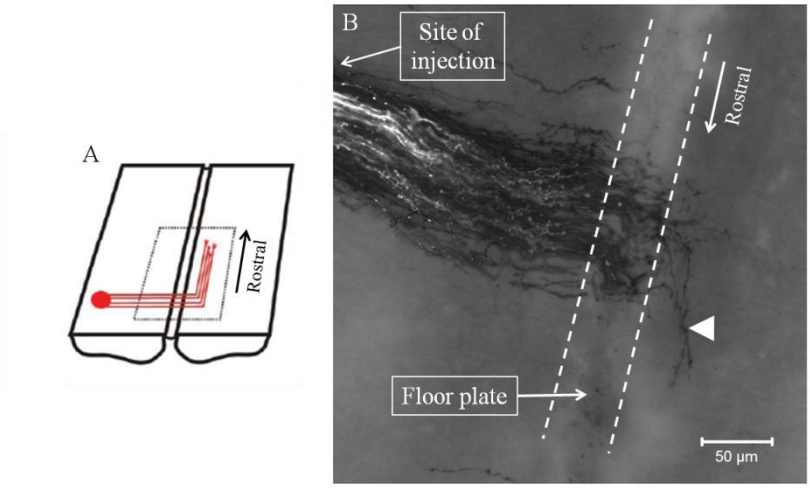

Figure 3.4: Labeling commissural neuron trajectories using DiI.
A. Schematic representation of the injection. The spinal cord was pinned to a silgard plate in an open book format and the commissural neuron cell bodies were targeted (modified from Joset P. et al., 2011), **B.** Image of the labelled commissural neurons following the DiI delivery. The characteristic rostral turn is seen for the post crossing axons. The image is inverted for better contrast. The arrow point to the rostral end.

3.2.3 Labeling trajectories with specific antibodies

Embryos were cryosectioned and stained with specific antibodies to label the neuronal trajectories. Antibodies like the neurofilament associated antigen (3A10, DSHB), Axonin-I (23.4-5, DSHB), Islet1 and Islet2 (39.4D5, DSHB), motor neuron marker HB9 (81.5C10, DSHB) were tested. These antibodies were not chosen to specifically label the commissural neurons but in addition to labeled other regions in the spinal cord as well. 3A10 and 23.4-5 allowed us to mark the neuronal trajectories while 39.4D5 and 81.5C10 allowed us to mark the cell nuclei. This allowed us to have a small panel of potential regions in the spinal cord that could be used for screening the phenotype after specific knockdowns in our experiments (Figure 3.5, below).

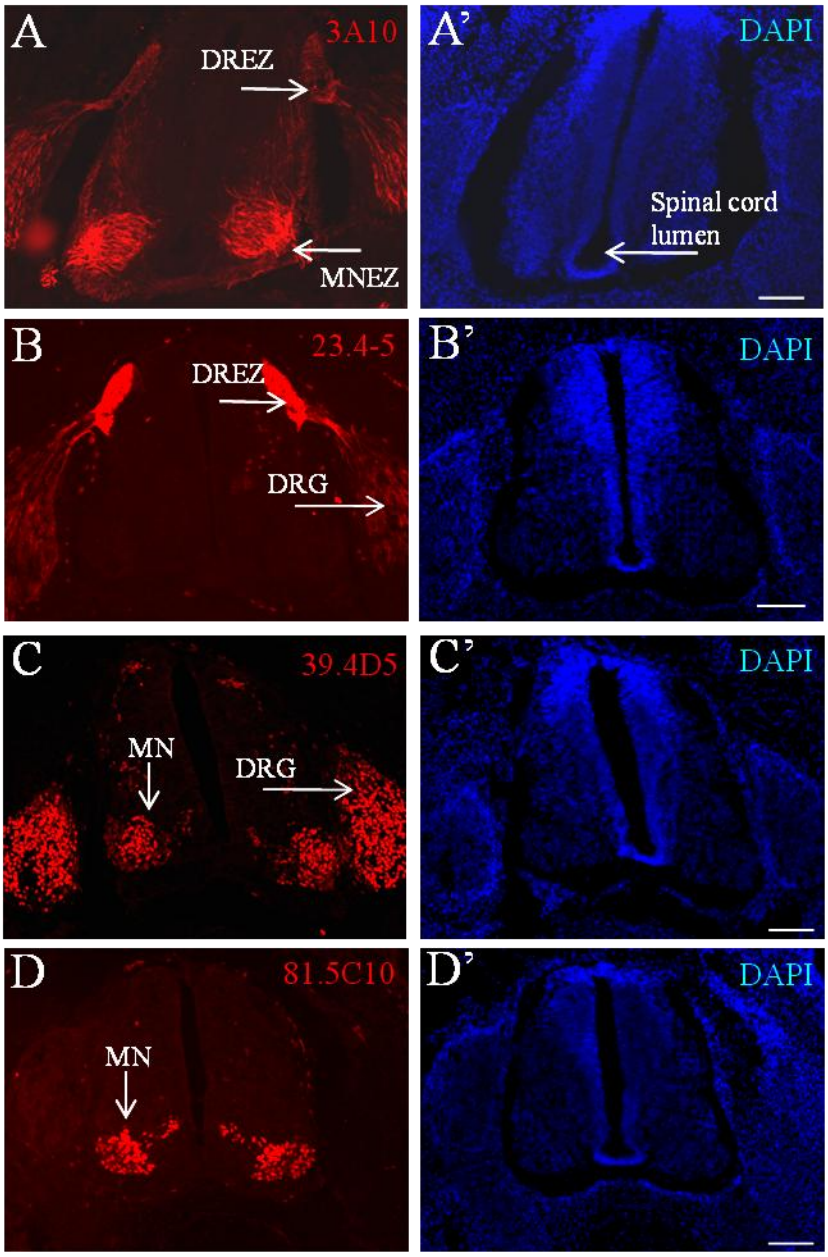

Figure 3.5: Labeling trajectories using antibodies.
A. Neuronal trajectories marked using an antibody against neurofilament associated antigen. Dorsal Root Entry Zones (DREZ) and the Motor Neuron Exit Zone (MNEZ) were labeled, **B.** Staining for cell adhesion molecule Axonin-I. DREZ and Dorsal Root Ganglia can be seen. **C.** Transcription factor Islet1 and Islet2 positive cells stained using 39.4D5 antibody. Motor Neuron (MN) and DRG cell nuclei were labeled. **D.** Motor neuron cell bodies were labeled using an antibody against HB9 trancription factor. **A'-D'.** DAPI staining for respective sections. Scale bar 100µm.

3.2.4 Primary neuronal cultures

It was important to establish a primary neuronal culture system which would allow analysis of cell biological aspects of the growth cone motility using high resolution imaging. Primary spinal neurons were successfully cultured for up to 48 hours. The developmental stage at which these neurons were dissected was found to be important for the health of the cultures. Spinal cultures from early stage embryos (before HH stage 22/23) were found to contain a lot of non-neuronal cells which overcrowded the cultures. This is largely because the patterning of the spinal and vertebral tissue is still ongoing. The patterning process involves migration of different cell types and segregation of the tissues. If the segregation is not complete, the isolated spinal cords contain cells from the surrounding tissue that interfere with the analysis of free growth cones in the culture plate. Late stage embryos (HH 27 and above) were difficult to dissect as by this stage the vertebral column has undergone closure from the dorsal side and the calcification of the vertebrae has begun. This restricts easy access to the spinal cord. The spinal tissue can still be isolated by breaking away the vertebral column, but in doing so the adjacent tissue needs to be carefully separated to avoid the carry over to the cultures. An absolutely pure culture of the spinal neurons is not practically achievable as the spinal cord contains other cell types like the glia and even within the neuronal population, there are various sub-types like the motor, sensory and the interneurons. Nonetheless, cultures obtained from stage 23 to stage 26 have a higher neuronal population with minimal fibroblast contamination. In addition the cultures obtained from these stages were healthier as compared to the other stages. For all subsequent experiments spinal neurons from Day 5 embryos (stage 26/27) were used (Figure 3.6, below).

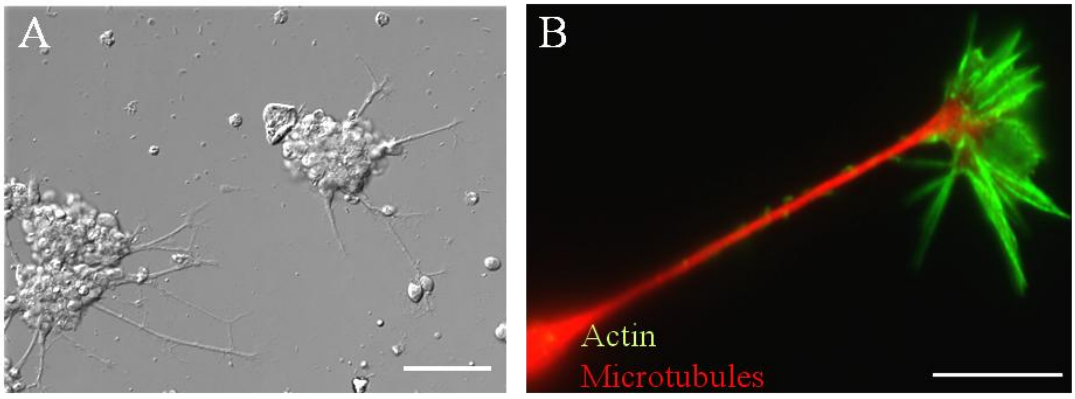

Figure 3.6: Primary neuronal cultures from the spinal cord.
A. DIC micrograph of explant culture of spinal neurons. The cell bodies are clumped together and axons growing outwards with the growth cones at the tip. B. Immunostaining for the growth cone marking the actin and microtubule cytoskeletal components using phalloidin and anti-tubulin antibody respectively. Scale bar 10μm.

3.2.5 Transfecting primary neurons

Expression of the desired proteins in the growth cone was achieved using plasmid electroporations in a cuvette. This method of transfecting the primary neurons was important not just for over-expression studies but also for the knockdown studies where morpholinos were electroporated in the primary neurons. A plasmid expressing monomeric GFP tagged to actin was co-transfected with the morpholino. In addition, morpholinos were fluorescently tagged to allow identification of the transfected neurons under the microscope (Figure 3.7, below). This allowed fluorescent imaging of the growth cones since the morpholino signal was found to be weak and sub-optimal for long term live imaging.

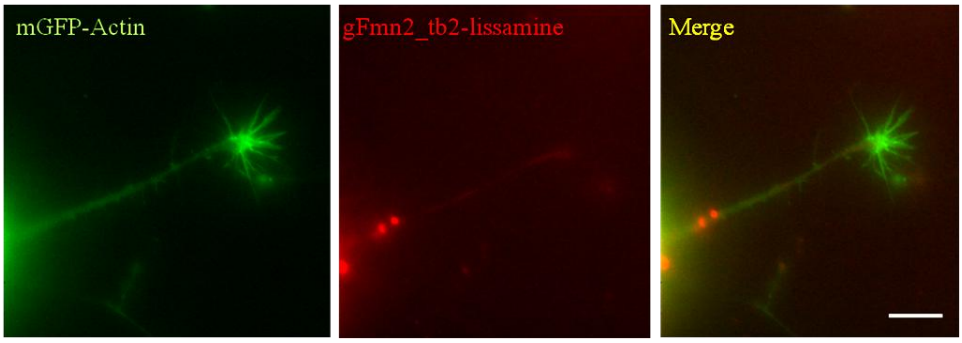

Figure 3.7: Transfections in primary spinal neurons.
Expression of mGFP-actin could be seen 24 hours post transfections. The cells that recieved the morpholino were marked by the fluoroscent tag on the morpholino. Scale bar 10μm.

3.3 Summary and Discussion

The tools necessary for analyzing the neuronal trajectories in the spinal cord were established in the lab. These included the ability to successfully electroporate desired reagents in the spinal cord and labeling the commissural neuron trajectories using enhancers/lipophilic dyes. This ability was crucial for the further studies, as marking the neuronal trajectories is the first step towards understanding the role of the genes of interest in the establishment of these trajectories. In addition, primary cultures of spinal neurons were successfully established in the lab which formed the basis of all the cell biological studies described later.

3.4 Materials and Methods

3.4.1 *In ovo* electroporations

The injections were done at stage 14/15. The eggs were kept horizontal on holder made out of packing foam. A small piece of sticky tape was put on the egg shell to avoid cracking of the eggs during the windowing procedure. Using an 18 gauge needle attached to a 5ml syringe, a small hole was punched near the pointed end of the egg. Through this opening, 10-12 ml of the thin albumin was removed from the egg to avoid spilling over during windowing. Using a pair of

scissors, a window was cut on the top of the egg big enough to reach the embryo with the injection needle and the electrodes. The DNA/morpholino solution was loaded in to glass capillaries pulled in to fine needles (5-10μm bore diameter). This needle was attached to the injector tubing that used nitrogen gas for injections. The injection pressure and time was adjusted according to the bore size of the needle. The DNA solution was injected in the spinal cord lumen until the spinal cords was completely filled. 0.1% fast green dye was added to the DNA solution to allow visualization during the injection procedure. When using morpholinos, the addition of the dye was avoided since the morpholino was fluorescently tagged and this made the morpholino solution visible without any addition of the dye. The electrodes were placed along the spinal cord and the pulse was applied using the desired settings. The time between the injection and the electroporation pulse was critical as a long period between the two leads to diffusion of the DNA/morpholino solution out of the spinal cord and the amount available for electroporation was reduced. Also the diffusion out of the lumen leads to undesired electroporation of the DNA/morpholino in the tissue surrounding the spinal cord. Following the electroporation, 1ml of DMEM+1x PenStrep was added on top of the embryo to prevent contamination during the incubation period. The windowed egg shell was taped back on to the egg and the egg was put back in the incubator for further incubation till the desired stage of development was reached.

3.4.2 Embedding, Cryosectioning and immunohistochemistry

The embryos were dissected out in PBS and fixed in 4% Paraformaldehyde (PFA) at 4°C overnight. The next day, the PFA was washed off using three washes of PBS, 30 minutes each at room temperature on a rocker. This was followed by a gradient of sucrose in PBS (10%, 20% and 30%). Each of the sucrose treatments was done till the embryo sank down to the bottom of

the vial. After the 30% sucrose treatment, the embryo was embedded in to the embedding and cutting medium OCT. A layer of OCT was added to a boat made out of aluminum foil and allowed to freeze at -20°C. Before the top of the OCT layer froze, the embryo was removed from the 30% sucrose solution and placed on the OCT layer. The orientation of the embryo was adjusted carefully under a stereo microscope and additional OCT was poured on top of the embryo until it was covered completely. The embryo was allowed to freeze in the OCT at -20°C for at least 30 min before moving on to the sectioning procedure. The embedded block was trimmed from the caudal end till the hind limb region. From here onwards, 10µm thick sections were collected on poly-l-lysine coated slides until the forelimb region was completely sectioned. Thus transverse sections of only the region between the hind limbs and the fore limbs were collected. The sections on the slide were allowed to air dry and the slides were stored at -20°C till further processing.

For immunohistochemistry, the slides were removed from -20°C and allowed to stand at room temperature for 15-20 min till the moisture evaporated. The sections were washed thrice, 10 minutes each with PBST (PBS+0.1%Triton-X 100) to remove the embedding medium. 250µl solution was sufficient to cover the entire slide surface. This also served as a permeabilization step. 5% normal goat serum in PBS was used as a blocking agent and the sections were incubated in this solution for 1 hour at room temperature. Blocking was followed by incubation with the primary antibody at 4°C overnight. The antibody dilutions were made in blocking solution. Next day the primary antibody solution was removed and stored for reuse. The slides were washed thrice with PBST, 10 minutes each. This was followed by a second blocking step. The secondary antibody was diluted in the blocking solution and added on the slides at room temperature. Secondary antibody incubation was done for 1 hour at room temperature. Finally

the slides were washed thrice with PBST. 20µl mounting medium (20mM Tris-HCL, pH-8.0 and 0.5% propyl galate in 90% glycerol) was spread on the slide carefully and the coverglass was mounted gently without air bubbles. The excess mounting medium was cleaned with a tissue paper and the coverglass was sealed using transparent nail polish. The slides were stored at 4°C until imaging.

All the antibodies from DSHB were procured in supernatant form and used in the range of 1:10-1:50 dilution. All secondary antibodies were used at 1:1000 dilution.

3.4.3 Open-book preparation and DiI labeling

Stage 22-26 embryos were used for the open-book preparations. The embryos were pinned down dorsal side up in PBS on a Silgard plate and using two sharp needles a shallow incision was made right along the midline. When the lumen of the spinal cord was exposed, two additional incisions are made on either wide of the spinal cord to separate the spinal tissue from the dorsal root ganglia (DRGs) and surrounding vertebral tissue. By sliding the flat end of the needle below the floor plate of the spinal cord, the spinal cord is separated from the vertebral tissue at the bottom. After the spinal cord is completely free it can be seen floating in the buffer. The spinal cord was pinned down on to the silgard using pins placed as far as possible from the midline with the luminal side facing up. The tissue was fixed using 4% PFA for 30 minutes and washed thoroughly with PBS to remove traces of PFA.

For the labeling, 1mM DiI solution in methanol/chloroform was used. Under a stereo microscope, a small amount was loaded in the glass needle used for *in ovo* injections. The needle was connected to rubber tubing and a small amount of the dye was injected using mouth pipetting. Under the stereo microscope, the cell bodies in the outer one-third of the open book preparation were targeted for injections. The injections were made at regular intervals along one

side of the spinal cord. The site of injection was visible under the microscope as the DiI solution is colored. Multiple spinal cords were processes in the same plate and the plate was covered with aluminum foil. The samples were stored at 4°C for up to a week and checked every day to assess the diffusion of the dye. Usually by the third day the entire commissural neuron trajectory was labeled and no further labeling was observed on the subsequent days.

3.4.4 Primary neuronal cultures from the spinal cord and transfections

Day 5/6 embryos were used for the spinal neuron cultures. The embryos were pinned down dorsal side up in PBS on a Silgard® plate and using two sharp needles a shallow incision was made right along the midline. When the lumen of the spinal cord is exposed, two additional incisions are made on either wide of the spinal cord to separate the spinal tissue from the dorsal root ganglia (DRGs) and surrounding vertebral tissue. By sliding the flat end of the needle below the floor plate of the spinal cord, the spinal cord is separated from the vertebral tissue at the bottom. After the spinal cord is completely free it can be seen floating in the buffer.

The entire spinal cord is transferred to 500µl of 0.05%Trypsin-EDTA in a 1.5ml tube and incubated at 37°C for 25-30min. Trypsin is removed and replaced with 500µl culture medium which contained 10% FBS, 1x PenStrep and 2mM L-glutamine (optional if L-15 already contains L-glutamine) in L-15 phenol red free medium to stop the trypsin action. The tissue is pelleted down by centrifuging at 3000 rpm for 5min at room temperature. The tissue is resuspended in 100µl of Optimem and is gently triturated by passing it through a 200µl tip until a uniform cell suspension is obtained. The cell density after trypsinization ranges from $2x10^5$ to $5x10^5$ depending on the amount of tissue successfully harvested. The cell suspension is then distributed equally in 4-5 30mm sterile cover-glass bottom culture dishes with 2ml culture medium. The dishes are transferred to a humidified 37°C incubator without CO_2.

For transfections, cells were resuspended in 100µl Optimem after trypsinization. The cell density was kept in the range of $2x10^5$ cells. The DNA/morpholino (10µg plasmid DNA and 10-100nM morpholino) was added to the cell suspension and mixed gently by tapping. The cell suspension along with the DNA/morpholino was transferred to the electroporation cuvette and the electric pulse was applied using the following parameters.

Poring pulse:		
Voltage (V)	-	125
Pulse length (msec)	-	5
Pulse interval (msec)	-	50
Number of pulses	-	2
Decay rate (%)	-	10
Polarity	-	+

Transfer pulse:		
Voltage (V)	-	20
Pulse length (msec)	-	50
Pulse interval (msec)	-	50
Number of pulses	-	5
Decay rate (%)	-	40
Polarity	-	+/-

Additional 400µl Optimem is added to the cuvette and the cells are allowed to recover for 5 min at 37°C in the incubator. After this the cell suspension is added to culture plates as done during regular cultures. Next morning the medium is replaced with fresh culture and cells are placed back in the incubator until the imaging time. This removes the free floating fluorescently labeled morpholino which hinders the background free imaging and also removes the debris in the culture plate.

3.4.5 Fixation and immunostaining of growth cones

After 24-48 hours after plating, the cells were briefly washed with PBS to remove the debris. The PBS wash is quick to avoid growth cone collapse due to osmotic shocks during the fluid changing process. This was quickly replaced with the fixative (4% Paraformaldehyde+0.05% gluteraldehyde in 1xPBS). Fixation was allowed for 10 minutes at room temperature followed by three washes of PBST, 10 minutes each for washing away the fixative and also permeablize the cells. Blocking was done using 3% BSA in PBS for 1 hour at room temperature. Desired primary antibody was diluted in the blocking solution and added to the cells. Primary antibody incubation was done overnight at 4°C. Next morning the primary antibody solution was washed using three PBST changes. Additional blocking was done using 3% BSA in PBS for 1 hour at room temperature. This was followed by the secondary antibody or phalloidin incubation for 1 hour at room temperature. Phalloidin was used at 1:100 dilution from and anti-tubulin antibody (DM1A, Sigma) was used at 1:5000. While comparing data sets across experiment, the antibody dilution and incubation times were kept constant.

4 ENRICHMENT AND ROLE OF FMN2 IN THE DEVELOPING SPINAL CORD

4.1 Introduction

Cappuccino (Capu), the *Drosophila* ortholog of Fmn2 was first described as maternal effect a gene which was related to the vertebrate limb deformity locus. Capu was found to be important for establishment of egg and embryo polarity in *Drosophila* (Emmons et al., 1995) and later for meiotic spindle positioning in mice (Leader et al., 2002). Further studies showed that Fmn2 is enriched in the developing central nervous system in mouse embryos (Leader and Leder, 2000) but later studies showed that this enrichment is not restricted to the nervous system (Leader et al., 2002). When $Fmn2^{-/-}$ males and $Fmn2^{+/-}$ females were mated together, fertility seemed to be normal as these mice produced an average litter size similar to that from wild-type parents. When mated to either $Fmn2^{+/+}$ or $Fmn2^{-/-}$ males, $Fmn2^{-/-}$ females did not produce any offspring that survived to weaning age (Leader et al., 2002). Further analysis showed that $Fmn2^{-/-}$ females were sub-fertile and ovary transplantations could rescue this defect. However, $Fmn2^{-/-}$ mice had neither gross abnormalities of the central nervous system, nor histological differences in brains when compared with $Fmn2^{+/+}$ mice. Recent studies though hint towards the importance of Fmn2 in the nervous system. Epigenetic studies revealed that altered histone signatures at Fmn2 lead to age-dependent memory impairment in mice and the lack of Fmn2 altered the dendritic spine morphologies in the hypocampus (Peleg et al., 2010). Moreover, mutation in Fmn2 has been linked to dendritic morphology and intellectual disability in humans (Law et al., 2014).

Thus it seems that Fmn2 could play an important cellular role in the fine scale organization of the nervous system may be indirectly through its ability to influence the actin architecture inside the neurons.

4.2 Results

4.2.1 RNA *in situ* hybridization for Fmn2 transcript

cDNA clones were selected from the BBSRC chick EST library (http://www.chick.manchester.ac.uk/) based on similarity with Fmn2 transcript. Two EST clones were identified, ChEST691l18 and ChEST709h8. Both the clones were reported to be expressed in the chicken ovaries. ChEST691l18 was located in the extreme 3' end of the coding sequence running in to the 3'UTR of the gFmn2 transcript (Figure 4.1, below) which prevented the detection of the conserved domains in the formin family. Using the ChEST691l18 EST clone, RNA probes were made and used for *in situ* hybridization on Stage HH21-25 whole embryos. The EST Fmn2 transcript was seen to be enriched in the spinal cord (Figure 4.2A and B, below).

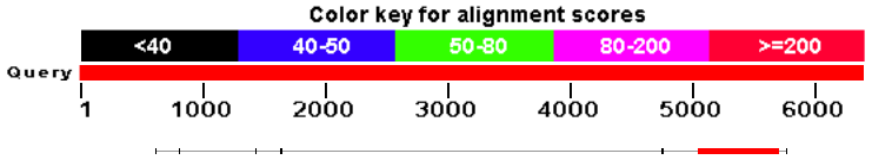

Figure 4.1: Alignment of the EST clone with the Fmn2 mRNA.
The alignment of the EST using BLAST showed that the EST overlapping with the extreme 3' end of the coding sequence and the 3'UTR of the mRNA. The coding sequence ended at nucleotide 5292 in the mRNA.

The results obtained from the RNA *in situ* hybridizations were not conclusive as a fair bit of staining was observed throughout the embryo. This staining was clearly not a technical error as the procedural control probe for FGF8 transcript gave a clean staining pattern as expected. Further, the control reactions using the sense strand as a probe were found to be clean with

minimal background staining. The signal from the Fmn2 probe was not as distinct as the FGF8 probe (Figure 4.2C and D, below) which suggested that either Fmn2 did not have a clean step gradient in the expression pattern or the sensitivity range of the technique did not allow us to detect small changes in the enrichment. Therefore, we decided to analyze the transcript enrichment using a more sensitive technique of quantitative real-time PCR (pRT-PCR).

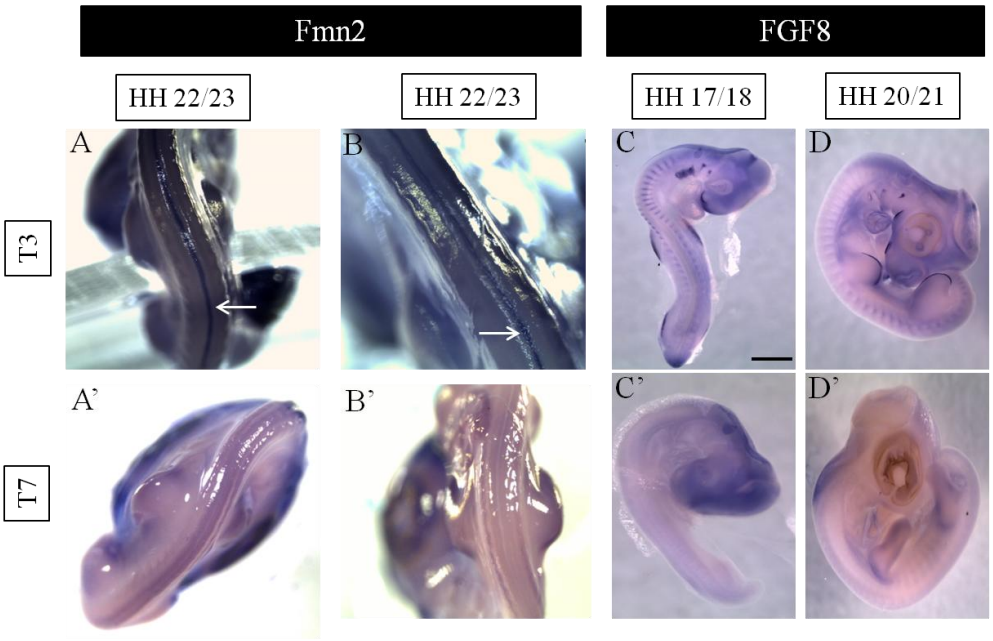

Figure 4.2: RNA in situ hybridization.
A. and B. Signal from Fmn2 antisense probe used for hybridization. The signal was seen along the spinal cord (arrows). **C. and D.** antisense probe for FGF8 used as a procedural control. The signal was detected at the somites and the tips of the limb buds. **A'-D'.** Sense strand probe controls for respective genes. (T3-antisense probe, T7-sense probe)

4.2.2 Enrichment of Fmn2 transcript in developing chick embryo

qRT-PCR analysis showed that Fmn2 transcript was enriched in the spinal cord as compared to other tissues examined. Tissues like the heart, lungs, and liver showed low abundance of the Fmn2 transcript whereas tissues like the brain and the spinal cord were enriched for Fmn2 transcript. The enrichment in the spinal cord was up to 4-times higher than the brain (Figure 4.3, below). The enrichment was not exclusive to the CNS and other tissues

were also seen to express Fmn2 though in much lower amounts. The observation that Fmn2 is enriched in the central nervous system (CNS) was in accordance with the earlier reports in the literature which used RNA *in situ* hybridization to map the expression pattern of the Fmn2 transcript in the developing mouse embryos.

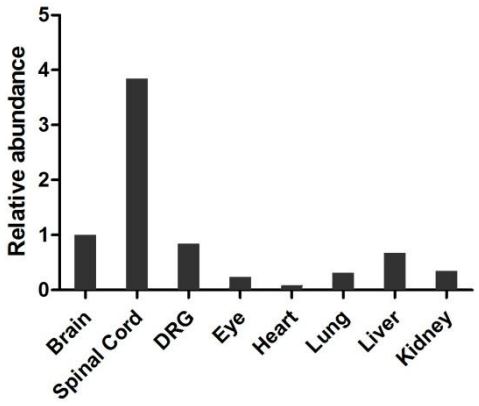

Figure 4.3: Enrichment of Fmn2 transcript in different tissues.
qRT-PCR analysis showing the levels of Fmn2 transcript in various tissues from Day 6 embryo. The data represents the mean of two independent quantifications with three technical replicates in each.

The qRT-PCR analysis has been reproduced independently in our laboratory (Ketakee Ghate, unpublished data) and found to be consistent with the above observation. In addition, the enrichment of other actin nucleators in addition to Fmn2 was studied during HH14 to HH26, the developmental window of commissural neuron outgrowth and midline crossing. It was seen that Fmn2 levels were sustained during the development of commissural neurons in the spinal cord whereas the levels of other actin nucleators dropped suggesting a role for Fmn2 during the developmental window from HH14 to HH26 (Ketakee Ghate, unpublished data).

4.2.3 Fmn2 depletion leads to failure of midline crossing by the commissurals

Axonin-I is a cell adhesions molecule responsible for mediating the midline crossing by the commissural neurons. During early development the commissural neurons express Axonin-I in

high amounts to navigate their way towards the midline. After encountering the midline, Axonin-I is no longer required by the commissural neurons and is down regulated as a result and by stage HH26, the Axonin-I expression on the commissural neurons is reduced (Baeriswyl and Stoeckli, 2008; Fitzli et al., 2000; Milev et al., 1996; Stoeckli and Landmesser, 1995).

Efficiency of two different translation blocking morpholino sequences was tested (Figure 4.4, below) using a custom made antibody against chick Fmn2 (antibody validation discussed in the next chapter). Analysis of the commissural neurons post morpholino treatment revealed that the commissural neurons failed to cross the midline in the Fmn2 morphant embryos. The observation was confirmed using two different techniques- using anti-Axonin-I antibody to mark the commissural neurons in cryosections. Fmn2 morphant embryos were seen to maintain high levels of Axonin-I even at stage HH26. The aberrant Axonin-I staining was seen only on the side of the spinal cord which received the morpholino while the opposite side served as an internal control which did not show this aberrant staining (Figure 4.5, below). This aberrant Axonin-I staining pattern was never observed in the control embryos. This result was supported by the observation that the commissural neurons failed to cross the midline in the Fmn2 morphant spinal cords as opposed to a stereotyped midline crossing in the control morpholino treated embryos, as seen by co-electroporation of commissural neuron specific enhancer Atoh1 to drive a marker fluorophore along with the morpholino (Figure 4.6, below). The failure of the commissural neurons to cross the midline in this case was not absolute. Due to the intrinsic variation during the electroporation, depending on how much morpholino was delivered inside the cells, the degree of this phenotype varied from complete lack of crossing to partial crossing and at times complete crossing. Recent detailed characterization of the phenotype in the

laboratory confirmed that 80% of the Fmn2 morphant embryos showed defective midline crossing (Ajesh Jacob, unpublished data).

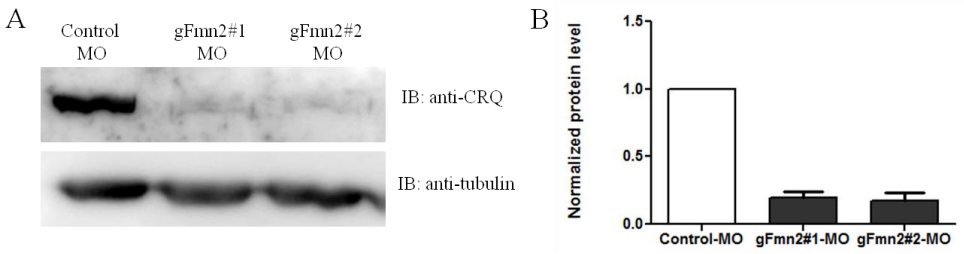

Figure 4.4: Verification of morpholino mediated knockdown.
A. Western blot showing the reduction in Fmn2 protein level as seen by anti-CRQ immunoblotting, tubulin used as loading control. B. Densitometric quantification for the western blot. The data represents mean and standard errors for three independent analyses.

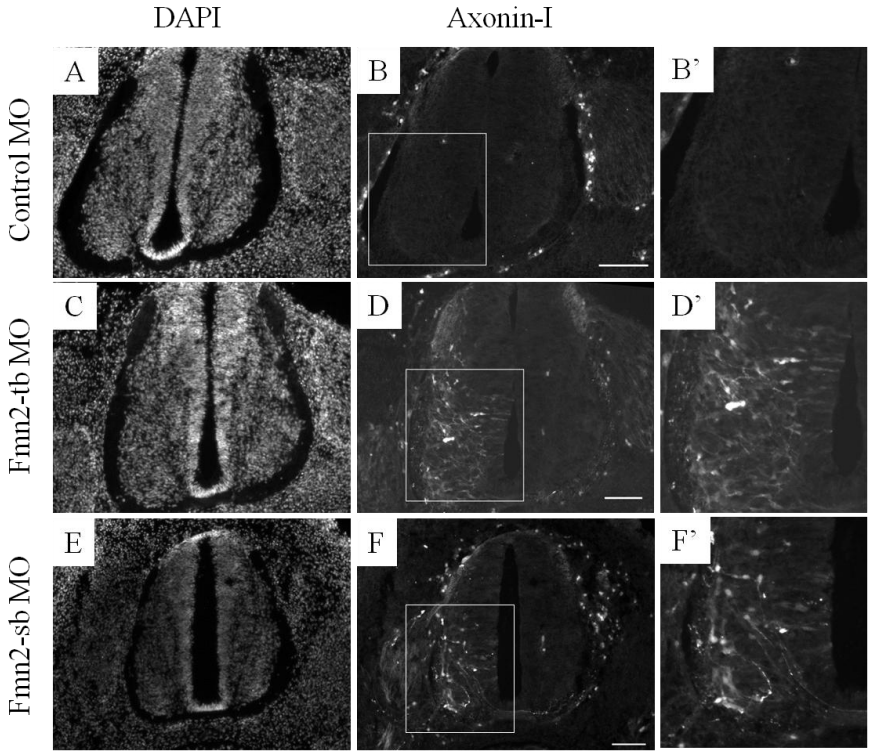

Figure 4.5: Aberrant Axonin-I staining upon Fmn2 depletion.
A, C and E. Transverse sections of the lumbosaccral region of the spinal cords at stage HH26 stained with DAPI. **B, D and F.** Abnormal Axonin-I staining in the Fmn2 morpholino treated spinal cords. **B', D' and F'.** Enlarged regions marked in B, D and F respectively. Axonin-I staining in the boxed regions can be seesn only in the Fmn2 morphant embryos on the side which received the morpholino. Control morpholino treated embryos do not show the Axonin-I expression due to the down regulation following midline encounter. The phenotype was reproducible over three independently transfected embryos.

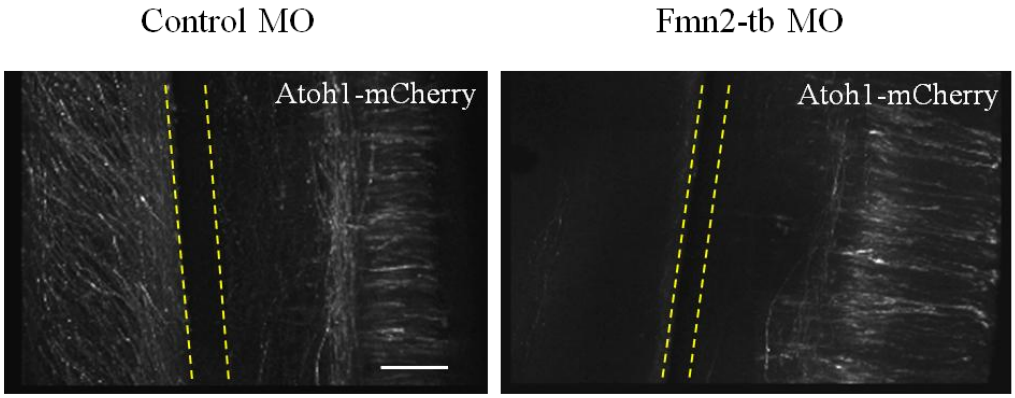

Figure 4.6: Failure of midline crossing by commissural neurons.
Atoh1-mCherry was coelectroporated with the morpholino and the spinal cords were analysed as open-books. The commissural neurons failed to cross the midline in the Fmn2 MO treated embryo as opposed to the Control MO treated embryos which showed the characteristic rostral sigmoid trajectories post-crossing. Scale bar 100μm.

4.3 Summary and Discussion

Using RNA *in situ* hybridization and qRT-PCR analysis, Fmn2 was seen to be enriched in the central nervous system. Fmn2 was seen to be differentially expressed even within the central nervous system with up to 4 times higher expression levels in the spinal cord as compared to the brain. Depletion of Fmn2 from developing spinal cord resulted in midline crossing failure by the commissural neurons. The requirement of Fmn2 was seen to be cell autonomous and conserved during evolution, as introduction of the mouse ortholog of Fmn2 only in Atoh1 positive neurons could rescue the midline crossing errors (Ajesh Jacob, unpublished data). Since Fmn2 is an actin nucleator, we hypothesized that the failure of midline crossing by the commissural neurons was a result of slower growth of axon due to perturbation of the actin polymerization machinery at the growth cone. The possible cell biological explanations in support of this hypothesis were investigated in the subsequent chapters.

4.4 Materials and Methods

4.4.1 RNA probe synthesis and hybridization.

The following components were mixed at room temperature in a PCR tube and incubated at 37°C for 2 hours. All the solutions were prepared in DEPC treated water.

5X Transcription buffer	-	4 µl
DIG-labeled Nucleotide mix	-	2 µl
RNase inhibitor	-	0.5 µl
T3/T7 polymerase	-	0.25 µl
DNA template	-	3 µl
DEPC-water to	-	20 µl

1 µl RNase free DNaseI was added to this reaction and incubated at 37°C for 15 min and reaction was checked for transcription by running 1 µl on a 1% agarose gel. For precipitation, 100µl TE pH8.0, 10µl 4M LiCl and 300µl ethanol were added to the reaction and the reaction was incubated overnight at -20°C. The probe was pelleted by spinning the tubes at 12000 rpm for 10min at 4°C. The pellet was washed with 500µl of 70% ethanol, air dried for 5min and dissolved in 50µl TE pH8.0 and 50µl of hybridization buffer. Probe was stored in 50 % hybridization buffer for few weeks at -80°C.

Hybridization

Embryos of desired stage were harvested and washed in PBS. Embryos were fixed in fresh 4% paraformaldehyde in PBS overnight at 4°C. Embryos were subjected to dehydration using a graded methanol/PBT series (25%, 50%, 75%, 100% methanol) by allowing embryos to rock gently at room temperature for 30 minutes in each wash solution. Dehydrated embryos were stored for up few weeks (not more than a month) at -20°C.

Day 1: Prehybridization and Hybridization

Embryos were rehydrated in a methanol/PBT series (75%, 50%, 25%, PBS) 30 minutes each. If necessary, the embryos were bleached with 6% hydrogen peroxide in PBT for 1 hour at room temperature with gentle rocking. (Note: bleaching time can be reduced or extended if desired.) Embryos were washed with PBT thrice, 10 minutes each. Embryos were treated with Proteinase K diluted in PBT to different concentrations depending on their embryonic age according the following guideline. (Incubation times in Proteinase K have to be optimized to achieve proper permeabilization).

Stg 14: 2.5 ug/ml	for 20min
Stg 18: 5 ug/ml	for 20min
Stg 22: 8 ug/ml	for 20min
Stg 25: 15 ug/ml	for 20min
Stg 26: 20 ug/ml	for 20min
Stg 28: 30 ug/ml	for 20min
Day7/8: 60ug/ml	for 20min
Day10: 120ug/ml	for 20min

Two washes 5 minutes each with PBT were given. Embryos were postfixed with 4% Paraformaldehyde (PFA) and 0.2% glutaraldehyde in PBT for 20 minutes at room temperature followed by two PBT washes minutes each. Embryos were subjected to a 10 minute wash in a 1:1 mixture of hybridization solution/PBT followed by a 10 minutes wash in hybridization solution and incubated at 70°C in hybridization solution for at least 1 hour. Old hybridization solution was replaced with fresh hybridization solution with the RNA probe (we used the total probe generated in a transcription reaction of 20µl or half of it and incubate overnight at 70°C (This incubation temperature has to be optimized depending on the sequence characteristics and probe length).

Day 2: Post-hybridization washes, blocking, and antibody incubation

Embryos were washed thrice for 30 minutes each at 70°C in prewarmed solution-I and thrice in prewarmed solution-III for 30 minutes each at 65°C. Embryos were washed thrice with fresh TBST for 5 minutes each at room temperature and blocked by incubating in 10% HIGS in TBST for at least 1hr at RT. Blocking solution was removed from embryos and anti-DIG AP conjugated antibody at 1:5000 dilution in TBST with 1% HIGS). Embryos were incubated in the antibody solution overnight at 4□C.

Day 3: Post-antibody washes

Embryos were washed thrice for 5 minutes each with TBST at room temperature followed by five TBST washed for 1 to 1.5 hours each at room temperature. A final TBST wash was given to the embryos overnight at 4□C with gentle rocking.

Day 4: Color development

Embryos were washed thrice in NTMT for at least 10 minutes each at room temperature. After removing NTMT, reaction mix (125 □g/ml BCIP and 250 □g/ml NBT in NTMT) was added and the reaction was allowed to proceed at room temperature with gentle rocking. Throughout the development reaction, the samples were kept covered with aluminum foil to protect them from light and checked periodically to monitor the progress of the reaction. When the reaction was judged complete, the embryos were washed with PBS or PBT and postfixed in 4% PFA/ 0.1% glutaraldehyde for 10 minutes followed by three washes with PBS 5 minutes each.

4.4.2 cDNA preparation and qRT-PCR

Total RNA was isolated from the tissues using TRIZOL. The tissue was crushed in 500µl TRIZOL. Additional 500µl TRIZOL was added and the tube was vortexed for 10 seconds to disrupt the tissue. 200µl chloroform was added to the tube and further vortexed for 10 seconds. This formed a uniform emulsion of TRIZOL/Chloroform and the disrupted tissue. The entire mix was allowed to sit at room temperature for 10 minute. The aqueous layer was separated by centrifugation at 12000rcf for 10 minutes at 4°C. The top layer (~500µl) was collected in a fresh RNase free tube and equal volume of isopropanol was added. After mixing the isopropanol, the tube was allowed to stand at room temperature for 30 minutes. The nucleic acids were pelletted down by centrifugation at 10000rcf for 10 minutes at 4°C. The pellet was resuspended in 70% ethanol and re-pelleted by centrifugation at 7500rcf for 10 minutes at 4°C. The supernatant was discarded and the pellet was allowed to air dry. After drying the nucleic acids were resuspended in 100µl of nuclease free water and 1 unit of RNase free DNase was added to degrade the entire DNA that was precipitated along with the RNA. The DNase treatment was allowed for 45 minutes at 37°C. 1µl of the sample was run of 1% agarose gel to verify the degradation of DNA and the integrity of the RNA. This was followed by removal of the DNase by repeating the entire TRIZOL RNA extraction process described earlier to get only the RNA pellet. The RNA pellet was dissolved in 20µl of nuclease free water and stored at -80°C for up to a week.

For the cDNA preparation, 2µg RNA was used. cDNA was prepared using oligo-dT primer and M-MLV RT (Invitrogen) according to the manufacturer's protocol.

Nuclease free water	-	12µl
100µM oligo-dT promer	-	1µl
dNTPs (10mM each)	-	1µl

This mix was heated to 65°C for 5 minutes and snap chilled on ice. After a brief centrifugation to collect the contents, following reagents were added to the above mix.

First strand buffer (5x)	-	4µl
DTT (0.1M)	-	1µl
RNase inhibitor	-	1µl
M-MLV RT	-	1µl

The reaction was mixed gently and incubated at 42°C for 2 hours. This was followed by heating the reaction to 70°C for 15 minutes to inactivate the reverse transcriptase. The cDNA obtained was stored at -20°C for up to two weeks.

The PCR reactoins were set in a 96 well plate with a dilution series (undiluted, 1:2, 1:4, 1:6 and 1:8) for the cDNA was used to plot a standard curve for estimating primer efficiencies for each primer pair. For all the quantification, 1:8 dilution of the cDNA was used. The PCR reaction composition was as follows,

5x master mix	-	5µl
Forward primer (1µM)	-	2µl
Reverse primer (1µM)	-	2µl
cDNA (1:8 dilution)	-	1µl

The reaction was set in a dark room and the plate was heat sealed using a transparent sealing film.

Table 4-1: Primer details for the qRT-PCR.

Primer Name	Location in the CDS	Sequence	Amplicon Length (bp)
RT-gβactin-f (994)	994	TTGCTGACAGGATGCAGAAGGAGA	158
RT-gβactin-r (1152)	1152	ACTCCTGCTTGCTGATCCACATCT	
RT-gFmn2-f(1486)	1486	TCAGCAGCGGATTCTGAGGCTAAA	155
RT-gFmn2-r(1641)	1641	ATGCAAGTCCTCTTGACTGGCTGA	

4.4.3 Morpholino treatment

500μM morpholino was injected in the spinal cord lumen and the elctoporation protocol for whole embryos described in Chapter 2 was followed.

Table 4-2: Details of the morpholinos used.

Morpholino Name	Sequence	Location	Mode of action
gFmn2#1 MO	TGCAATGCAGGCAATAAAAACCGTG	5' UTR (159-183)	Translation blocking
gFmn2#2 MO	CCATCTTGATTCCCCATGATTTTTC	Spans (ATG)	Translation blocking
gFmn2-sb	ACAACCATATAACTTACCTTTTACT	E5-I junction	Splice blocking

4.4.4 Western blotting

Spinal cords were isolated from the electroporated embryos and the electroporated halves from five embryos were pooled together. The tissue was crushed using a motorized mortar and pestle compatible with 1.5ml tubes. The tissue was lysed using RIPA lysis buffer for 30 minutes at 4°C. After the lysis, the debris was separated by centrifugation at 10,000 rpm for 10 minutes at 4°C. The supernatant was carefully removed and collected in a fresh tube. The protein concentration in the lysate was estimated at 280nm using a nanodrop. 20μg protein was loaded per well on 8% SDS PAGE gel.

Post electrophoresis, the proteins were transferred overnight to a PVDF membrane at 30mA current using Tris-Glycine buffer with 0.1% SDS and 20% methanol. The membrane was subsequently blocked with 5% skimmed milk and incubated with 1:200 dilution of the anti-CRQ anti-sera from the VIth bleed overnight at 4°C. This incubation was followed by three washed of PBST (1xPBS+0.1% tween-20) 10 minutes each and secondary antibody incubation for 1 hr at

room temperature. Secondary antibody was washed away using PBST, three washed 10 minutes each. The blot was visualized using Millipore western developer reagent on a CCD based imaging system.

4.4.5 Cryosectioning and immunohistochemistry

The procedure described in Section 3 was followed. Axonin-I antibody was used at 1:10 dilution.

4.4.6 Commissural neuron labeling and open book preparations

Electroporations in the spinal cord were done as described in Section 3. After the required time of incubation post electroporations, open book preparations were done as described in Chapter 2. Images were acquired on a confocal system. The entire Z-stack was compressed in to a maximum intensity projection for representation.

5 FMN2 IN GROWTH CONE MORPHOLOGY AND DYNAMICS

5.1 Introduction

Precise neuronal connections are a result of efficient growth cone motility and path finding. Thus understanding the role of Fmn2 in the process of growth cone motility becomes important to understand the behavior of axons *in ovo*. Using primary neurons from the spinal cords of developing chick embryo, we analyzed the effect of morpholino mediated Fmn2 depletion on the growth cone morphology and motility *ex vivo*.

5.1.1 Growth cone motility

Growth cone motility has been divided into three distinct stages- protrusion, engorgement and consolidation (Dent and Gertler, 2003) (Figure 5.1, below). When a growth cone encounters a favorable growth cue, the intracellular signaling cascade prepares the assembly of the molecular clutch (described in the main introduction) linking the actin cytoskeleton to the ECM in the P-domain. The resultant attenuation of the F-actin retrograde flow enables anchoring of the plasma membrane at these locations while the actin polymerization continues at the leading edge. Thus the existing P-domain is converted to the new C-domain and a new P-domain is created. This completes the protrusion phase. In engorgement phase, the actin filaments between the peripheral adhesions and the C-domain because of severing of the actin filaments after the clutch strengthening. MTs from the C-domain enter the site of new growth and provide the stability. Finally the proximal part of the growth cone undergoes compaction adding to the axon shaft resulting in consolidation.

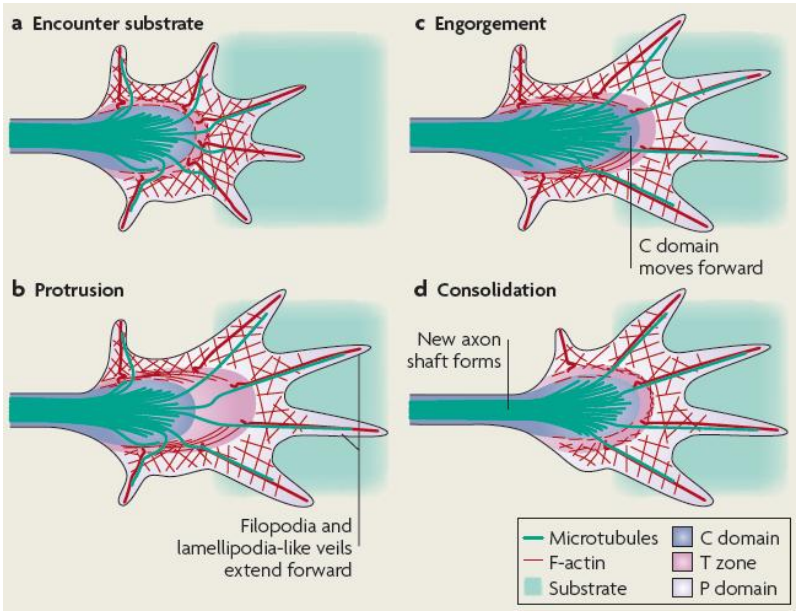

Figure 5.1: Stages of growth cone motility.
The growth cone undergoes repeated cycles of engorgement, protrusion and consolidation as it moves forward. Adapted from (Lowery and Van Vactor, 2009).

5.1.2 Point contacts in growth cones

Motility of the growth cone depends on stable anchorage to the ECM via the integrin receptors. Stable adhesions to the ECM in turn promote stabilization of filopodia and lamellipodia. Stable adhesions act as positive growth regulators and thus promote neurite elongation. Integrin engagement promotes a multi-molecular assembly of adaptor proteins and signaling proteins (Geiger et al., 2009). Growth cones do not exhibit large focal adhesions like non-neuronal cells but rather have small point contacts distributed throughout the growth cone (Robles and Gomez, 2006). The molecular markers for these point contact are similar to the ones found in focal adhesions of the non-neuronal cells (Renaudin et al., 1999). The point contacts essentially serve the same purpose as the focal adhesions. They are the sites of coupling between the intracelluar cytoskeleton and the ECM the only difference being in the size of these marcomolecular assemblies and hence the amount of traction force generated at these sites.

Signaling proteins like FAK have been shown to be important for the growth cone to respond to a chemotropic cue by modulating the intracellular signalling to promote turning towards an attractive cue (Myers and Gomez, 2011). FAK is auto-phosphorylated at Y397 upon integrin tethering (Shi and Boettiger, 2003) and is an important step for subsequent downstream signaling which is necessary for stabilization of leading edge focal adhesions (Tomar et al., 2009). Attractive response of the growth cone to Netrin-1 is known to work via the FAK mechanotransduction pathway (Moore et al., 2012). The cell biological functions of FAK ultimately impact the process of axon guidance as reported in the retinotopic mapping of neurons (Woo et al., 2009) and commissural interneurons (Robles and Gomez, 2006).

This shows that the cell biological deficiencies in the process of motility have significant *in vivo* manifestations leading to axon guidance errors.

5.1.3 Importance of Filopodia in the growth cone motility and axon guidance

Filopodia are finger like structures with a core of bundles F-actin at the centre. Importance of filopodia in growth cone motility and guidance has been studied widely. Growth cones depend on filopodia for motility (Marsh and Letourneau, 1984) and guidance (Bentley and Toroian-Raymond, 1986) *in vivo*. Filopodia have also been shown to the site of intracellular signal initiation (Gomez et al., 2001). Filopodia have been shown to orient towards a guidance cue preceding the actual movement of the growth cone towards the cue (Zheng et al., 1996). In addition to this integrins have been shown to cluster at filopodial tips upon induction with NGF (Grabham and Goldberg, 1997). Filopodia are also important for substrate choice (Gomez and Letourneau, 1994).

Although the importance of filopodia has been undisputedly demonstrated, what remains elusive is the mechanism of filopodia formation. Various actin related proteins have been

demonstrated to be important in the process of filopodia formation in different models (Barzik et al., 2014; Faix, 2008; Goh and Ahmed, 2012; Gonçalves-Pimentel et al., 2011; Johnston et al., 2008; Korobova and Svitkina, 2008; Lebrand et al., 2004; Mellor, 2010; Schirenbeck et al., 2005a; Steffen et al., 2006; Yang et al., 2007). However, neuronal filopodia present a special case where the mechanism of filopodia formation and subsequent growth cone motility remains highly debated (Korobova and Svitkina, 2008; Strasser et al., 2004). Thus the process of filopodia formation seems to be a complex interplay between different molecules and no single molecule can be implicated to be the sole filopodia generator or elongator.

Formins over the years have emerged as one major class of actin nucleators members of which have been studied with respect to their role in filopodial dynamics in non-neuronal cells (Barzik et al., 2014; Dent et al., 2007; Faix, 2008; Goh and Ahmed, 2012; Mellor, 2010; Schirenbeck et al., 2005a; Schirenbeck et al., 2005b; Yang et al., 2007). To test whether Fmn2 could potentially affect the filopodial dynamics and in turn the growth cone motility, we tested the effects of Fmn2 depletion on filopodia, growth cone morphology and motility in cultured spinal neurons.

5.2 Results

5.2.1 Antibody design and assessment of morpholino mediate knockdown of gFmn2

The knockdown efficiency in a particular experiment can be assessed at two levels, the reduction in mRNA using qRT-PCR or the reduction in the protein level using western blots. In our case the first approach was not suitable as morpholinos do not degrade the transcript but instead act like a sequestrating agent which tightly binds to the mRNA and prevents the translation machinery from binding to the mRNA. Thus the transcript remains intact and can still be detected in a PCR reaction. Therefore, the reduction in the protein level was the only way

to assess the knockdown. This required an antibody which faithfully recognized Fmn2 on a western blot.

We tested a few commercially available antibodies like HPA004937 (Sigma), H00056776-A01 (Abnova) and ab72052 (AbCam) generated against the mouse or human ortholog of Fmn2. These antibodies were not found to be satisfactory as they did not detect the desired band at the expected size on the blots and hence it was decided to raise a custom antibody against the chick ortholog of Fmn2 using a peptide sequence. A peptide antibody against the mouse orhtolog was already reported (Kwon et al., 2011). We chose a similar region in the chick ortholog by aligning the two sequences (Figure 5.2, below).

```
Alignment with gFmn2

Query  1630  CRQKKGKSLYNIRPK  1644 -------- chick
             CRQKKGKSLY ++P+
Sbjct  1     CRQKKGKSLYKVKPR  15   -------- mouse
```

Figure 5.2: Sequence alignment for the peptide chosen for antibody generation.
The 15aa peptide sequence towards the C-terminus of gFmn2 was used for the antibody generation.

This region was also checked for surface accessibility and antigenic potential. Both these parameters were found to be satisfactory and hence the region from aa.1632-aa.1646 (CRQKKGKSLYNIRPK) chosen for peptide synthesis and antibody generation in rabbit. Peptide synthesis and antibody generation was done by Bioklone, Bangalore, India. The antibody is referred to hereafter as anti-CRQ.

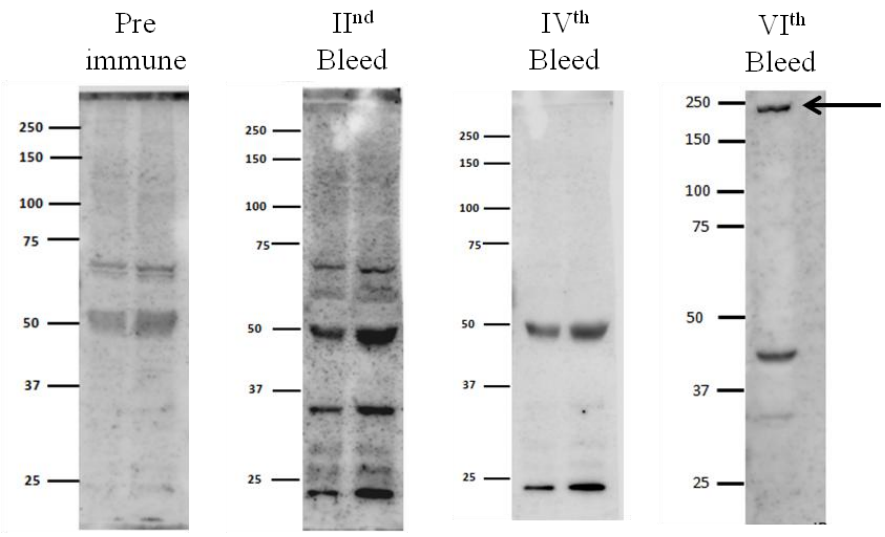

Figure 5.3: Testing the antibody by western blot.
Different bleeds were tested against spinal cord lysates. The VIth bleed detected a band at the expected size on the blot (Arrow).

Antisera from different bleeds were tested on western blot to detect the desired band (Figure 5.3, above). The validity of the antibody was confirmed when the morpholino treated samples showed a reduction in the densitometric analysis of the western blots. The blots showed around 50% reduction in the proteins levels at the population level in cultured spinal cords (Figure 5.4, below). During the electroporation, not all cells of the spinal cord receive the morpholino. Given this limitation of the delivery of the morpholino inside the cells of the spinal cord, 50% reduction at population level would mean a higher reduction at individual cell level.

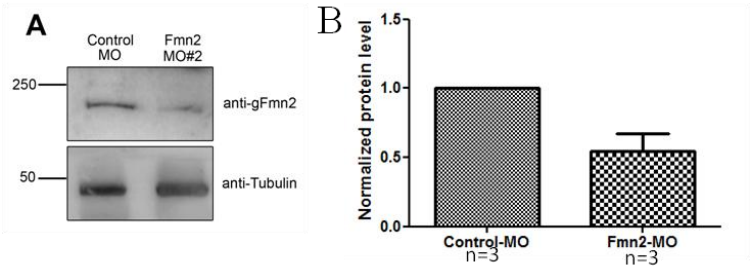

Figure 5.4: Morpholino mediated knockdown of gFmn2 in cultured spinal neurons.
A. Western blot showing the reduction in Fmn2 levels as seen by anti-CRQ immunoblot, **B.** Densitometric quantification for the western blots from three independent set of electroporations. Error bars represent standard error of mean.

5.2.2 Fmn2 localization in the growth cone

The antibody was tested using immunofluorescence on neuronal growth cones from the spinal cords. This revealed the distribution of the endogenous Fmn2 in the growth cone where Fmn2 decorated F-actin bundles in some filopodia as seen by the colabeling with phalloidin. Fmn2 signal was also seen at the tip of some of the filopodia suggesting it might be involved in elongating the actin filaments in the bundle (Figure 5.5A-A"). Quantification of the anti-CRQ signal per unit area of the growth cone revealed a drop in the signal after Fmn2 depletion (Figure 5.6, below).

The localization of Fmn2 to the F-actin bundles in the growth cone was also seen to when the GFP tagged mouse ortholog was overexpressed in the neurons (Figure 5.7, below) suggesting functional and evolutionary conservation between the avian and murine variants of Fmn2.

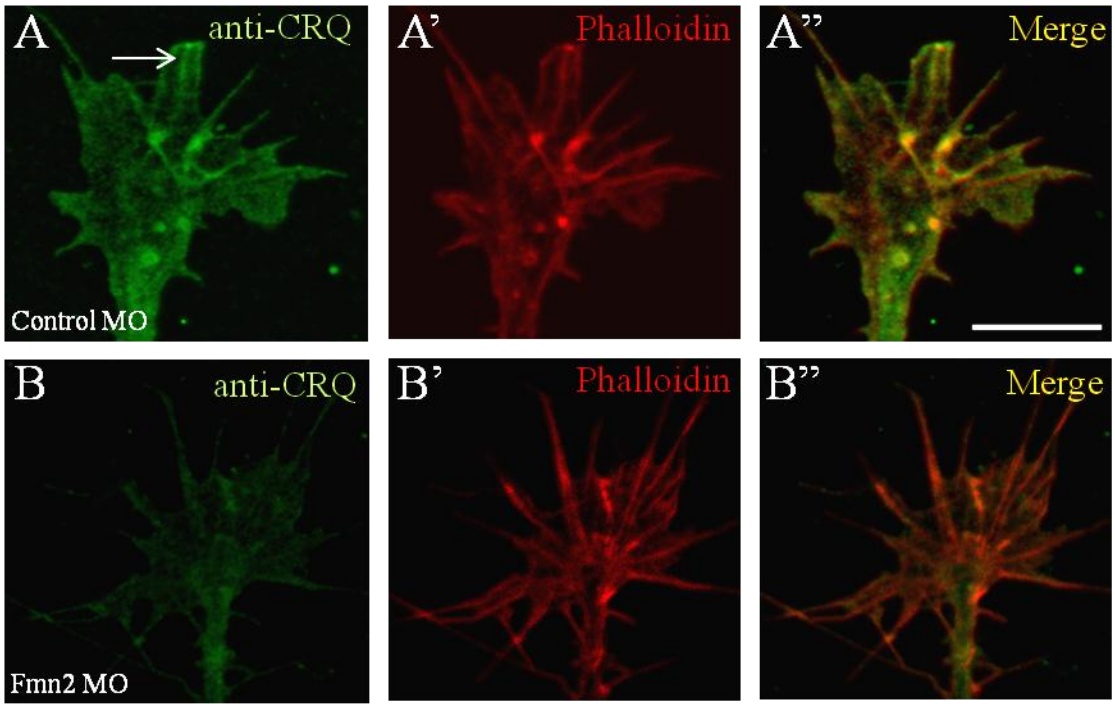

Figure 5.5: Testing the knockdown efficiency by immunostaining.
A. Control MO treated growth cone with endogenous gFmn2 distribution as seen by anti-CRQ immunostaining. Arrow points the bundle like distribution of gFmn2, **A'.** F-actin labelled with phalloidin in the control growth cone, **A".** Control growth cone showing colabeling of F-actin structures with gFmn2, **B.** Fmn2-MO treated growth cone shows reduction in the anti-CRQ staining intensity along, The bundle like distribution is lost, **B'.** F-actin labelled with phalloidin in the Fmn2 morphant growth cone, **B".** Merge image for the Fmn2 morphant growth cone showing loss of gFmn2 staining along the F-actin bundles. Scale bar 10μm.

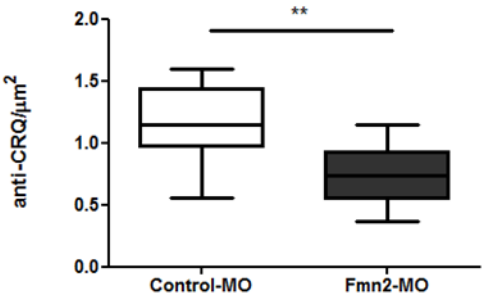

Figure 5.6: Quantification of gFmn2 at the growth cone after the morpholino treatment.
The graph shows reduction in anti-CRQ staining intensity per unit growth cone area as seen by immunostaining after the morpholino treatment. (**, $p<0.01$)

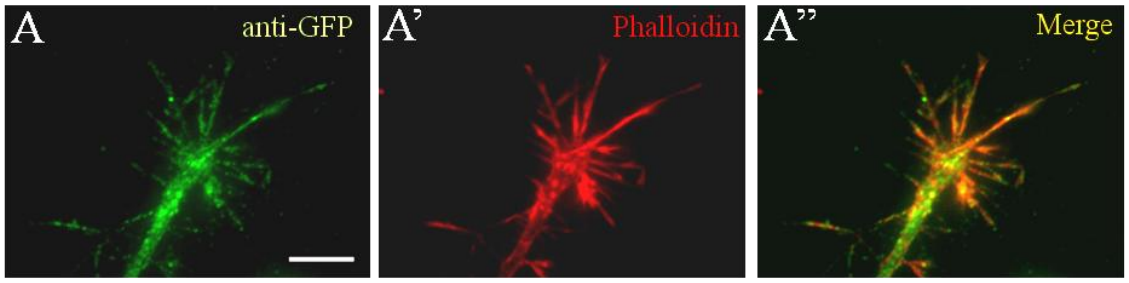

Figure 5.7: Distribution of GFP tagged mouse Fmn2 in the growth cone.
Secondary staining with anti-GFP antibody was used to visualize GFP after fixation. The localization resembles the distribution of endogenous gFmn2 as seen by anti-CRQ immunostaining earlier. Scale Bar 10μm.

5.2.3 Effect of Fmn2 depletion on growth cone area

Transfected growth cones were fixed and stained with phalloidin for imaging. Using the polygon selection tool in Image J, the outline of the growth cone was drawn by hand in the phalloidin channel and the area enclosed was measured. It was seen that Fmn2 depleted growth cones had a significant reduction in the total area of the growth cone (Figure 5.8, below) as compared to the area of the control morpholino treated growth cones.

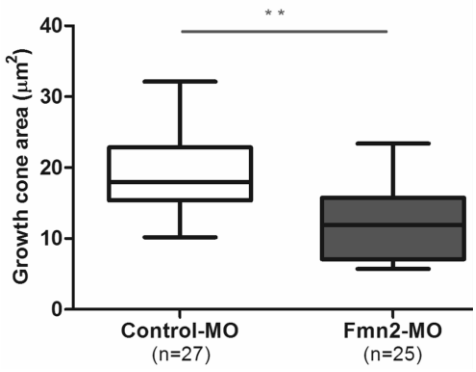

Figure 5.8: Quantification of growth cone area upon Fmn2 knockdown.
Area of the growth cone is seen to decrease significantly upon Fmn2 depletion. (**, p=0.0019).

5.2.4 Effect of Fmn2 depletion on growth cone filopodia

Fmn2 depletion resulted in significant reduction in the number of filopodia per growth cone (Figure 5.9A, below). Fmn2 knockdown also resulted in shortening of the filopodia when compared to control growth cones (Figure 5.9B, below). This shows that Fmn2 has might have a dual role in generating new filopodia and also to elongate or stabilize already generated filopodia. Given the involvement of multiple actin associated proteins in the process of filopodia formation (Chacón et al., 2012; Faix, 2008; Korobova and Svitkina, 2008; Steffen et al., 2006), maintenance (Barzik et al., 2014; Schirenbeck et al., 2005b; Yamada et al., 2013) and elongation (Applewhite et al., 2007; Barzik et al., 2014; Lebrand et al., 2004), it is difficult to comment on the exact function of Fmn2 or mechanism of Fmn2 function in filopodial dynamics from the current analysis.

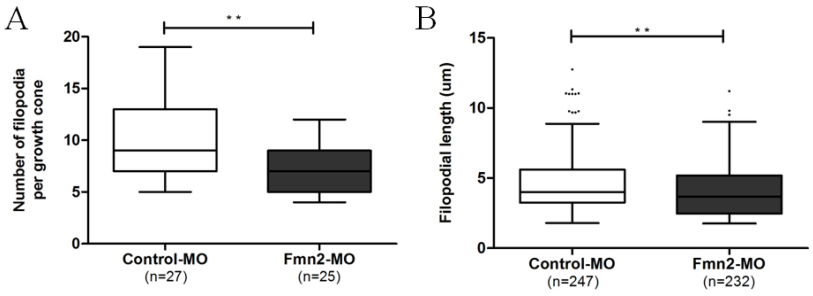

Figure 5.9: Analysis of the filopodial after Fmn2 knockdown.
A. Reduction in number of filopodia per growth cone, **B.** Reduction in the length of individual filopodia after Fmn2 depletion. (**, $p<0.01$).

5.2.5 Fmn2 depletion leads to compromised growth cone motility

To understand the importance of Fmn2 in the process of motility, the growth cones were imaged live after co-transfection of mGFP-Actin along with the morpholinos. Analysis of the time-lapse movies showed that the growth cones treated with Fmn2 morpholino exhibit

compromised motility. These growth cones moved slower (Figure 5.10A and B, below) and thus travelled less distance than the control growth cones (Figure 5.10C and D, below). In addition to this, it was seen that Fmn2 morphant growth cones failed to maintain a persistent directional migration, measured as the ratio of the Euclidian distance to the total distance covered by the growth cones in unit time (Figure 5.10E, below).

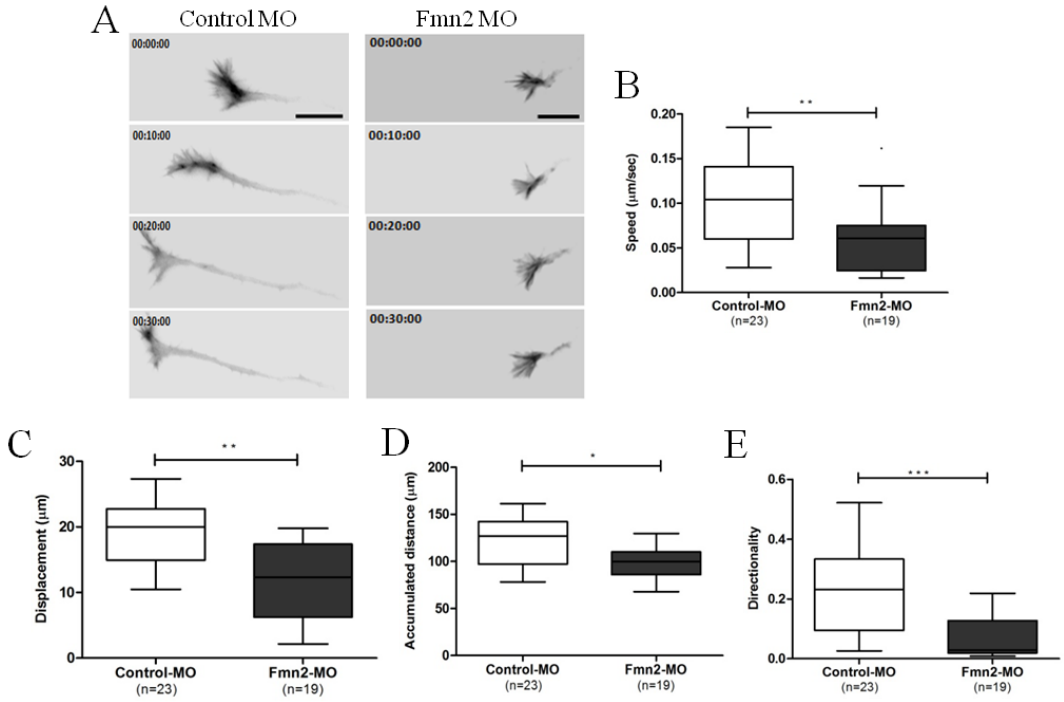

Figure 5.10: Quantification of motility of the growth after Fmn2 depletion.
A. Representative images from the time series for growth cones in Control morpholino and Fmn2 morpholino treatments. The lack of forward motion in Fmn2 morphant growth cones can be seen, **B.** reduction in the motility speeds of Fmn2 morphant growth cones, **C.** Fmn2 morphants show reduced displacement, **D.** total distance travelled by the Fmn2 depleted growth cones is also reduced, **E.** reduction in the persistent directionality of the Fmn2 morphant growth cones. (*p<0.05, ** p<0.01, *** p<0.001).

Occasionally the Fmn2 morphant growth cones were seen to split and then fused again to form one single growth cone (Figure 5.11, below). These splitting events were never observed in the control set. Quantification for these events was not performed due to their rare occurrence.

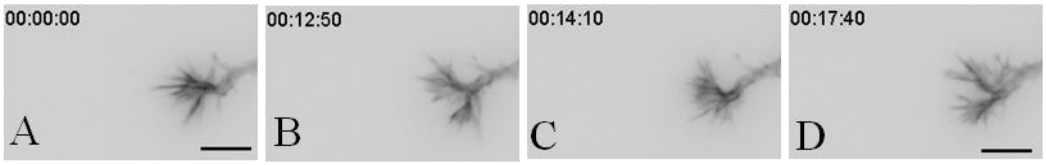

Figure 5.11: Splitting events in Fmn2 morphant growth cones.
Fmn2 morphant growth cones split and fuse as they move. Timestamp represents hrs:min:sec. Scale bar 10μm

5.2.6 Fmn2 depletion affects point contacts in the growth cones

Evidence from non-neuronal cells has shown that Fmn2 is present at the focal adhesions, the sites of attachment with the extrecellular matrix (Kuo et al., 2011). We analyzed the point contacts, the focal adhesion equivalents in the growth cone (Gomez et al., 1996). Immunofluorescence has shown that the integrin receptors are distributed throughout the growth cone and are concentrated in the filopodia (Grabham and Goldberg, 1997). Using pFAK-397 as an early marker for integrin engagement and subsequent point contact formation (Figure 5.12, below), we observed that upon Fmn2 knockdown the number of filopodia showing pFAK punctae at the tip did not change significantly suggesting a normal integrin engagement and initiation of point contact assembly Figure 5.13A, below). However, the mean pFAK signal at the growth cone reduced significantly as compared to the control growth cones (Figure 5.13B, below). Point contacts along the filopodia are crucial for growth cone advancement as described earlier. Thus we analyzed the total pFAK signal along the filopodia by dividing the total length of the filopodia in to initial 50% and distal 50% segments. This allowed us to overcome the length differences in the filopodia after Fmn2 knockdown and the initial and distal segments could be directly compared. It was found that the pFAK signal in the initial segment of the filopodia remained unchanged between the Fmn2 morphant group and the control group but the distal segment showed a significant decrease in pFAK accumulation when Fmn2 was depleted

(Figure 5.14A, below). The phalloidin signal in the filopodial segments remained comparable between the control and Fmn2 morphant group removing the possibility of a length dependent bias in the quantification (Figure 5.14B, below). Further, line scans for the intensity along the individual filopodia revealed reduced pFAK accumulation towards the distal end (tip) of the filopodium (Figure 5.15, below).

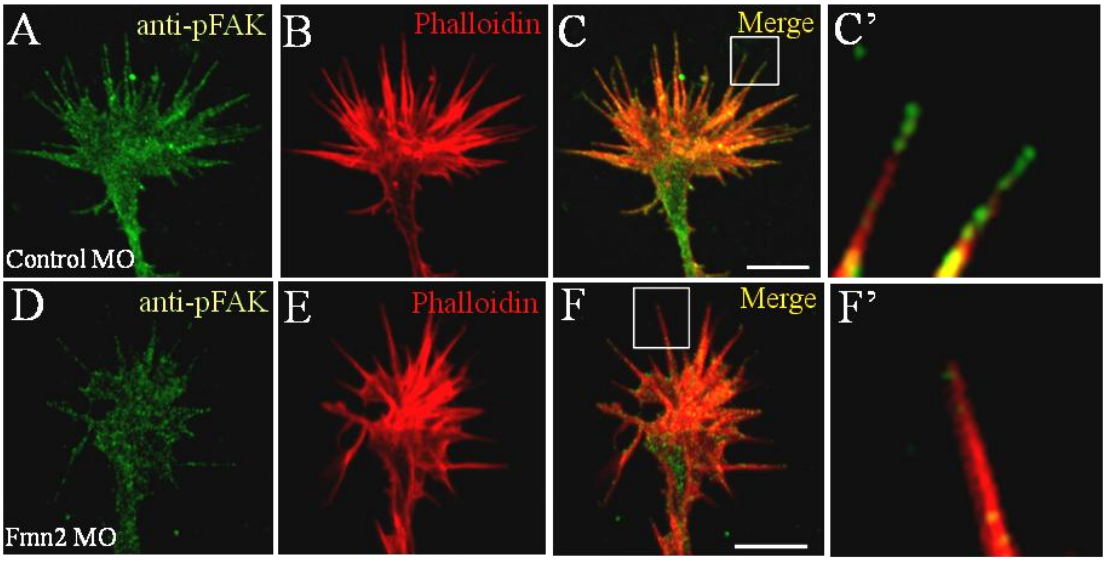

Figure 5.12: pFAK immunostaining after Fmn2 knockdown in spinal growth cones.
A-C. Control morpholino treated growth cones showing pFAK and F-actin labelling, **C'.** Magnified view of the filopodia tips from C showing terminal point contacts. **D-F.** Fmn2 morpholino treated growth cone with pFAK and F-actin labelling, **F'.** Magnified view of the ROI in F. The pFAK signal at the filopidal tips is seen to diminish. Scale Bar 10µm.

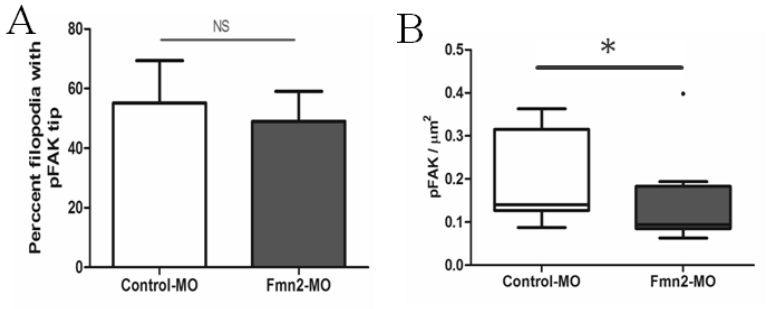

Figure 5.13: Quantification of pFAK signal at the growth cones.
A. The percentage of filopodia with pFAK labelled tip does not change upon Fmn2 depletion, **B.** pFAK signal per unit are of the growth cone is seen to reduce significantly. (* $p<0.05$)

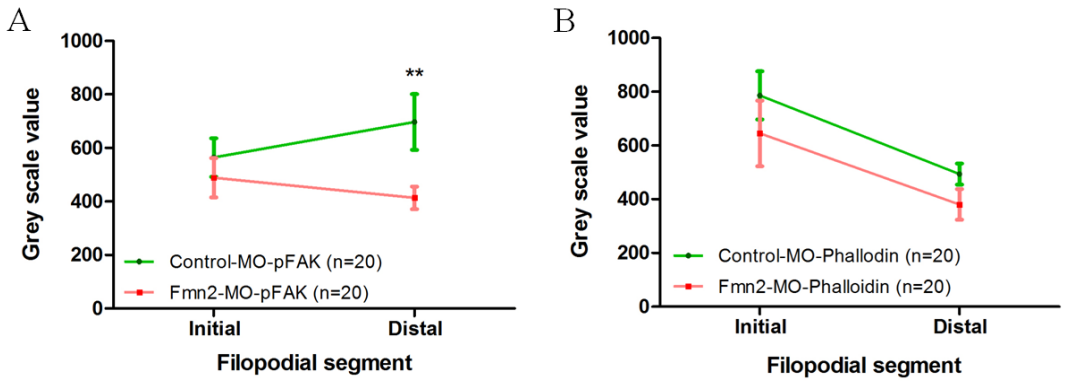

Figure 5.14: pFAK distribution in the filopodia.
The filopodia were divided in to initial and distal segments. The total pFAK signal in these segments was used for quantification. **A.** Comparison in the two filopodial segments showed a significant difference in the pFAK signal in the distal segment of Fmn2 morphant growth cones as compared to the controls. **B.** Comparison of the phalloidin signal in the two filopodial segments did not show a significant change. (**, p<0.01)s

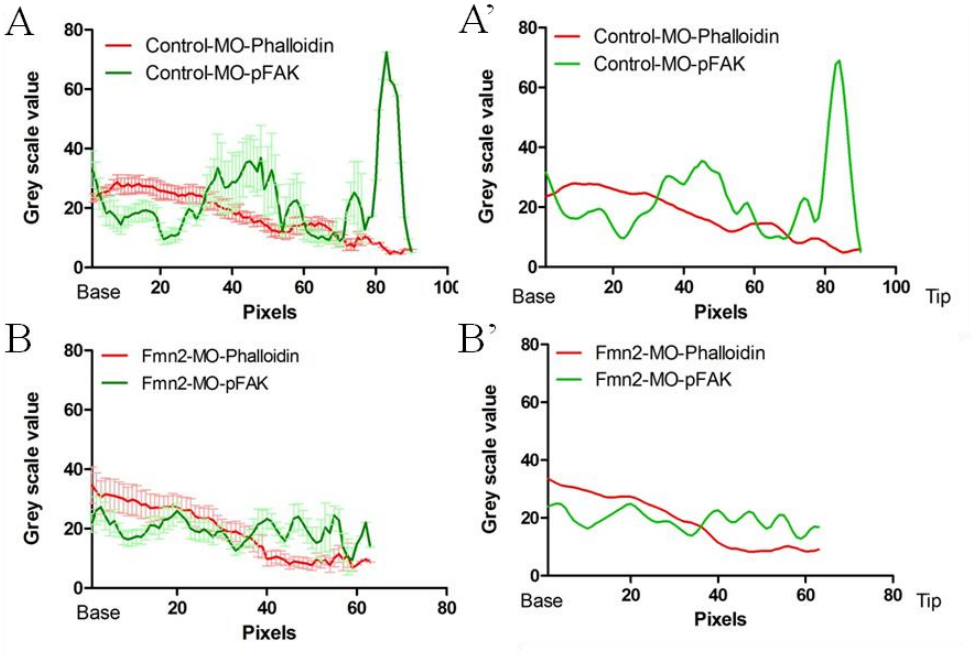

Figure 5.15: Line traces for pFAK along the filopodia.
A and B. Raw intensity traces along the filopodia in control and Fmn2 morphant growth cones respectively, A' and B'. Second order smoothening of the curves in A and B. A peak for pFAK trace at the tip of the filopodia can be seen in control morpholino treated growth cones as opposed to the baseline signal in the filopodia of Fmn2 morphant growth cones.

These observations suggested that reduction in Fmn2 levels compromises the ability of the growth cone to either form new point contacts or maintain the already existing set of point contacts. Studying the dynamics of point contacts in the growth cone is technically challenging because of the small size of the point contacts. Thus we decided to use focal adhesions in the non-neuronal cell culture system to gain better understanding of the dynamics of the substrate attachment upon Fmn2 depletion (See next Chapter).

5.2.7 Fmn2 depletion alters the actin ordering inside the growth cone

Anisotropy measurements utilize the information about the rotational freedom of a fluorophore to infer about the organizational complexity of a structure. The parallel and perpendicular components of the emission signal, and the level of asymmetry between these two components is measured. A free floating fluorophore will have perfectly symmetrical i.e. isotropic signal. As the rotational freedom of the fluorophore is restricted, the anisotropy increases as the emission is preferentially restricted to a particular fluorophore orientation. Thus a compact organization results in lower anisotropy values whereas a disordered organization has higher anisotropy values. In conventional anisotropy measurements, higher values of anisotropy mean more ordering. In the case of bundled actin, it has been reported that there is a component of homoFRET among the molecules in both cases, GFP-Actin as well as phalloidin labeling (Iyer et al., 2012). Due to the homoFRET, there is a loss of fluorescence signal in highly ordered conformations like bundled actin which results in reduced anisotropy. As the compaction decreases the effects of homoFRET are less noticeable and the fluorescence signal increases. Thus in case of homoFRET anisotropy, more compaction leads to reduced anisotropy.

Phalloidin stained morpholino treated growth cones were probed for the actin ordering by anisotropy measurements (Figure 5.16, below). It was seen that the anisotropy inside the growth cone increased upon Fmn2 depletion (p=0.014) as compared to the control growth cones (Figure 5.17, below). The change in actin ordering was complemented by an observation that in non-neuronal cells, the actin filaments at the stress fibers show reduced actin monomer turnover in Fmn2 depleted scenario (See next Chapter).

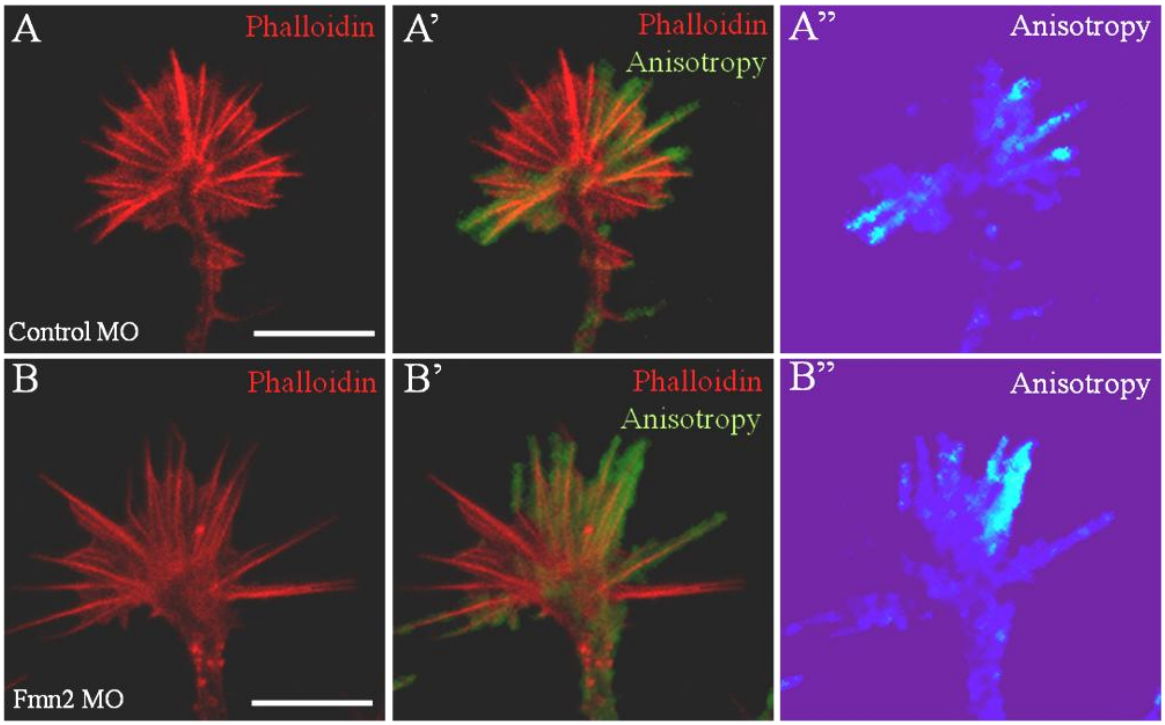

Figure 5.16: homoFRET anisotropy measurements in the growth cone using phalloidin.
A and B. F-actin in the growth cone as visualized by phalloidin staining. **A' and B'.** Anisotropy image overlayed on the F-actin channel. **A" and B".** Heat map for the anisotropy image (blue, low anisotropy; white, high anisotropy). Scale bar 10μm.

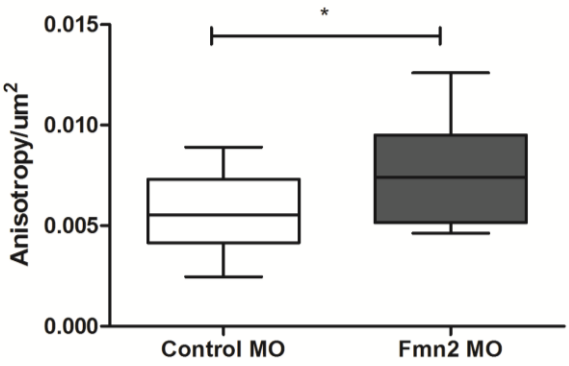

Figure 5.17: Quantification of anisotropy at the growth cone.
Anisotropy measurement per unit area of the growth cone increases upon Fmn2 depletion. (* $p<0.05$)

5.3 Summary and Discussion

We successfully raised a custom designed peptide antibody against chick Fmn2 and validated it on western blots. Using the same antibody, we reported the distribution of endogenous Fmn2 in the growth cones. Here, Fmn2 was found to localize to filopodial actin bundles along with occasional Fmn2 punctae at the filopodial tips. These observations indicated that Fmn2 might have a role in filopodia generation or elongation. Fmn2 reduction resulted in growth cones that have shorter and fewer filopodia. This shows that Fmn2 can either generate new filopodia and/or elongate or stabilize the existing filopodia. However, the two activities could not be separated using our experimental design. In addition to changes in filopodia, the overall spread area of the growth cones was reduced in Fmn2 morphant growth cones. Further, for motile growth cones, the motility speed and persistent directionality was compromised upon Fmn2 knockdown. The point contacts in the growth cone and along the filopodia as seen by pFAK-397 were compromised after Fmn2 depletion. The substrate attachments over the entire growth cone were found to be sub-optimal. This effect was pronounced near the tips of the filopodia where new point contacts are established. These tip adhesions are crucial for filopodia

stabilization which is followed by the lamellipodial advance between two stable filopodia ultimately resulting in net forward movement of the growth cone. Failure to stabilize the filopodia as seen by the low pFAK signal at the filopodial tips could make the Fmn2 morphant growth cones unable to consolidate the advance of the lamellipodium and thus exhibit reduced motility rates. Given the importance of filopodia in guidance, the effect of Fmn2 depletion on filopodial structures could be crucial to the ability of the growth cone to respond to the surrounding guidance cues and thus could affect the connectivity within the nervous system. In addition, the anisotropy measurements in the growth cone showed that the actin ordering was affected on Fmn2 depletion. Higher anisotropy values suggest a compromised actin organization in the growth cone. This could be in the form of the F-actin bulk in the growth cone or insufficient budling activity, both of which could be an effect of reduced Fmn2 levels. However the exact mechanism of this organization could not be explained using our experimental design.

Our results show that Fmn2 has an important role in establishing the overall morphology of the growth cone. The effect of Fmn2 depletion on the ability of the cell to form substrate attachments was subsequently assessed using non-neuronal cells and the observations are discussed in the next chapter.

5.4 Material and Methods

5.4.1 Culturing spinal neurons

As described in Section 3.

5.4.2 Morpholino and plasmid electroporation in neurons

As described in Section 3 and 4.

5.4.3 Live imaging of the growth cones

Growth cones were imaged on at 60x PlanApo objective at 10 second intervals for 30 minutes in the culture medium. The entire imaging setup was maintained at 37°C. If growth cone health was judged unfit, 1x Oxyrase was added to the medium during imaging. Intensity of the illumination source was kept at the minimum required to achieve good contrast.

5.4.4 Fixation and immunostaining of growth cones

As described in Section 3. pFAK (397) (Cell Signaling) was used at 1:1000 dilution.

5.4.5 Anisotropy measurements

The growth cones were stained with phalloidin-488 as described earlier and imaged on a confocal system equipped with the anisotropy module. The same growth cone was imaged without any polarizer in the emission path to get a reference image of the total fluorescence signal from F-actin. Subsequently, individual images were acquired with the parallel and perpendicular polarizer in the emission path. These images were then subjected to the following mathematical transformation;

$$D = ((S1-G*S2)/(S1+2G*S2))*255$$

where, D is the anisotropy, S1 and S2 are the parallel and perpendicular components of emission respectively and G is grating factor for the imaging system which is used to correct any bias towards a particular emission component. To scale the output image to an 8-bit image a factor of 255 is incorporated in the equation. In our case the grating factor was calculated using 1mM FITC solution in water. Under ideal conditions G should be 1.18 for FITC, but due to the inaccuracies in the optical path, G is found to deviate from the ideal value. In our experimental setup G was found to be 0.98.

The growth cone outline was hand drawn on the reference image and the ROI was transferred to the final anisotropy image. Only the gray scale values in side this ROI were used for further analysis and normalized to the growth cone area.

5.4.6 Quantification, data representation and statistics

Densitometric analysis was done on the western blots using Image J. Uniform sized area was selected around the band and the intensity was plotted using Analyze>Gel>Plot lanes. The area under the curve was cut-off using the line tool and area under the curve was selected using the wand tool. This area was measure using Analyze>Measure. The signal for anti-CRQ was normalized to the anti-tubulin signal from the respective lanes. The ratios so obtained were put in GraphPad Prism to get the graphical representation.

Growth cone outline was hand drawn using the segmented line tool in Image J on the Phalloidin channel of the image. This ROI was used to obtain the growth cone area. The raw area in pixel^2 was converted to μm^2 by multiplying with corresponding scaling factor. The same ROI was transferred to the anti-CRQ or pFAK channel and the mean intensity in this region was recorded using Analyze>Measure. The mean anti-CRQ signal was normalized to the growth cone area. The ratios so obtained were put in GraphPad Prism to get the graphical representation.

Growth cone motility was measured using the manual tracking tool Image J. The centre of the growth cone was manually marked. The raw coordinates so obtained were imported to the Chemotaxis and Migration tool developed by Ibidi. The values for accumulated distance, Euclidean distance and velocity were obtained from this tool and complied in GraphPad Prism for graphical representation.

Finger like membrane protrusions with F-actin cores as seen in the phalloidin channel were used for filopodia analysis. They were traced using the segmented line tool in Image J and the

lengths were obtained using Analyze>Measure. The measurements were complied as raw pixel lengths and converted to μm by multiplying with corresponding scaling factor. Only those filopodia which were longer than 2μm were considered for analysis. The number and length of these filopodia were compiled in GraphPad Prism for graphical representation.

The filopodia were traced using segmented line tool in Image J and the intensities in both the channels, Phalloidin and pFAK were obtained using Analyze>Plot profile. The traces for multiple filopodia were compiled in GraphPad Prism for graphical representation.

The graphical representations show the data using Box and Whisker plots and the bars show the spread of the data using the Tukey method. For bar graphs and the line traces, the error bars represent the standard error of mean (SEM) unless mentioned otherwise.

All the data sets were compared using Mann-Whitney test where the data is represented as Box and Whisker plots. For comparing the data sets represented as bar graphs, student's t-test was used to compare the data sets. Comparisons were done in GraphPad Prism.

6 ROLE OF FMN2 IN STRESS FIBER AND FOCAL ADHESION DYNAMICS

6.1 Introduction

Focal adhesion complexes in non-neuronal cells are comparable to the point contacts in growth cones described earlier. Both these structures essentially perform the same function of crosslinking the actin cytoskeleton to the ECM via the integrins and aid in generation of the traction forces required by the cell to move. Focal adhesions are multimolecular complexes which contain signaling and scaffolding proteins (Geiger et al., 2009). Some of these proteins are also involved in mechanosensing and in turn initiate intracellular biochemical signaling cascades (Geiger and Bershadsky, 2001).

6.1.1 Complexity and organization of focal adhesions

Numerous proteins have been reported to be a part of the focal adhesion complex over the years. Network analysis has shown that there is a huge cross talk between the individual molecular members of the complex (Figure 6.1, below). These studies have also revealed the design and organization principles such as a binary outcome of tyrosine phosphorylation/dephosphorylation status of the proteins in the complex (Geiger et al., 2009).

Different approaches have been used to study the complexity of the adhesions. High throughput proteomic studies have listed the components of the focal adhesions (Kuo et al., 2011). Novel imaging studies have revealed the organization of various components in the adhesion complex. One such approach is the compositional imaging where multicolour data from the microscope is used to create a multidimensional pixel clusters according to the compositional signatures and finally displayed as cellular distribution of individual component (Zamir et al.,

2008). Using Interferometric photo-activated localization microscopy (iPALM), a nanoscale map of the focal adhesion component was developed (Kanchanawong et al., 2010) which revealed a multilaminar architecture made up of spatial and functional compartments that mediate the interdependent functions of focal adhesions: an integrin signaling layer, a force transduction layer, and an actin regulatory layer.

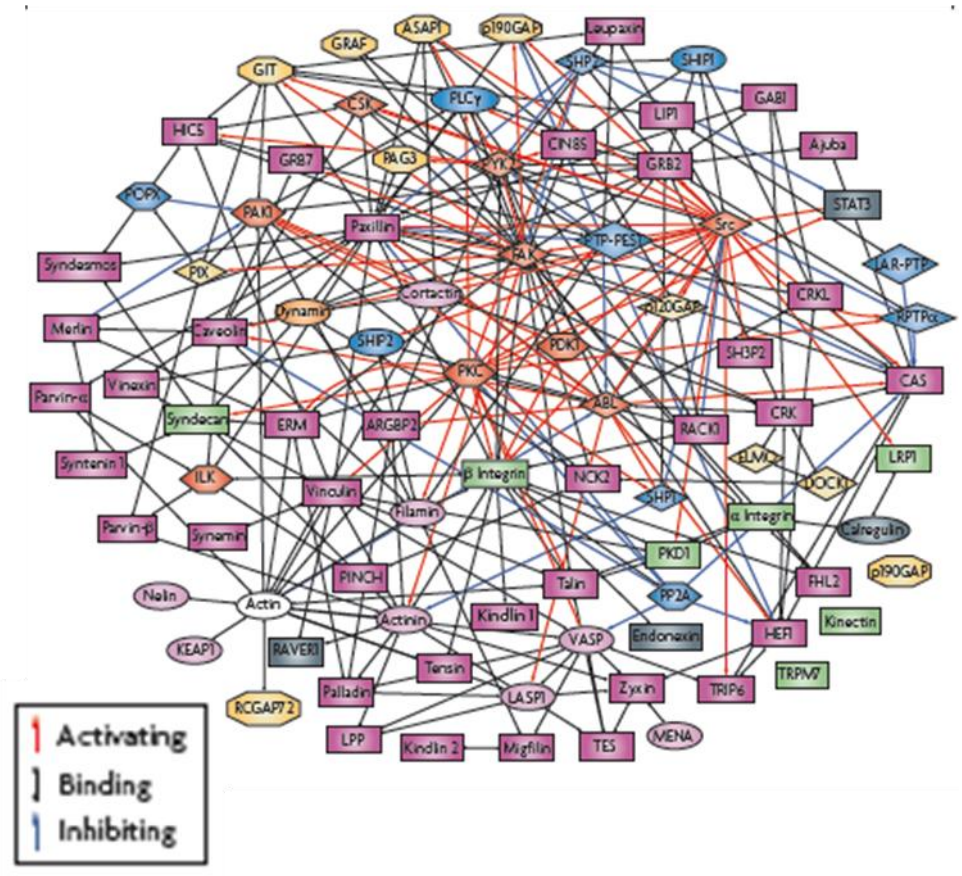

Figure 6.1: Interaction network within the focal adhesion
The entire network contains about 700 links, majority of which are binding interactions and the remaining are modifications where one component activates or inhibits the activity of another component. The biological activities components include several actin regulators that affect the organization of the attached cytoskeleton, adaptor proteins that link actin to integrins either directly or indirectly, and a wide range of signalling molecules, such as kinases, phosphatases and G proteins and their regulators. *(Adapted from Geiger et al.,2009)*

6.1.2 Focal adhesions assembly and dynamics

Actin cytoskeleton is linked to the ECM via the transmembrane integrin receptors at the focal adhesions. This cross linking is mediated by anchoring proteins like Talin (Nayal et al., 2004). Talins together with essential integrin binding proteins, kindlins, are responsible for integrin activation (Montanez et al., 2008; Moser et al., 2008). Subsequent steps in focal adhesion assembly include the recruitment of additional components to promote clustering of the nascent complexes and stabilization of the integrin–cytoskeleton bonds. The binding of vinculin to talin triggers the clustering of activated integrins (Humphries et al., 2007) and lead to strengthening of the intergrin-actin interaction (Galbraith et al., 2002).

The focal adhesions transition between assembly and disassembly cycles as the cell migrates (Figure 6.2, below). Small nascent adhesions (<0.25μm) at the leading edge of the cell initiate the process of focal adhesion assembly. A subset of these nascent adhesions develop in to focal complexes (<0.5μm) and then mature in to focal adhesions (1-5μm) (Gardel et al., 2010). Mechanical tension has been shown to stimulate the process of maturation (Balaban et al., 2001). Bundling of F-actin mediated by α-actinin at the nascent adhesion and myosin-II mediated retrograde flow transmits the force from the actin cytoskeleton to the ECM. The bundles of F-actin serve as bridges between focal adhesions and the myosin driven tension across this bundle contributes towards the maturation of focal adhesions (Oakes et al., 2012b).

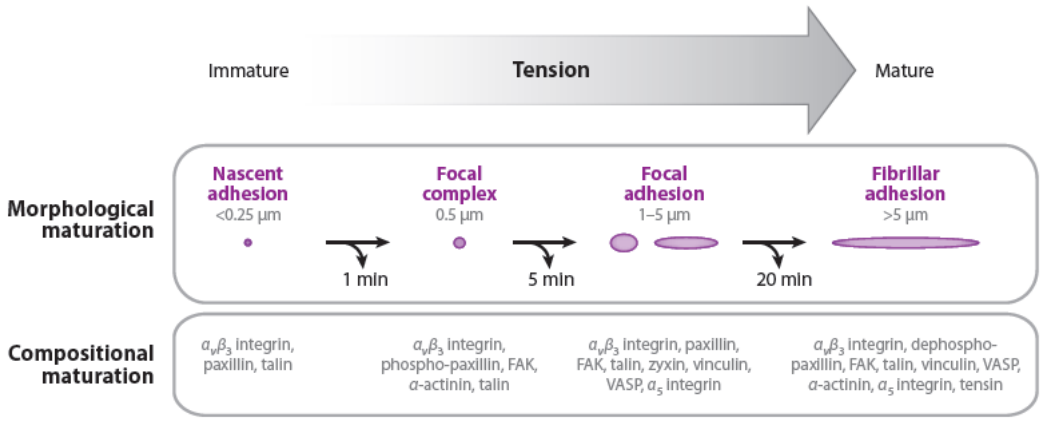

Figure 6.2: Phases of focal adhesion maturation.
The focal adhesion undergoes a series compositional changes ultimately leading to the maturation. The maturation of focal adhesions occurs in response to the mechanical tension experienced at each stage.

The ECM engagement with the integrin induces the auto-phosphorylation of FAK at tyrosine 397 (pY397) (Shi and Boettiger, 2003). This initiates a phosphorylation cascade resulting in tyrosine phosphorylation of Paxillin and p130Cas (Ballestrem et al., 2006) and binding of SH2-domain containing proteins that results in further growth of the adhesion.

Mechanical coupling of the actin retrograde flow to the ECM via the focal adhesions immobilizes the actin mesh inside the cell relative to the ECM. This has two potential outcomes, one is the transmission of filament polymerization at the leading edge in to the protrusion of the cell membrane and secondly, the transmission of moysin driven pulling forces in to traction against the ECM to pull the cell body forward. This coupling could be locally regulated by a 'molecular clutch' to allow tunable transmission of myosin- or polymerization-driven retrograde flow into leading edge protrusion and/or traction.

Disassembly of focal adhesions is equally important for migration of the cell. If the nascent adhesions are not stimulated enough, the default outcome is their disassembly. FAK is implicated in the disassembly of focal adhesions via p190RhoGAP phosphorylation that may decrease Rho-ROCK mediated myosin-II activity (Holinstat et al., 2006). FAK deficient cells

show larger and stable peripheral focal adhesions (Ilić et al., 1995). An alternative explanation for FAK mediated focal adhesion disassembly is by upregulating Rac1 activity and thus opposing the Rho mediated myosin activity (Arthur and Burridge, 2001). Evidence also shows that FAK is involved in regulation of Dynamin mediated integrin endocytosis (Ezratty et al., 2005).

6.1.3 Role of forces and focal adhesion dynamics in cell motility

Directional forces at the protein level are thought to induce conformational changes in the proteins at the nascent adhesions (Gardel et al., 2010). The new binding site thus exposed recruit additional proteins of the focal adhesion complex. *In vitro*, force induced unfolding of talin allows binding of vinculin (del Rio et al., 2009). In addition to the structural changes in proteins that lead to the enhanced recruitment of additional components at the nascent adhesion, 'catch bond' behavior of integrins increases the bond life time of individual receptor-ligand combination (Marshall et al., 2003).

Actin bundles at the nascent adhesion sites have been shown to elongate in a formin dependent manner in response to the tension development (Gupton et al., 2007b). Thus tension-mediated adhesion maturation is important for supplying new actin filaments which are integrated in the actomysin machinery for further tension development. The intimate coupling of the F-actin and the focal adhesion translates in to tractional forces at the focal adhesions which help the cell in directional motility(Le Clainche and Carlier, 2008). The focal adhesion acts as amolecular clutch (described in the main introduction) that controls the mechanical coupling between actin dynamics and the substrate. When the clutch is engaged, the force generated by actin assembly at the leading edge of the lamellipodium is converted into protrusion whereas,

when the clutch is disengaged, the slippage that occurs between the polymerizing actin network and adhesions increases the retrograde flow and decreases the protrusion rate .

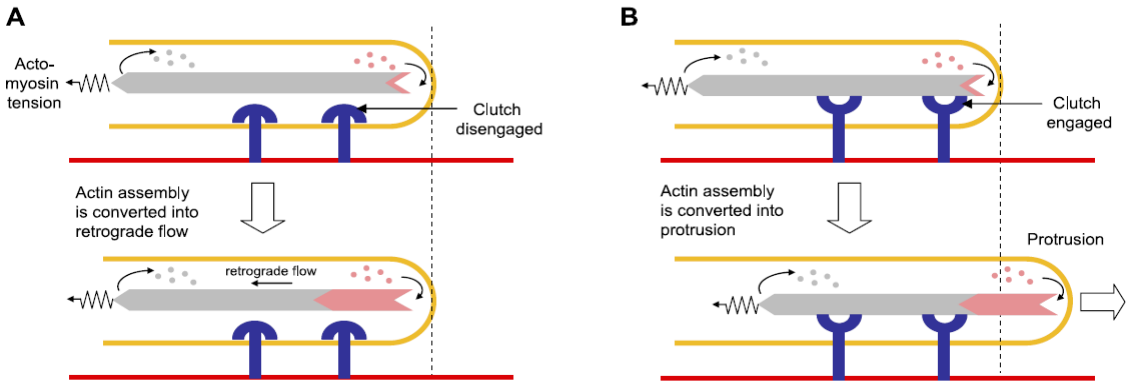

Figure 6.3: Clutch engagement and force transmission at focal adhesions.
A. Disengaged molecular clutch with no linkage between the F-actin and the focal adhesion complex. Under this condition, no protrusion can occur as the system is biased towards the retrograde flow. **B.** An engaged molecular clutch. The F-actin and the focal adhesion complex are tightly coupled and the actin polymerization leads to protrusion of the leading edge membrane. The actomyosin contractile forces are converted to traction enabling the cell to move forward. Adapted from *(Le Clainche and Carlier, 2008)*.

6.1.4 Stress fibers in non-neuronal cells

Stress fibers are contractile actomyosin bundles important in cell adhesion and motility. They are composed of short actin filaments with graded polarity (Cramer et al., 1997). Actin bundling proteins like α-actinin are involved in cross linking these short actin filaments. Stress fibers are classified in three broad categories, ventral stress fibers, transverse arcs and dorsal stress fibers (Hotulainen and Lappalainen, 2006) (Figure 6.4, below). Ventral stress fibers are the contractile bundles that are associated with focal adhesions at both the ends and play a crucial role in cell adhesion and motility. Transverse arcs do not associate with the focal adhesions on either end and are curved bundles that show a characteristic flow from the leading edge of migrating cell towards the centre. Dorsal stress fibers are attached at one end to the focal adhesion on the ventral side and terminate in to the transverse arcs on the other end (Hotulainen and Lappalainen, 2006). Dorsal stress fibers have uniform polarity and are thus thought to be

only motor tracks for transport rather than contractile structures (Pellegrin and Mellor, 2007). Contraction of the ventral stress fibers is thought to occur because of a ratcheting effect from the bundle originating from either of the focal adhesions at the ends (Pellegrin and Mellor, 2007). In contrast to this hypothesis, studies by Burridge and colleagues have shown that the contractility is maximum at the ends (Peterson et al., 2004). Nonetheless, it has been observed that majority of the contractile forces generated in non-muscle cells are aligned to the axis of ventral stress fibers (Pellegrin and Mellor, 2007).

Owing to their unique organization, the stress fibers couple distant focal adhesions in a cell and help in coordinating the forces across the cell. Impaired stress fibers have been shown to result in impaired focal adhesion compositional maturation and ECM remodeling (Oakes et al., 2012a). Laser ablation studies have shown that disrupting a single stress fiber reduces tension on individual vinculin molecules at the focal adhesion across the cell (Chang and Kumar, 2013a). Stress fiber mediated assembly and maturation of focal adhesions is well documented. The tension generated due to the actomyosin sliding at the stress fibers leads to focal adhesion maturation (Oakes et al., 2012a). These studies relate stress fiber tension to the adhesion stability and cell shape.

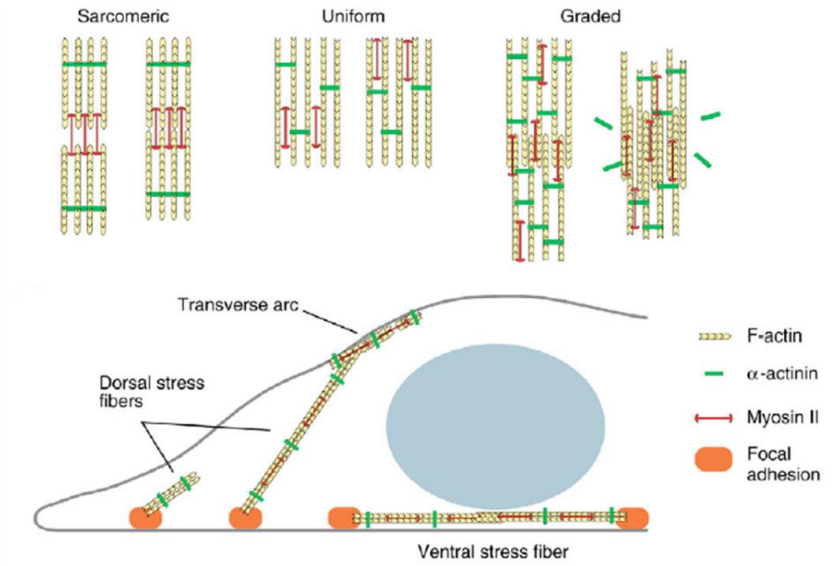

Figure 6.4: Organization of actin stress fibers.
Schematic representation of three possible arrangements of actin filament with different outcomes for contractility and organization of different types of stress fibres in the cell. Adapted from *(Pellegrin and Mellor, 2007)*.

6.2 Results

6.2.1 Fmn2 is expressed in NIH3T3 fibroblasts

Using primers against unique region in the mouse Fmn2 transcript, endogenous transcript for Fmn2 could be detected in NIH3T3 cells (Figure 6.5, below). This supported the earlier observation that Fmn2 is not exclusive to the nervous system as NIH3T3 cells belong to the embryonic fibroblast lineage.

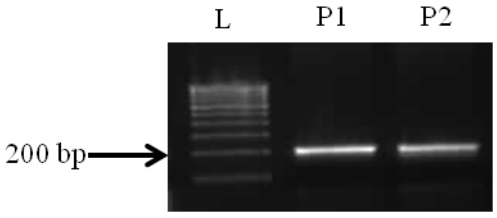

Figure 6.5: Expression of Fmn2 in NIH3T3 cells.
Agarose gel showing the amplified PCR product for mFmn2 in NIH3T3 cells using two different primer pairs P1 and P2.

6.2.2 Fmn2 depletion reduces the size of focal adhesions

Knockdown of Fmn2 in NIH3T3 cells was performed using siRNA. The efficiency of knockdown was assessed using realtime qPCR. Up to 70% reduction in the transcript level was achieved in 24 hours. The knockdown persisted up to 48 hours post treatment but only around 50% (Figure 6.6, below). The cells were co-transfected with EGFP-Paxillin to mark the focal adhesions for analysis 24 hours post transfection (Figure 6.7A and B, below). The focal adhesions were imaged in live cells and were analyzed using the Focal Adhesion Analysis Server (FAAS, http://faas.bme.unc.edu/). This analysis used high pass and round averaging filters in combination with water algorithm to segment and identify focal adhesions. Once identified, the focal adhesions were tracked over the entire image sequence entered in the server. The physical parameters for the focal adhesions like size, length of the long and short axis, distance from the cell edge etc. were calculated from the thresholded images. Analysis of focal adhesions over a 30 minute period showed that Fmn2 depletion did not change the number of FAs per cell significantly (Figure 6.7C, below) but resulted in smaller FAs (Figure 6.7D, below) when compared to the cells treated with LacZ siRNA as a control.

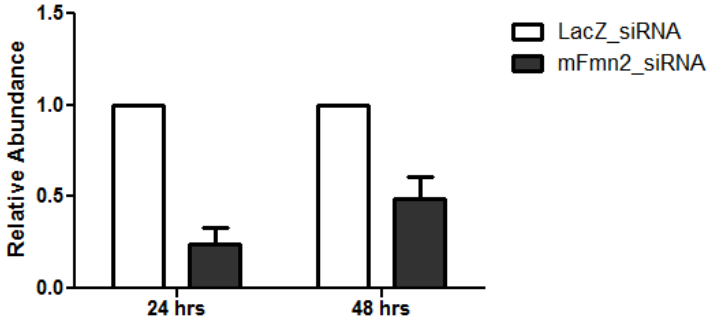

Figure 6.6: Assessment of Fmn2 knockdown using siRNA.
Quantification for the relative transcript levels after siRNA mediated knockdown of Fmn2 as assessed by realtime qPCR. The data is normalized to actin. After 24 hrs of siRNA treatment, about 70% reduction in the Fmn2 transcript was seen.

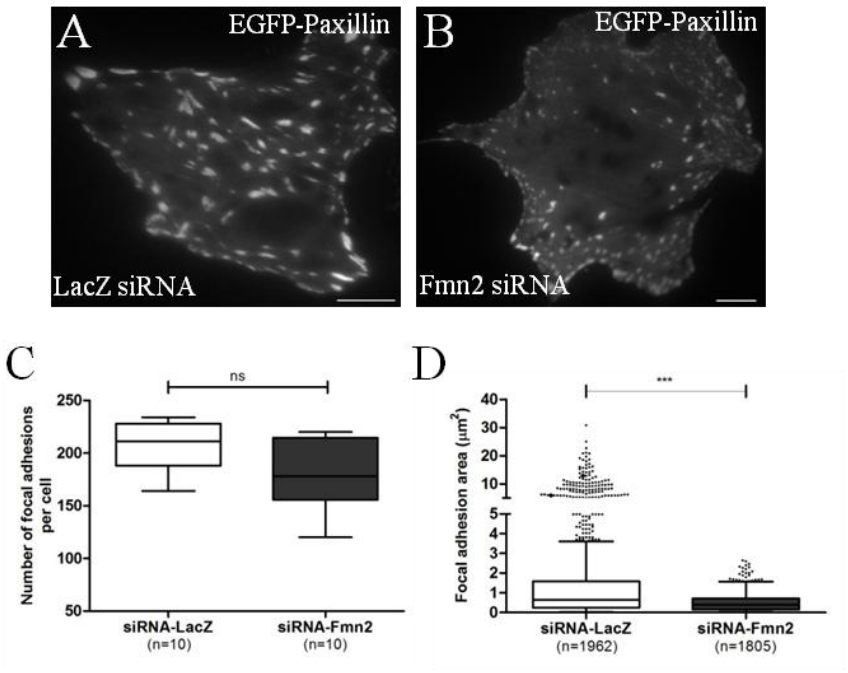

Figure 6.7: Effect of Fmn2 knockdown on focal adhesion number and size.
A and B. Focal adhesions in marked with EGFP-Paxillin in LacZ and Fmn2 siRNA treated cells respectively, **C.** Number of focal adhesions per cell did not show a change, **D.** Focal adhesion size was reduced significantly after Fmn2 knockdown. Scale Bar 10μm. (ns, non-significant, ***$p<0.0001$).

6.2.3 Focal adhesions stability is compromised upon Fmn2 depletion

Tracking the intensity change for each of the focal adhesions over the entire imaging period provided an understanding about assembly and disassembly kinetics. Increase in the EGFP-Paxillin signal at the focal adhesion corresponded to more recruitment and thus assembly of the focal adhesion whereas the decreasing signal corresponded to disassembly. Using the change in intensity per unit time the assembly and disassembly rates were calculated. Analysis of the rate of focal adhesion assembly and disassembly, showed that after Fmn2 depletion, the focal adhesion assembly rates are unchanged (Figure 6.8A, below), but the disassembly rates are increased (Figure 6.8B, below) in comparison to the control cells. Further, upon Fmn2 depletion, the time spent by the focal adhesions in the assembly phase was reduced (Figure 6.8C,

below) and they spent more time in the disassembly phase (Figure 6.8D, below). As a result, the mean size of focal adhesions was reduced.

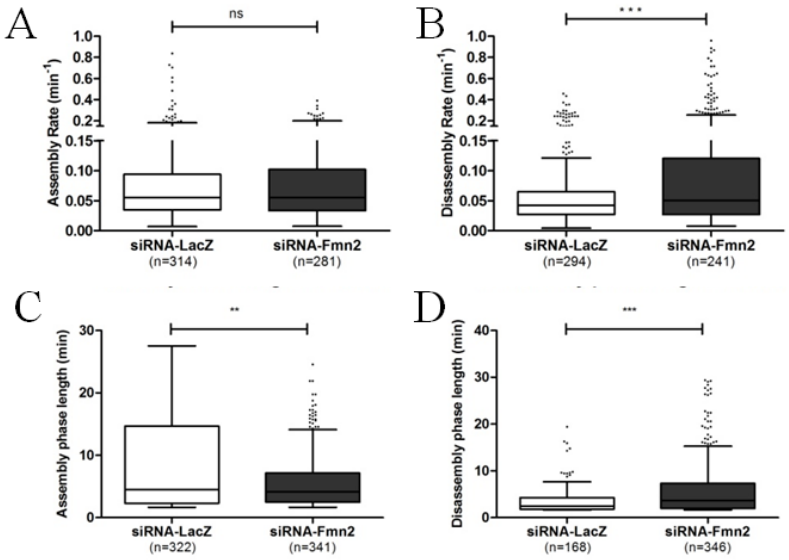

Figure 6.8: Effect of Fmn2 reduction on focal adhesion dynamics.
A. Focal adhesion assembly rate did not show a change after Fmn2 knockdown, **B.** Disassembly rates of the focal adhesions were enhanced following Fmn2 depletion, **C.** Assembly phase length of the focal adhesions lasted for a shorter duration in Fmn2 depleted cells, **D.** Disassembly phase length of the focal adhesions was seen to be longer in the Fmn2 depleted cell. (ns non-significant, ** $p<0.01$, *** $p<0.001$)

6.2.4 N-terminus of Fmn2 directs the localization to stress fibers

Continuing from the observation in growth cones where Fmn2 was seen along actin bundles, we tested if Fmn2 also localizes to actin bundles in non-neuronal cells. Over expression of mFmn2-EGFP in NIH3T3 cells showed that Fmn2 distribution resembles stress fibers in the cell (Figure 6.9, below). Further co-labeling the stress fibers using lifeact to mark the F-actin strucures showed that the distribution of full length Fmn2 resembled the bundled actin template in the cells (Kalyanee Shirlekar and Ketakee Ghate, unpublished data).

To better understand the distribution of Fmn2, smaller fragments of gFmn2 were expressed in the cells along with stress fiber and focal adhesion markers. It was seen that the N-terminal (1-

400 aa.) localized to the stress fibers as seen by co-labeling the stress fibers with Lifeact-GFP (Figure 6.10, below).

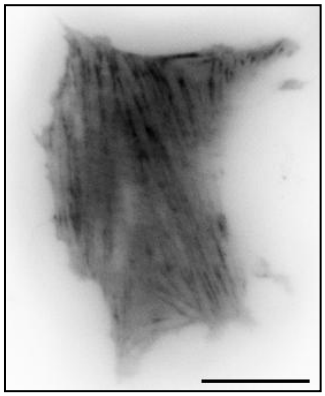

Figure 6.9: Distribution of mFmn2 in NIH3T3 cells.
mFmn2-EGFP distribution resembled stress fibre like pattern in NIH3T3 cells. The image was inverted for better contrast. Scale Bar 10 μm.

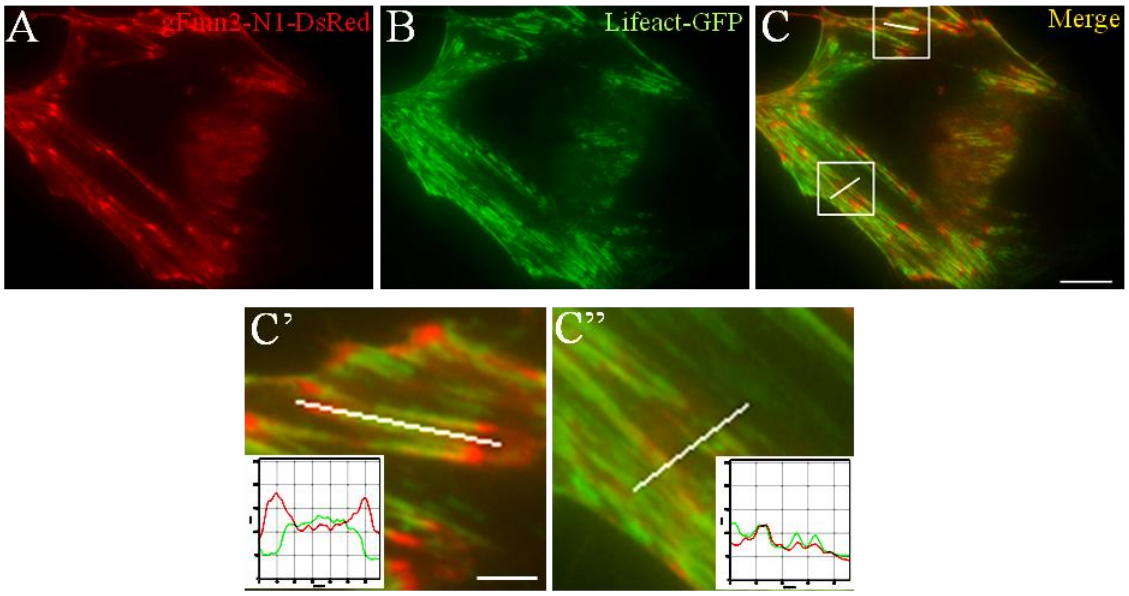

Figure 6.10: N-terminus of gFmn2 is sufficient for stress fibre localization.
A. Expression of gFmn2 N-terminus in NIH3T3 fibroblast, **B.** Stress fibres labelled with lifeact, **C.** Merged image showing colabelling of Fmn2 N-terminus with stress fibers, **C' and C"** Magnified regions marked in C. Insets show the intensity profiles along the marked lines. Scale Bar 10μm for A, B and C. Scale Bar 2 μm for C' and C"

Although the images showed that the N-terminus was labeling the entire stress fiber, closer inspection of the intensity profiles showed that the ends of the stress fibers had higher accumulation of the N-terminus as compared to the central region of the stress fibers. The ventral stress fibers terminate in focal adhesions at both the ends (Hotulainen and Lappalainen, 2006; Pellegrin and Mellor, 2007). Thus the higher accumulation of Fmn2 N-terminus at the stress fiber ends suggests that the N-terminus of Fmn2 directed the localization to the focal adhesions in addition to the stress fibers. This hypothesis is supported by previous biochemical evidence for Fmn2 being present at the focal adhesions (Kuo et al., 2011). However, further colabeling studies using paxillin did not show colocalization at the focal adhesions (Figure 6.11, below). We therefore hypothesize that Fmn2 is not recruited to the focal adhesions, but is present juxta-focal adhesion and along the actin bundle in the stress fiber.

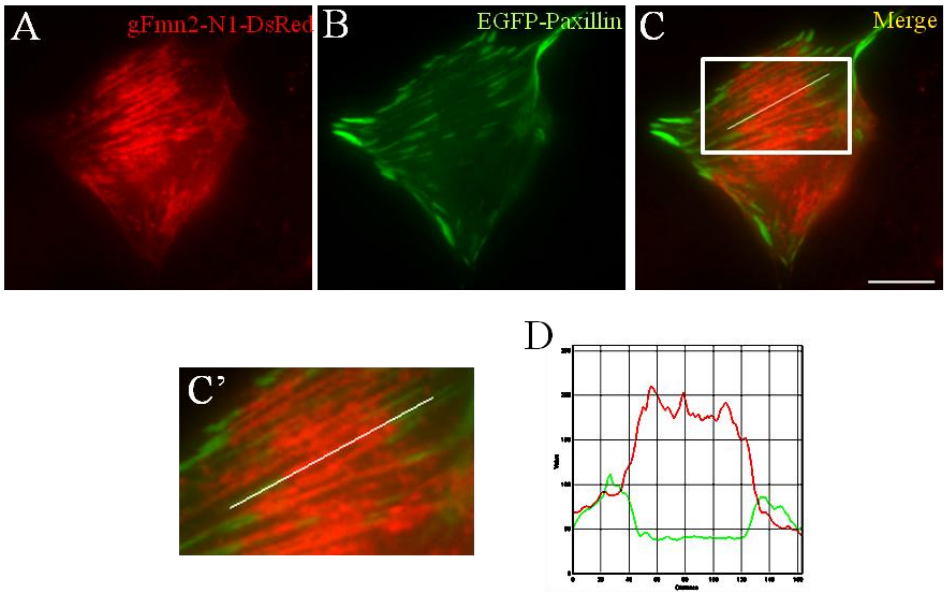

Figure 6.11: N-terminus of gFmn2 does not localise to the focal adhesions.
A. Expression of gFmn2 N-terminus, **B.** Focal adhesions labelled with EGFP-Paxillin, **C.** Merge, **C'.** Magnified view of the marked region in C, **D.** Intensity profile along the marked line in C'.

6.2.5 Fmn2 has a role in stress fiber turnover

Since Fmn2 was seen at the stress fibers, we tested whether Fmn2 functions in formation or maintenance of the stress fibers. We analyzed the turnover of actin at the stress fibers using the Fluorescence Recovery after Photobleaching (FRAP) technique with mGFP-βactin.

As NIH3T3 cells did not exhibit the different types of stress fibers as evidently as described for other cell types (Pellegrin and Mellor, 2007), we decided to focus on the clearly distinguishable ventral stress fibers. FRAP analysis on the central regions of the ventral stress fibres showed that in conditions where Fmn2 is depleted the actin turnover was slowed down ($t_{1/2}$=86±13.4) as compared to control conditions ($t_{1/2}$=54.31±7.4) (Figure 6.12, below).

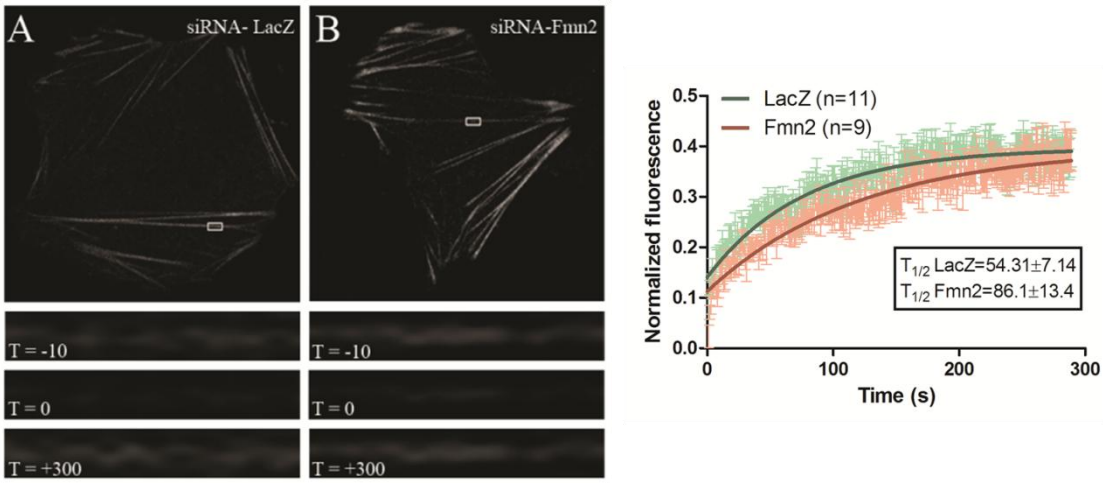

Figure 6.12: mGFP-actin recovery at the stress fibers following Fmn2 knockdown.
(A and B) LacZ and Fmn2 siRNA treated cells respectively showing stress fibres marked using mGFP-actin. The marked regions represent the section of the stress fibre used for bleaching and FRAP analysis. The FRAP regions with the time stamp (seconds) are enlarged for the corresponding cell. The graph shows the fluorescence recovery in control and Fmn2 depleted scenarios. The data is represented as a single exponential fit to the raw values and the error bars represent SEM. The $T_{1/2}$ values are represented in seconds along with the SD.

Though the difference in the FRAP curves for Fmn2 depleted and the control cells is subtle, it nonetheless is significant and suggests that the localization of Fmn2 at the stress fibers as seen earlier is of functional relevance.

6.3 Summary and Discussion

Fmn2 was found to be endogenously expressed in NIH3T3 cells. Fmn2-EGFP was not detected at the focal adhesions in our experimental setup but the truncated N-teminus was found to be juxta-focal adhesion and along the stress fibers. In spite of this lack of localization to the focal adhesions, siRNA mediated Fmn2 depletion affected focal adhesion parameters like the size and dynamics of assembly and disassembly. Fmn2 depletion did not affect the number of focal adhesions per cell but it did result in smaller and less stable focal adhesions in the cell. It was found that under Fmn2 depleted conditions; the focal adhesions failed to stabilize and thus disassembled faster than the focal adhesions in the control cells. As described in the literature, focal adhesion stabilization and subsequent maturation depends on the tension generated across the stress fibers that link two distant focal adhesions (Burridge and Wittchen, 2013; Chang and Kumar, 2013b; Colombelli et al., 2009; Oakes et al., 2012b). Owing to their actomyosin organization, the stress fibers exert contractile forces at the two ends where they are coupled to the focal adhesions. The contractile force is transmitted to the focal adhesions resulting in stabilization and further maturation of the focal adhesions. Thus, we hypothesized that Fmn2 could mediate the focal adhesion stabilization via the stress fiber template. In support of our hypothesis, we showed that the incorporation of actin monomers at the stress fibers is retarded under conditions of reduced Fmn2. Therefore we conclude that, sub-optimal levels of Fmn2 in the cell, hampers the steady state dynamics of the actin filaments within the stress fibers. This reduced incorporation of actin monomers would lead to shorter actin filaments within the stress fibers and thus lower myosin II recruitment which ultimately results in weaker forces, lower tension and compromised force transmission along the stress fiber that is insufficient to stabilize the focal adhesions. In addition, Fmn2 could also play a bundling function as suggested for other

formins (Machaidze et al., 2010; Schönichen et al., 2013) and could be responsible for maintaining the integrity of the stress fiber via its bundling and the resultant stabilization. In such a scenario however, the polymerization and bundling activity of Fmn2 would have to be separately regulated as the predicted configuration of the dimmer for either of these activities would be different (Machaidze et al., 2010).

6.4 Material and methods

6.4.1 RNA isolation and cDNA preparation from NIH3T3 cells

All the solutions and plasticware used in the procedure were DEPC treated. The cells were trypsinized and collected in a 15ml centrifuge tube and pelleted by centrifuging at 100 rcf for 5 minutes. The supernatant was discarded and 1ml TRIZOL was added to the cell pellet. The pellet was resuspended in TRIZOL gently and 200µl Chloroform was added. After a short vortex (10 seconds), the mixture was allowed to sit at room temperature for 10-15 minutes. The aqueous layer was separated by centrifugation at 12,000 rcf to 10 minutes at 4°C and collected in a fresh tube. Equal volume of isopropanol was added and RNA was allowed to precipitate for 30 minutes at room temperature. RNA pellet was obtained by centrifugation at 10,000 rcf for 10 minutes at 4°C. The pellet was resuspended in 70% ethanol and centrifuged again at 7,500 rcf for 10 minutes at 4°C. The supernatantwas discarded and the RNA pellet was allowed to air dry at room temperature. Finally the RNA was dissolved in 20µl nuclaese-free water and stored at -80°C for up to 2 weeks.

cDNA was prepared as described in Section 3.

6.4.2 siRNA and plasmid transfection

For real-time, (Concentration) of siRNA and 1µg plasmid DNA was used for transfection. Approximately 10^5 cells were seeded in each well of a 6-well cell culture dish. After allowing the cells to attach overnight, the culture medium was replaced with 2ml of Optimem and the cells were kept back at 37°C until the transfection mix was ready. Transfections were done using Lipofectamine 2000 (Invitrogen). siRNA and plasmid were added to 200µl Optimem and incubated at room temperature for 5 minutes. Simultaneously, 2.5µl Lipofectamine was added to a separate tube with 200µl Optimem. The Lipofectamine and Optimem mix was incubated at room temperature for 5 minutes and was then added to the siRNA+plasmid+Optimem mix. This entire mixture was incubated at room temperature for 15 minutes and was then added to the cells with Optimem. The cells with siRNA+plasmid+lipofectamine+Optimem were incubated at 37°C with 5% CO_2 for 4 hours. After 4 hours, the medium was replaced with culture medium (DMEM+10FBS+1x PenStrep) and cells were put back in the incubator for 24 hours.

For live imaging of the cells after siRNA treatment, the cells were cultured on fibronectin coated coverglass chambers.

6.4.3 Imaging of cell post transfection and analysis using FAAS

After 24 hours of siRNA treatment, the culture medium was replaced with imaging medium (L-15 without phenol red+10% heat inactivated FBS+1x PenStrep) to allow imaging without additional CO_2 supply. The entire imaging setup was maintained at 37°C. Using the TIRF mode, a penetration depth of approximately 200nm was fixed and the focal adhesions were imaged at 10 second interval for 30 minutes using minimum laser power required for good contrast.

The image sequence was saved as TIFF and uploaded to the FAAS. All the parameters for analysis were kept default in the server. Data obtained from the server was analysed using GraphPad Prism.

Focal adhesion number per cell and the size of the focal adhesions were obtained for only the first frame of the image sequence. The assembly rates, disassembly rates, and phase lengths for the entire time series was used for analysis.

For the N-terminus localization images, the cells were imaged in wide field mode using appropriate filters. The line profiles for the stress fibers were obtained using Image J, Plugins>RGB profiler.

6.4.4 FRAP analysis

Cells were transfected with mGFP-βactin and imaged at 63x on a confocal microscope 24 hours post transfection. A uniform sized ROI (5x14 pixels) was selected for bleaching. Bleaching was done using the 488nm laser at 100% intensity while the imaging was done at 4% laser intensity. Ten pre-bleach images were acquired for reference and post-bleach images were acquired at 1 second interval for 300 seconds.

For analysis, the mean ROI signal from the bleached area was subjected to background subtraction and normalization using the mean intensity of the whole cell. The curve fitting and analysis of $t_{1/2}$ was done using one phase association model in Prism GraphPad.

6.4.5 Data representation and statistics

The graphical representations show the data using Box and Whisker plots and the bars show the spread of the data using the Tukey method where the outliers are represented outside the box as individual data points. For bar graphs and the line traces, the error bars represent the standard error of mean (SEM) unless mentioned otherwise. All the data sets were compared

using Mann-Whitney test where the data is represented as Box and Whisker plots. For comparing the data sets represented as bar graphs, student's t-test was used to compare the data sets. Comparisons were done in GraphPad Prism.

7 DISCUSSION

In this study, we characterized the cell biological role of Fmn2 in growth cone motility and commissural axon guidance *in vivo*. Importance of actin dynamics for the process of growth cone motility is well documented (Bentley and Toroian-Raymond, 1986; Marsh and Letourneau, 1984) and our study demonstrates the involvement of Fmn2 in this process.

Fmn2 in maintenance of the growth cone morphology

As described in earlier results, growth cones depleted of Fmn2 show reduced spread area. We attribute this defect to two major functional aspects of Fmn2; first is the polymerization potential of Fmn2 and second is the stabilization of the substrate attachments. The polymerization activity of Fmn2 might contribute to the protrusive forces at the leading edge resulting in spreading of the growth cone membrane either via the lamellipodium directly or indirectly via the growth and subsequent stabilization of the filopodia which is followed by lamellipodial advance between two stable filopodia. Though we do not show any evidence that Fmn2 participates in the lamellipodial dynamics, we do find the endogenous Fmn2 decorating the actin bundles in the filopodia. We hypothesize a role for Fmn2 in the generation and elongation of filopodia in the growth cone. In support of this hypothesis, we show that Fmn2 depletion leads to smaller and fewer filopodia at the growth cone. Formin mediated filopodia formation has been reported in non-neuronal cells (Barzik et al., 2014; Faix, 2008; Goh and Ahmed, 2012; Homem et al., 2009; Mellor, 2005; Mellor, 2010; Schirenbeck et al., 2005a; Schirenbeck et al., 2005b) but the evidence in growth cone filopodia is limited (Matusek et al., 2008). The evidence for the involvement of the classical actin nucleator Arp2/3 in the process of filopodia formation remains controversial in the growth cone (Korobova and Svitkina, 2008;

Strasser et al., 2004).Perhaps Arp2/3 function is required for filopodia formation but Arp2/3 might not be the sole regulator or generator of filopodia at the growth cone and therefore additional players apart from Arp2/3 are likely to participate in this process. Indeed, formin family members like DAAM and mDia1 are needed for filopodia formation in neurons or neuron like cells (Goh et al., 2011; Matusek et al., 2008). Our study demonstrates the requirement of Fmn2 in filopodia formation and elongation at the neuronal growth cone. Further, the Fmn2 morphant growth cones show reduced spread area. The possible reason for this decrease in area could be the lack of addition of F-actin bulk in the growth cone or due to the lack of stabilization of substrate attachment as discussed below.

Fmn2 in stabilization of substrate attachments

During each protrusive phase of the leading edge, the growth cone gains additional area due to the assembly and stabilization of new substrate attachments at the periphery. Failure to stabilize the substrate attachments during the leading edge advancement results in retraction of the unstable leading edge. As demonstrated by the lower levels of pFAK (Y397) intensity in the Fmn2 morphant growth cones, we speculate that these growth cones fail to stabilize the substrate attachments. To further strengthen our speculation, we show using a non-neuronal cell system that under conditions of Fmn2 depletion, the cells form smaller focal adhesions which are less stable and thus disassemble faster when compared to unperturbed Fmn2 levels. Even in the non-neuronal cells, the pFAK-397 levels are seen to decrease upon Fmn2 depletion (Ketakee Ghate, unpublished data). Thus we ascribe a role to Fmn2 in stabilization of substrate attachments which is consistent between the neuronal growth cone and non-neuronal systems. Altered growth cone motility can be a result of compromised substrate attachment and in turn disrupt *in vivo*

growth cone pathfinding (Robles and Gomez, 2006). In line with this observation, we show that Fmn2 depletion leads to midline crossing errors by the commissural axons as discussed later.

Focal adhesion stability depends on the amount of tension developed via the actomyosin machinery in the stress fibers that connect two focal adhesions with each other or to the actomyosin network (Chang and Kumar, 2013b; Oakes et al., 2012b; Roca-Cusachs et al., 2013; Wolfenson et al., 2011; Zimerman et al., 2004). Fmn2 depletion affects the actin monomer turnover at the stress fibers. Further, we show that Fmn2 does localize to the stress fibers in NIH3T3 cells. In line with these two observations, we propose that Fmn2 controls the adhesion stability indirectly through the stress fiber template. Earlier studies have shown formins like mDia2 to be present at the focal adhesions and aid in maintenance of polymerization competent barbed ends at the focal adhesions (Gupton et al., 2007a). This provided an elegant mechanism for focal adhesion stabilization by linking it to the actomyosin machinery via the actin filaments generated out of the focal adhesions. We propose that Fmn2 might help in point contact stabilization similar to mDia2. Although stress fiber like structures have not been reported in the growth cone due to the highly dense meshwork of actin, similar structures that aid direct crosstalk between two distant point contacts or indirectly via the actin mesh in the growth cone can be anticipated.

Fmn2 in growth cone motility

With respect to the growth cone motility, Fmn2 depletion results in slow moving growth cones with compromised persistent directionality. This is in contrast to the accelerated growth cone motility when a nucleator like Arp2/3 is depleted (Strasser et al., 2004). The slower motility rates of the Fmn2 depleted growth cones can be explained by the compromised substrate attachments as discussed earlier. Lack of proper attachment could make the growth cone spend

more time in finding an optimal attachment site and thus lead to more exploratory behavior by the growth cone ultimately resulting in the failure to maintain persistent directionality by the growth cone.

Fmn2 in actin organization

Fmn2 was seen along actin bundles in the filopodia in the growth cones. Full-length mFmn2 localized to the stress fibers in NIH3T3 cells and this localization was governed by the N-terminus. In addition, the N-terminus of Fmn2 also localized to the focal adhesions in some cells. From the FRAP analysis on stress fibers in NIH3T3 cells and phalloidin anisotropy measurements in the growth cone, it is apparent that Fmn2 is involved in bundled actin organization inside the growth cone as well as in non-neuronal cells. The actin monomer turnover at the stress fibers can be attributed to the polymerization activity of Fmn2 assuming that Fmn2 has steady state presence along the stress fibers and is involved in elongating the existing actin filaments within the stress fiber bundle.

***In vivo* manifestation of Fmn2 depletion**

Finally we show that the commissural neurons in the spinal cord fail to cross the midline when Fmn2 is reduced. This effect seems to be cell autonomous, as overexpression of mouse ortholog of Fmn2 is able to partially rescue the phenotype (Ajesh Jacob, unpublished data) and shows the functional conservation of Fmn2 between the avian and mammalian forms. Further, the expression of the presumably dominant negative form of Fmn2 in commissural neurons shows a similar midline crossing defect (Ajesh Jacob, unpublished data).

Taken together our results ascribe a previously unknown cellular role to Fmn2 in the process of actin organization and substrate adhesion stability, both in neuronal growth cones as well as NIH3T3 cells. The lack of Fmn2 in growth cones results in improper substrate

attachment possibly due to the lack of coordination between the actomyosin network and the point contacts. This would in turn result in compromised growth cone motility and thus larger *in ovo* manifestation in the form of midline crossing failure by the commissural neurons in the spinal cord.

Predicted model for the action of Fmn2

A subset of filopodia in the growth cone shows a marked localization of Fmn2 along the F-actin bundle that forms the core of the filopodia. Depletion of Fmn2 leads to reduction in the number of filopodia as well as the length of filopodia and in addition, results in reduced growth cone spread area. Reduction of Fmn2 levels results in a possible destabilization or failure of the terminal point contacts in the filopodium to mature in to stable attachments with the substrate, as seen by the reduction in pFAK signal at the filopodial tips. Based on these observations, we contemplate that Fmn2 is needed at the growth cone filopodia for generation, elongation and stabilization; either individually or in combination. Stabilization of the filopodia is critical for process like lamellipodial advance, directional persistence during motility and response to guidance cues as discussed earlier. Failure of point contact stabilization would lead to unstable filopodia and in turn failure of the lamellipodium to consolidate the advance between two filopodia. Tip adhesions are important for filopodial stabilization which is brought about via the tension induced stabilization and maturation of the point contacts (Bornschlögl, 2013). The actomyosin activity near the base of the filopodium and towards the central region of the growth cone is coupled to the filopodial actin bundles (Bornschlögl et al., 2013; Mallavarapu and Mitchison, 1999). The tension required for point contact stabilization/maturation is thought to be transmitted along the filopodial actin bundle which is linked to the point contact at one end

and embedded in the lamellipodial actomyosin network on the other end by the contractile actomyosin bulk near the leading edge of the lamellipodium (Figure 7.1, below).

Previous high throughput proteomics study had detected Fmn2 at the focal adhesions (Kuo et al., 2011) but lacked the functional description for this localization. In our study, although Fmn2 could not be colocalized with the focal adhesions, the depletion of Fmn2 affected the focal adhesion dynamics. Depletion of Fmn2 resulted in compromised reduced actin turnover at the stress fiber. Based on these observations, we speculate that Fmn2 is not recruited to the focal adhesions *per se* but is rather involved in polymerization or bundling activity of the existing actin filaments growing out of the adhesions. The effect on the substrate attachments in this scenario would be indirect via the actomyosin mediated tension acting at the sites of attachment.

Lack of tension generated by either of the two mechanism described above would lead to unstable point contacts at the filopodial tips for a growth cone and unstable focal adhesions in non-neuronal cells. Suboptimal substrate attachments would lead to further defects in the motility of the growth cone and offset the temporal coordination with the guidance cues ultimately leading to compromised axon path finding *in vivo*.

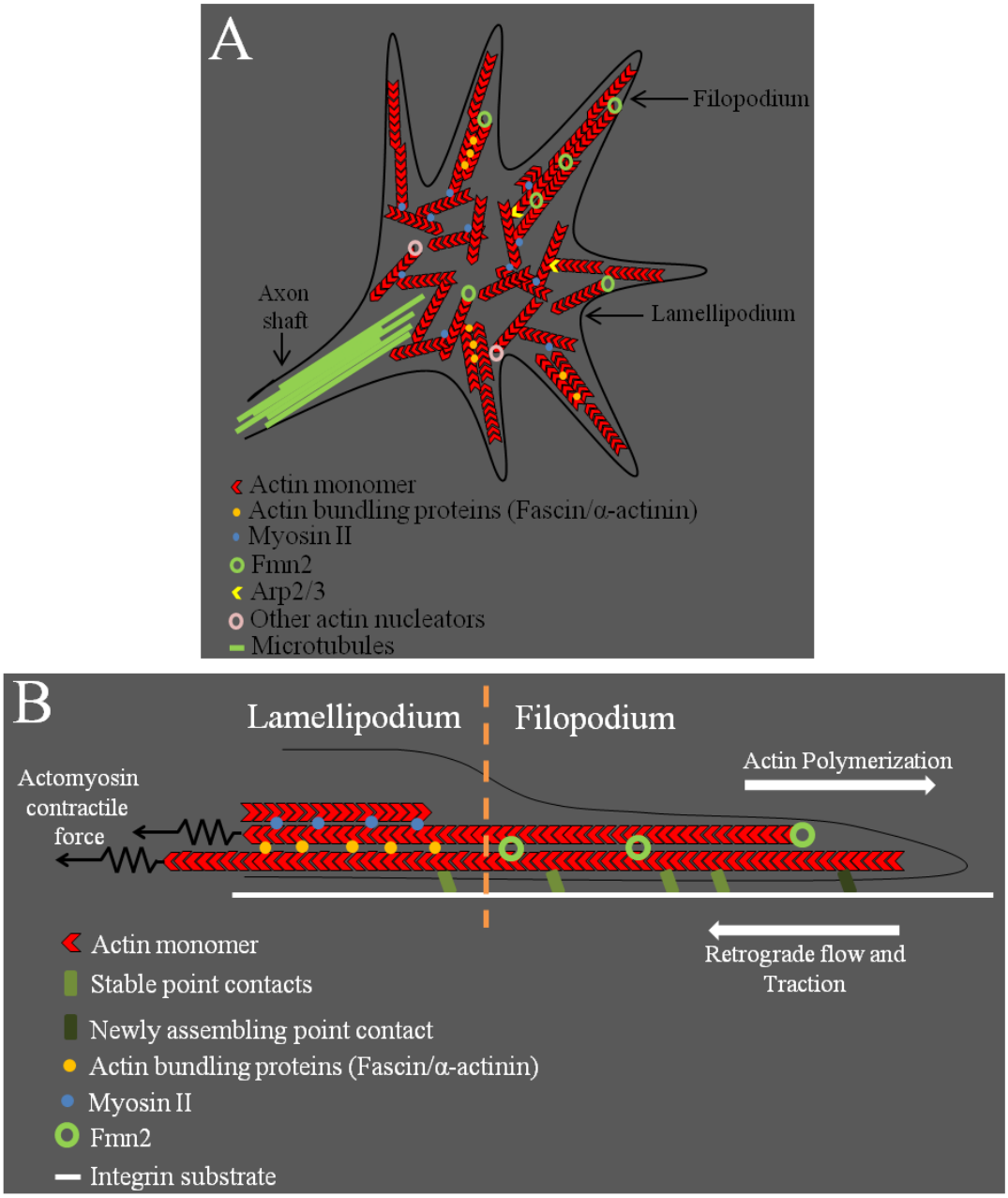

Figure 7.1: Model for Fmn2 activity in the growth cone.
A. Top view of a growth cone. The central region of the growth cone shows a dense meshwork of crosslinked actin filaments. In addition to Fmn2, the central region contains other nucleators that bring about actin polymerization. **B.** Side view of a growth cone. Polymerization activity of Fmn2 helps in elongation of some of the filopodial actin filaments which are bundled together via the bundling proteins or possibly Fmn2 itself. The myosin II activity in the central region results in a highly contractile network which is connected to the filopodial actin bundles. The force generated by the actomyosin activity is transmitted to ECM via the integrin receptors due to their coupling with the filopodial actin bundles. This force transmission results in stabilization of the point contacts.

8 FUTURE DIRECTIONS

This study describes Fmn2 activity only at the functional level in the process of growth cone motility and axon guidance. However, the mechanistic understanding of Fmn2 activity still remains to be explored.

Immediate directions

We speculate that Fmn2 is indirectly responsible for the stabilization of substrate attachments with the ECM. In our model Fmn2 is involved in maintenance of the F-actin bundles that are physically coupled to the integrins and due to the tensional forces actin on these actin bundles, the substrate attachments undergo stabilization and maturation. The lab has started testing our hypothesis using techniques like Traction Force Microscopy (TFM) to validate our hypothesis. Using the displacements of the beads embedded in a soft gel, TFM enables estimation of traction forces that the cell/growth cone exerts on the substrate. Traction forces in such experiments could be estimated over the entire area of the growth cone or the analysis can be restricted to only the filopodia. If our model holds true, Fmn2 depleted cells/growth cones should exert weaker forces on the substrate compared to the control cells/growth cones.

Using Fluorescence Resonance Energy Transfer (FRET) sensors like Vinculin-TS (Grashoff et al., 2010), to visualize the tension experienced by the focal adhesions, the lab is currently investigating the effect of Fmn2 depletion on forces acting at the focal adhesions. This sensor informs about the magnitude of the force experienced by the vinculin molecule; higher intramolecular FRET is observed under low tension conditions while higher tension on the vinculin molecule results in reduction of the intramolecular FRET signal.

For a detailed biophysical analysis of the effect of Fmn2 knockdown on the forces along filopodia, optical traps can be used. These have been previously used to estimate the forces exerted by filopodia (Bornschlögl, 2013). Using similar analysis the effect of Fmn2 on filopodial pulling can be investigated.

Long term future directions

Regulation of Fmn2

In vitro studies show that capu undergoes autoinhibition (Bor et al., 2012b) but in absence of a clear recognizable Rho-binding domain, the regulation of this autoinhibition remains poorly understood. In *Drosophila,* capu has been shown to interact with Rho1 and Spir during the process of oocyte maturation (Rosales-nieves et al., 2006) but in vitro studies show that Fmn2 and Spire can act together in absence of Rho (Montaville et al., 2014). Nonetheless, Fmn2 and Spire have been shown to act together during oocyte maturation and a Spire interaction domain has been mapped to the C-terminus of Fmn2 (Pfender et al., 2011; Quinlan et al., 2007). It would be interesting to investigate whether the phenotypes that we describe in our study have a component of Fmn2-Spire interaction.

Preliminary bioinformatic analysis in our lab predicts presence of DEP-domain in the N-terminal half of Fmn2. This potentially could provide a previously unknown regulatory mechanism for Fmn2. DEP domain was first identified in *Drosophila* Dishevelled, *C. elegans* EGL-10, and mammalian Pleckstrin, and is found in a number of mammalian protein families involved in Wnt signaling (Chen and Hamm, 2006). The lab is currently in the process of exploring if the DEP domain in Fmn2 is functionally relevant.

A mechanism of Fmn2 regulation independent of any regulatory interaction would be worth exploring where a tension dependent activation of Fmn2 occurs similar to other proteins like talin. Force induced unfolding of the autoinhibited conformation of Fmn2 could expose the FH1-FH2 domains and enable the polymerization activity.

Interactors of Fmn2

Analysis of Fmn2 protein sequence reveals multiple proline rich motifs that are similar to the (F/L/W/Y)PPPP motifs that interact with Class1 EVH1 domains. These motifs could provide Fmn2 the ability to interact with EVH1-domain containing proteins like Ena and enable focal adhesion or membrane targeting via Ena. Whether these motifs are functional in Fmn2 remains to be understood.

Fmn2 in receptor recycling

Involvement of Fmn2 in the receptor recycling at the growth cone cannot be denied given that evidence in support of other formins in the process of endocytosis (Girao et al., 2008; Prosser et al., 2011) and Fmn2 in long range vesicle transport (Schuh, 2011). Receptor recycling and its role in axon guidance are well established where temporal regulation is achieved for the expression of specific receptors depending on the extracellular cues (Winckler and Mellman, 2010).

9 REFERENCES

Abe, Y., Chen, W., Huang, W., Nishino, M. and Li, Y.-P. (2006). CNBP regulates forebrain formation at organogenesis stage in chick embryos. *Dev. Biol.* **295**, 116–27.

Applewhite, D. A., Barzik, M., Kojima, S., Svitkina, T. M., Gertler, F. B. and Borisy, G. G. (2007). Ena / VASP Proteins Have an Anti-Capping Independent Function in Filopodia Formation □. *Mol. Biol. Cell* **18**, 2579–2591.

Arthur, W. T. and Burridge, K. (2001). RhoA inactivation by p190RhoGAP regulates cell spreading and migration by promoting membrane protrusion and polarity. *Mol. Biol. Cell* **12**, 2711–2720.

Avraham, O., Zisman, S., Hadas, Y., Vald, L. and Klar, A. (2010). Deciphering Axonal Pathways of Genetically Defined Groups of Neurons in the Chick Neural Tube Utilizing in ovo Electroporation. *J. Vis. Exp.* **39**, e1792.

Baeriswyl, T. and Stoeckli, E. T. (2008). Axonin-1/TAG-1 is required for pathfinding of granule cell axons in the developing cerebellum. *Neural Dev.* **3**,.

Balaban, N. Q., Schwarz, U. S., Riveline, D., Goichberg, P., Tzur, G., Sabanay, I., Mahalu, D., Safran, S., Bershadsky, A., Addadi, L., et al. (2001). Force and focal adhesion assembly : a close relationship studied using elastic micropatterned substrates. *Nat. Cell Biol.* **3**, 466–472.

Ballestrem, C., Erez, N., Kirchner, J., Kam, Z., Bershadsky, A. and Geiger, B. (2006). Molecular mapping of tyrosine-phosphorylated proteins in focal adhesions using fluorescence resonance energy transfer. *J. Cell Sci.* **119**, 866–875.

Bartolini, F., Moseley, J. B., Schmoranzer, J., Cassimeris, L., Goode, B. L. and Gundersen, G. G. (2008). The formin mDia2 stabilizes microtubules independently of its actin nucleation activity. *J. Cell Biol.* **181**, 523–36.

Barzik, M., Mcclain, L. M., Gupton, S. L., Gertler, F. B. and Ginsberg, M. H. (2014). Ena / VASP regulates mDia2-initiated filopodial length , dynamics , and function. *Mol. Biol. Cell* **25**, 2604–2619.

Bentley, D. and Toroian-Raymond, a (1986). Disoriented pathfinding by pioneer neurone growth cones deprived of filopodia by cytochalasin treatment. *Nature* **323**, 712–715.

Bor, B., Vizcarra, C. L., Phillips, M. L. and Quinlan, M. E. (2012a). Autoinhibition of the formin Cappuccino in the absence of canonical autoinhibitory domains. *Mol. Biol. Cell* **23**, 3801–13.

Bor, B., Vizcarra, C. L., Phillips, M. L. and Quinlan, M. E. (2012b). Autoinhibition of the formin Cappuccino in the absence of canonical autoinhibitory domains. *Mol. Biol. Cell* **23**, 3801–13.

Bornschlögl, T. (2013). How filopodia pull: What we know about the mechanics and dynamics of filopodia. *Cytoskeleton* **70**, 590–603.

Bornschlögl, T., Romero, S., Vestergaard, C. L., Joanny, J.-F., Van Nhieu, G. T. and Bassereau, P. (2013). Filopodial retraction force is generated by cortical actin dynamics and controlled by reversible tethering at the tip. *Proc. Natl. Acad. Sci. U. S. A.* **110**, 18928–33.

Burridge, K. and Wittchen, E. S. (2013). The tension mounts: stress fibers as force-generating mechanotransducers. *J. Cell Biol.* **200**, 9–19.

Campellone, K. G. and Welch, M. D. (2010). A nucleator arms race: cellular control of actin assembly. *Nat. Rev. Mol. Cell Biol.* **11**, 237–51.

Chacón, M. R., Navarro, A. I., Cuesto, G., del Pino, I., Scott, R., Morales, M. and Rico, B. (2012). Focal adhesion kinase regulates actin nucleation and neuronal filopodia formation during axonal growth. *Development* **139**, 3200–10.

Chang, C.-W. and Kumar, S. (2013a). Vinculin tension distributions of individual stress fibers within cell-matrix adhesions. *J. Cell Sci.* **126**, 3021–30.

Chang, C.-W. and Kumar, S. (2013b). Vinculin tension distributions of individual stress fibers within cell-matrix adhesions. *J. Cell Sci.* **126**, 3021–30.

Chen, S. and Hamm, H. E. (2006). DEP domains: More than just membrane anchors. *Dev. Cell* **11**, 436–8.

Chen, Y., Pasapera, A. M., Koretsky, A. P. and Waterman, C. M. (2013). Orientation-speci fi c responses to sustained uniaxial stretching in focal adhesion growth and turnover.

Chesarone, M. a and Goode, B. L. (2009). Actin nucleation and elongation factors: mechanisms and interplay. *Curr. Opin. Cell Biol.* **21**, 28–37.

Chesarone, M., Gould, C. J., Moseley, J. B. and Goode, B. L. (2009). Displacement of Formins from Growing Barbed Ends by Bud14 Is Critical for Actin Cable Architecture and Function. *Dev. Cell* **16**, 292–302.

Chesarone, M. a, DuPage, A. G. and Goode, B. L. (2010). Unleashing formins to remodel the actin and microtubule cytoskeletons. *Nat. Rev. Mol. Cell Biol.* **11**, 62–74.

Chilton, J. K. (2006). Molecular mechanisms of axon guidance. *Dev. Biol.* **292**, 13–24.

Colombelli, J., Besser, a., Kress, H., Reynaud, E. G., Girard, P., Caussinus, E., Haselmann, U., Small, J. V., Schwarz, U. S. and Stelzer, E. H. K. (2009). Mechanosensing in actin stress fibers revealed by a close correlation between force and protein localization. *J. Cell Sci.* **122**, 1928–1928.

Cramer, L. P., Siebert, M. and Mitchison, T. J. (1997). Identification of novel graded polarity actin filament bundles in locomoting heart fibroblasts: Implications for the generation of motile force. *J. Cell Biol.* **136**, 1287–1305.

Del Rio, A., Perez-Jimenez, R., Liu, R., Roca-Cusachs, P., Fernandez, J. M. and Sheetz, M. P. (2009). Stretching single talin rod molecules activates vinculin binding. *Science* **323**, 638–641.

Dent, E. W. and Gertler, F. B. (2003). Cytoskeletal Dynamics and Transport in Growth Cone Motility and Axon Guidance. *Neuron* **40**, 209–227.

Dent, E. W., Kwiatkowski, A. V, Mebane, L. M., Philippar, U., Barzik, M., Rubinson, D. A., Gupton, S., Van Veen, J. E., Furman, C., Zhang, J., et al. (2007). Filopodia are required for cortical neurite initiation. *Nat. Cell Biol.* **9**, 1347–59.

Dent, E. W., Gupton, S. L. and Gertler, F. B. (2011). The growth cone cytoskeleton in axon outgrowth and guidance. *Cold Spring Harb. Perspect. Biol.* **3**,.

Dettenhofer, M., Zhou, F. and Leder, P. (2008). Formin 1-isoform IV deficient cells exhibit defects in cell spreading and focal adhesion formation. *PLoS One* **3**, e2497.

Dumont, J., Million, K., Sunderland, K., Rassinier, P., Lim, H., Leader, B. and Verlhac, M.-H. (2007). Formin-2 is required for spindle migration and for the late steps of cytokinesis in mouse oocytes. *Dev. Biol.* **301**, 254–65.

Emmons, S., Phan, H., Calley, J., Chen, W., James, B. and Manseau, L. (1995). Cappuccino, a Drosophila maternal effect gene required for polarity of the egg and embryo, is related to the vertebrate limb deformity locus. *Genes Dev.* **9**, 2482–2494.

Ezratty, E. J., Partridge, M. a and Gundersen, G. G. (2005). Microtubule-induced focal adhesion disassembly is mediated by dynamin and focal adhesion kinase. *Nat. Cell Biol.* **7**, 581–90.

Faix, J. (2008). Filopodia formation induced by active mDia2 / Drf3. *J. Microsc.* **231**, 506–517.

Fitzli, D., Stoeckli, E. T., Kunz, S., Siribour, K., Rader, C., Kunz, B., Kozlov, S. V, Buchstaller, a, Lane, R. P., Suter, D. M., et al. (2000). A direct interaction of axonin-1 with NgCAM-related cell adhesion molecule (NrCAM) results in guidance, but not growth of commissural axons. *J. Cell Biol.* **149**, 951–68.

Forscher, P. and Smith, S. J. (1988). Actions of cytochalasins on the organization of actin filaments and microtubules in a neuronal growth cone. *J. Cell Biol.* **107**, 1505–16.

Galbraith, C. G., Yamada, K. M. and Sheetz, M. P. (2002). The relationship between force and focal complex development. *J. Cell Biol.* **159**, 695–705.

Gardel, M. L., Schneider, I. C., Aratyn-Schaus, Y. and Waterman, C. M. (2010). Mechanical integration of actin and adhesion dynamics in cell migration. *Annu. Rev. Cell Dev. Biol.* **26**, 315–33.

Geiger, B. and Bershadsky, a (2001). Assembly and mechanosensory function of focal contacts. *Curr. Opin. Cell Biol.* **13**, 584–92.

Geiger, B., Spatz, J. P. and Bershadsky, A. D. (2009). Environmental sensing through focal adhesions. *Nat. Rev. Mol. Cell Biol.* **10**, 21–33.

Gilestro, G. F. (2008). Redundant mechanisms for regulation of midline crossing in Drosophila. *PLoS One* **3**, e3798.

Girao, H., Geli, M. I. and Idrissi, F. Z. (2008). Actin in the endocytic pathway: From yeast to mammals. *FEBS Lett.* **582**, 2112–2119.

Goh, W. I. and Ahmed, S. (2012). mDia1-3 in mammalian filopodia. *Commun. Integr. Biol.* **5**, 340–344.

Goh, W. I., Sudhaharan, T., Lim, K. B., Sem, K. P., Lau, C. L. and Ahmed, S. (2011). Rif-mDia1 interaction is involved in filopodium formation independent of Cdc42 and Rac effectors. *J. Biol. Chem.* **286**, 13681–94.

Goley, E. D. and Welch, M. D. (2006). The ARP2/3 complex: an actin nucleator comes of age. *Nat. Rev. Mol. Cell Biol.* **7**, 713–26.

Goley, E. D., Rodenbusch, S. E., Martin, A. C. and Welch, M. D. (2004). Critical conformational changes in the Arp2/3 complex are induced by nucleotide and nucleation promoting factor. *Mol. Cell* **16**, 269–79.

Gomez, T. M. and Letourneau, P. C. (1994). Filopodia Initiate Choices Made by Sensory Neuron Growth Cones at Laminin / Fibronectin Borders in vitro. *J. Neurosci.* **7414**, 5959–5972.

Gomez, T. M., Roche, F. K. and Letourneau, P. C. (1996). Chick sensory neuronal growth cones distinguish fibronectin from laminin by making substratum contacts that resemble focal contacts. *J. Neurobiol.* **29**, 18–34.

Gomez, T. M., Robles, E., Poo, M. and Spitzer, N. C. (2001). Filopodial calcium transients promote substrate-dependent growth cone turning. *Science (80-.).* **291**, 1983–1987.

Gonçalves-Pimentel, C., Gombos, R., Mihály, J., Sánchez-Soriano, N. and Prokop, A. (2011). Dissecting regulatory networks of filopodia formation in a Drosophila growth cone model. *PLoS One* **6**, e18340.

Grabham, P. W. and Goldberg, D. J. (1997). Nerve growth factor stimulates the accumulation of beta1 integrin at the tips of filopodia in the growth cones of sympathetic neurons. *J. Neurosci.* **17**, 5455–5465.

Grashoff, C., Hoffman, B. D., Brenner, M. D. and Zhou, R. (2010). Measuring mechanical tension across vinculin reveals regulation of focal adhesion dynamics. *Nature* **466**, 263–266.

Gungabissoon, R. A. and Bamburg, J. R. (2003). Regulation of Growth Cone Actin Dynamics by ADF / Cofilin 1. *J. Histochem. Cytochem.* **51**, 411–420.

Gupton, S. L., Eisenmann, K., Alberts, A. S. and Waterman-Storer, C. M. (2007a). mDia2 regulates actin and focal adhesion dynamics and organization in the lamella for efficient epithelial cell migration. *J. Cell Sci.* **120**, 3475–87.

Gupton, S. L., Eisenmann, K., Alberts, A. S. and Waterman-Storer, C. M. (2007b). mDia2 regulates actin and focal adhesion dynamics and organization in the lamella for efficient epithelial cell migration. *J. Cell Sci.* **120**, 3475–87.

Helms, A. W. and Johnson, J. E. (1998). Progenitors of dorsal commissural interneurons are defined by MATH1 expression. *Development* **928**, 919–928.

Higgs, H. N. and Peterson, K. J. (2005). Phylogenetic analysis of the formin homology 2 domain. *Mol. Biol. Cell* **16**, 1–13.

Holinstat, M., Knezevic, N., Broman, M., Samarel, A. M., Malik, A. B. and Mehta, D. (2006). Suppression of RhoA activity by focal adhesion kinase-induced activation of p190RhoGAP: Role in regulation of endothelial permeability. *J. Biol. Chem.* **281**, 2296–2305.

Homem, C. C. F., Peifer, M. and Hill, C. (2009). Exploring the Roles of Diaphanous and Enabled Activity in Shaping the Balance between Filopodia and Lamellipodia. *Mol. Biol. Cell* **20**, 5138–5155.

Hotulainen, P. and Lappalainen, P. (2006). Stress fibers are generated by two distinct actin assembly mechanisms in motile cells. *J. Cell Biol.* **173**, 383–94.

Humphries, J. D., Wang, P., Streuli, C., Geiger, B., Humphries, M. J. and Ballestrem, C. (2007). Vinculin controls focal adhesion formation by direct interactions with talin and actin. *J. Cell Biol.* **179**, 1043–1057.

Ilić, D., Furuta, Y., Kanazawa, S., Takeda, N., Sobue, K., Nakatsuji, N., Nomura, S., Fujimoto, J., Okada, M. and Yamamoto, T. (1995). Reduced cell motility and enhanced focal adhesion contact formation in cells from FAK-deficient mice. *Nature* **377**, 539–544.

Iskratsch, T., Yu, C.-H., Mathur, A., Liu, S., Stévenin, V., Dwyer, J., Hone, J., Ehler, E. and Sheetz, M. (2013). FHOD1 Is Needed for Directed Forces and Adhesion Maturation during Cell Spreading and Migration. *Dev. Cell* **27**, 545–59.

Iyer, K. V., Pulford, S., Mogilner, a. and Shivashankar, G. V. (2012). Mechanical activation of cells induces chromatin remodeling preceding MKL nuclear transport. *Biophys. J.* **103**, 1416–1428.

Johnston, S. a, Bramble, J. P., Yeung, C. L., Mendes, P. M. and Machesky, L. M. (2008). Arp2/3 complex activity in filopodia of spreading cells. *BMC Cell Biol.* **9**, 65.

Kalil, K., Li, L. and Hutchins, B. I. (2011). Signaling Mechanisms in Cortical Axon Growth, Guidance, and Branching. *Front. Neuroanat.* **5**, 1–15.

Kanchanawong, P., Shtengel, G., Pasapera, A. M., Ramko, E. B., Davidson, M. W., Hess, H. F. and Waterman, C. M. (2010). Nanoscale architecture of integrin-based cell adhesions. *Nature* **468**, 580–4.

Kaprielian, Z., Imondi, R. and Runko, E. (2000). Axon guidance at the midline of the developing CNS. *Anat. Rec.* **261**, 176–97.

Kaprielian, Z., Runko, E. and Imondi, R. (2001). Axon Guidance at the Midline Choice Point. *Dev. Dyn.* **221**, 154–181.

Koka, S., Neudauer, C. L., Li, X., Lewis, R. E., McCarthy, J. B. and Westendorf, J. J. (2003). The formin-homology-domain-containing protein FHOD1 enhances cell migration. *J. Cell Sci.* **116**, 1745–1755.

Korobova, F. and Svitkina, T. (2008). Arp2 / 3 Complex Is Important for Filopodia Formation , Growth Cone Motility , and Neuritogenesis in Neuronal Cells. *Mol. Biol. Cell* **19**, 1561–1574.

Kos, R., Tucker, R. P., Hall, R., Duong, T. D. and Erickson, C. a (2003). Methods for introducing morpholinos into the chicken embryo. *Dev. Dyn.* **226**, 470–7.

Kuo, J.-C., Han, X., Hsiao, C.-T., Yates, J. R. and Waterman, C. M. (2011). Analysis of the myosin-II-responsive focal adhesion proteome reveals a role for β-Pix in negative regulation of focal adhesion maturation. *Nat. Cell Biol.* **13**, 383–93.

Kwon, S., Shin, H. and Lim, H. J. (2011). Dynamic interaction of formin proteins and cytoskeleton in mouse oocytes during meiotic maturation. *Mol. Hum. Reprod.* **17**, 317–327.

Lai, F. P. L., Szczodrak, M., Block, J., Faix, J., Breitsprecher, D., Mannherz, H. G., Stradal, T. E. B., Dunn, G. a, Small, J. V. and Rottner, K. (2008). Arp2/3 complex interactions and actin network turnover in lamellipodia. *EMBO J.* **27**, 982–992.

Lammers, M., Rose, R., Scrima, A. and Wittinghofer, A. (2005). The regulation of mDia1 by autoinhibition and its release by Rho*GTP. *EMBO J.* **24**, 4176–4187.

Lavelin, I., Wolfenson, H., Patla, I., Henis, Y. I., Medalia, O., Volberg, T., Livne, A., Kam, Z. and Geiger, B. (2013). Differential effect of actomyosin relaxation on the dynamic properties of focal adhesion proteins. *PLoS One* **8**, e73549.

Law, R., Dixon-Salazar, T., Jerber, J., Cai, N., Abbasi, A. a, Zaki, M. S., Mittal, K., Gabriel, S. B., Rafiq, M. A., Khan, V., et al. (2014). Biallelic Truncating Mutations in FMN2, Encoding the Actin-Regulatory Protein Formin 2, Cause Nonsyndromic Autosomal-Recessive Intellectual Disability. *Am. J. Hum. Genet.* **95**, 721–8.

Le Clainche, C. and Carlier, M.-F. (2008). Regulation of actin assembly associated with protrusion and adhesion in cell migration. *Physiol. Rev.* **88**, 489–513.

Leader, B. and Leder, P. (2000). Formin-2 , a novel formin homology protein of the cappuccino subfamily , is highly expressed in the developing and adult central nervous system. *Mech. Dev.* **93**, 221–231.

Leader, B., Lim, H., Carabatsos, M. J., Harrington, A., Ecsedy, J., Pellman, D., Maas, R. and Leder, P. (2002). Formin-2, polyploidy, hypofertility and positioning of the meiotic spindle in mouse oocytes. *Nat. Cell Biol.* **4**, 921–8.

Lebrand, C., Dent, E. W., Strasser, G. A., Lanier, L. M., Krause, M., Svitkina, T. M., Borisy, G. G. and Gertler, F. B. (2004). Critical Role of Ena / VASP Proteins for Filopodia Formation in Neurons and in Function Downstream of Netrin-1. *Neuron* **42**, 37–49.

Li, F. and Higgs, H. N. (2003). The Mouse Formin mDia1 Is a Potent Actin Nucleation Factor Regulated by Autoinhibition. *Curr. Biol.* **13**, 1335–1340.

Lowery, L. A. and Van Vactor, D. (2009). The trip of the tip: understanding the growth cone machinery. *Nat. Rev. Mol. Cell Biol.* **10**, 332–43.

Lu, J., Meng, W., Poy, F., Maiti, S., Goode, B. L. and Eck, M. J. (2007). Structure of the FH2 Domain of Daam1: Implications for Formin Regulation of Actin Assembly. *J. Mol. Biol.* **369**, 1258–1269.

Machaidze, G., Sokoll, A., Shimada, A., Lustig, A., Mazur, A., Wittinghofer, A., Aebi, U. and Mannherz, H. G. (2010). Actin filament bundling and different nucleating effects of mouse Diaphanous-related formin FH2 domains on actin/ADF and actin/cofilin complexes. *J. Mol. Biol.* **403**, 529–45.

Mallavarapu, A. and Mitchison, T. (1999). Regulated actin cytoskeleton assembly at filopodium tips controls their extension and retraction. *J. Cell Biol.* **146**, 1097–1106.

Marsh, L. and Letourneau, P. C. (1984). Growth of Neurites without Filopodial or Lamellipodial Activity in the Presence of Cytochalasin B. *J. Cell Biol.* **99**, 2041–2047.

Marshall, B. T., Long, M., Piper, J. W., Yago, T., McEver, R. P. and Zhu, C. (2003). Direct observation of catch bonds involving cell-adhesion molecules. *Nature* **423**, 190–193.

Matusek, T., Gombos, R., Szécsényi, A., Sánchez-Soriano, N., Czibula, A., Pataki, C., Gedai, A., Prokop, A., Raskó, I. and Mihály, J. (2008). Formin proteins of the DAAM subfamily play a role during axon growth. *J. Neurosci.* **28**, 13310–9.

Mellor, H. (2005). The Rho Family GTPase Rif Induces Filopodia through mDia2. *Curr. Biol.* **15**, 129–133.

Mellor, H. (2010). The role of formins in filopodia formation. *Biochim. Biophys. Acta* **1803**, 191–200.

Mende, M., Christophorou, N. a D. and Streit, A. (2008). Specific and effective gene knock-down in early chick embryos using morpholinos but not pRFPRNAi vectors. *Mech. Dev.* **125**, 947–62.

Milev, P., Maurel, P., Ha, M., Margolis, K. and Margolis, R. U. (1996). TAG-1 / Axonin-1 Is a High-affinity Ligand of Neurocan , Phosphacan / Protein-tyrosine Phosphatase- / , and N-CAM *. *Biochemistry* **271**, 15716–15723.

Montanez, E., Ussar, S., Schifferer, M., Bösl, M., Zent, R., Moser, M. and Fässler, R. (2008). Kindlin-2 controls bidirectional signaling of integrins. *Genes Dev.* **22**, 1325–1330.

Montaville, P., Jégou, A., Pernier, J., Compper, C., Guichard, B., Mogessie, B., Schuh, M., Romet-Lemonne, G. and Carlier, M. F. (2014). Spire and Formin 2 Synergize and Antagonize in Regulating Actin Assembly in Meiosis by a Ping-Pong Mechanism. *PLoS Biol.* **12**, 1–20.

Moore, S. W., Zhang, X., Lynch, C. D. and Sheetz, M. P. (2012). Netrin-1 attracts axons through FAK-dependent mechanotransduction. *J. Neurosci.* **32**, 11574–11585.

Moser, M., Nieswandt, B., Ussar, S., Pozgajova, M. and Fässler, R. (2008). Kindlin-3 is essential for integrin activation and platelet aggregation. *Nat. Med.* **14**, 325–330.

Mozhui, K., Ciobanu, D. C., Schikorski, T., Wang, X., Lu, L. and Williams, R. W. (2008). Dissection of a QTL hotspot on mouse distal chromosome 1 that modulates neurobehavioral phenotypes and gene expression. *PLoS Genet.* **4**, e1000260.

Myers, J. P. and Gomez, T. M. (2011). Focal Adhesion Kinase Promotes Integrin Adhesion Dynamics Necessary for Chemotropic Turning of Nerve Growth Cones. *J. Neurosci.* **31**, 13585–13595.

Nakamura, H., Katahira, T., Sato, T., Watanabe, Y. and Funahashi, J. I. (2004). Gain- and loss-of-function in chick embryos by electroporation. *Mech. Dev.* **121**, 1137–1143.

Nalbant, P. (2014). FHOD1 regulates stress fiber organization by controlling transversal arc and dorsal fiber dynamics. *J. Cell Sci.*

Nayal, A., Webb, D. J. and Horwitz, A. F. (2004). Talin: An emerging focal point of adhesion dynamics. *Curr. Opin. Cell Biol.* **16**, 94–98.

O'Donnell, M., Chance, R. K. and Bashaw, G. J. (2009). Axon growth and guidance: receptor regulation and signal transduction. *Annu. Rev. Neurosci.* **32**, 383–412.

Oakes, P. W., Beckham, Y., Stricker, J. and Gardel, M. L. (2012a). Tension is required but not sufficient for focal adhesion maturation without a stress fiber template. *J. Cell Biol.* **196**, 363–74.

Oakes, P. W., Beckham, Y., Stricker, J. and Gardel, M. L. (2012b). Tension is required but not sufficient for focal adhesion maturation without a stress fiber template. *J. Cell Biol.* **196**, 363–74.

Otomo, T., Tomchick, D. R., Otomo, C., Panchal, S. C., Machius, M. and Rosen, M. K. (2005). Structural basis of actin filament nucleation and processive capping by a formin homology 2 domain. *Nature* **433**, 488–494.

Paul, A. and Pollard, T. (2008). The Role of the FH1 Domain and Profilin in Formin-Mediated Actin-Filament Elongation and Nucleation. *Curr. Biol.* **18**, 9–19.

Pekarik, V., Bourikas, D., Miglino, N., Joset, P., Preiswerk, S. and Stoeckli, E. T. (2003). Screening for gene function in chicken embryo using RNAi and electroporation. *Nat. Biotechnol.* **21**, 93–6.

Peleg, S., Sananbenesi, F., Zovoilis, A., Burkhardt, S., Bahari-Javan, S., Agis-Balboa, R. C., Cota, P., Wittnam, J. L., Gogol-Doering, A., Opitz, L., et al. (2010). Altered histone acetylation is associated with age-dependent memory impairment in mice. *Science* **328**, 753–6.

Pellegrin, S. and Mellor, H. (2007). Actin stress fibres. *J. Cell Sci.* **120**, 3491–9.

Perrin, F. E. and Stoeckli, E. T. (2000). Use of Lipophilic Dyes in Studies of Axonal Pathfinding In Vivo. *Microsc. Res. Tech.* **48**, 25–31.

Peterson, L. J., Rajfur, Z., Maddox, A. S., Freel, C. D., Chen, Y., Edlund, M., Otey, C. and Burridge, K. (2004). Simultaneous Stretching and Contraction of Stress Fibers In Vivo. **15**, 3497–3508.

Pfender, S., Kuznetsov, V., Pleiser, S., Kerkhoff, E. and Schuh, M. (2011). Spire-type actin nucleators cooperate with Formin-2 to drive asymmetric oocyte division. *Curr. Biol.* **21**, 955–60.

Pollard, T. D. and Cooper, J. a (2009). Actin, a central player in cell shape and movement. *Science* **326**, 1208–12.

Polleux, F., Ince-Dunn, G. and Ghosh, A. (2007). Transcriptional regulation of vertebrate axon guidance and synapse formation. *Nat. Rev. Neurosci.* **8**, 331–340.

Ponti, a, Machacek, M., Gupton, S. L., Waterman-Storer, C. M. and Danuser, G. (2004). Two distinct actin networks drive the protrusion of migrating cells. *Science* **305**, 1782–1786.

Prosser, D. C., Drivas, T. G., Maldonado-Báez, L. and Wendland, B. (2011). Existence of a novel clathrin-independent endocytic pathway in yeast that depends on Rho1 and formin. *J. Cell Biol.* **195**, 657–671.

Quinlan, M. E., Hilgert, S., Bedrossian, A., Mullins, R. D. and Kerkhoff, E. (2007). Regulatory interactions between two actin nucleators, Spire and Cappuccino. *J. Cell Biol.* **179**, 117–28.

Rao, M., Baraban, J. H., Rajaii, F. and Sockanathan, S. (2004). In vivo comparative study of RNAi methodologies by in ovo electroporation in the chick embryo. *Dev. Dyn.* **231**, 592–600.

Reinhard, M., Halbrugge, M., Scheer, U., Wiegand, C., Jockusch, B. M. and Walter, U. (1992). The 46/50 kDa phosphoprotein VASP purified from human platelets is a novel protein associated with actin filaments and focal contacts. *EMBO J.* **11**, 2063–2070.

Renaudin, a, Lehmann, M., Girault, J. and McKerracher, L. (1999). Organization of point contacts in neuronal growth cones. *J. Neurosci. Res.* **55**, 458–471.

Robles, E. and Gomez, T. M. (2006). Focal adhesion kinase signaling at sites of integrin-mediated adhesion controls axon pathfinding. *Nat. Neurosci.* **9**, 1274–83.

Roca-Cusachs, P., del Rio, A., Puklin-Faucher, E., Gauthier, N. C., Biais, N. and Sheetz, M. P. (2013). Integrin-dependent force transmission to the extracellular matrix by α-actinin triggers adhesion maturation. *Proc. Natl. Acad. Sci. U. S. A.* **110**, E1361–70.

Romero, S., Clainche, C. Le, Didry, D., Egile, C., Pantaloni, D. and Carlier, M. (2004). Formin Is a Processive Motor that Requires Profilin to Accelerate Actin Assembly and Associated ATP Hydrolysis. *Cell* **119**, 419–429.

Rosales-nieves, A. E., Johndrow, J. E., Keller, L. C., Magie, C. R., Pinto-Santini, D. M. and Parkhurst, S. M. (2006). Coordination of microtubule and microfilament dynamics by Drosophila Rho1, Spire and Cappuccino. *Nat. Cell Biol.* **8**, 367–376.

Rose, R., Weyand, M., Lammers, M., Ishizaki, T., Ahmadian, M. R. and Wittinghofer, a (2005). Structural and mechanistic insights into the interaction between Rho and mammalian Dia. *Nature* **435**, 513–518.

Schirenbeck, A., Arasada, R., Bretschneider, T., Schleicher, M. and Faix, J. (2005a). Formins and VASPs may co-operate in the formation of filopodia. *Biochem. Soc. Trans.* **33**, 1256–1259.

Schirenbeck, A., Bretschneider, T., Arasada, R., Schleicher, M. and Faix, J. (2005b). The Diaphanous-related formin dDia2 is required for the formation and maintenance of filopodia. *Nat. Cell Biol.* **7**, 619–25.

Schönichen, A., Alexander, M., Gasteier, J. E., Cuesta, F. E., Fackler, O. T. and Geyer, M. (2006). Biochemical characterization of the diaphanous autoregulatory interaction in the formin homology protein FHOD1. *J. Biol. Chem.* **281**, 5084–5093.

Schönichen, A., Mannherz, H. G., Behrmann, E., Antonina, J. and Geyer, M. (2013). FHOD1 is a combined actin filament capping and bundling factor that selectively associates with actin arcs and stress fibers Accepted manuscript Journal of Cell Science * Corresponding authors : Accepted manuscript.

Schuh, M. (2011). An actin-dependent mechanism for long-range vesicle transport. *Nat. Cell Biol.* **13**, 1–7.

Schuh, M. and Ellenberg, J. (2008). A new model for asymmetric spindle positioning in mouse oocytes. *Curr. Biol.* **18**, 1986–92.

Shi, Q. and Boettiger, D. (2003). A Novel Mode for Integrin-mediated Signaling : Tethering Is Required for Phosphorylation of FAK Y397. *Mol. Biol. Cell* **14**, 4306–4315.

Steffen, A., Faix, J., Resch, G. P., Linkner, J., Wehland, J., Small, J. V., Rottner, K. and Stradal, T. E. B. (2006). Filopodia Formation in the Absence of Functional WAVE- and Arp2 / 3-Complexes. *Mol. Biol. Cell* **17**, 2581–2591.

Stern, C. D. (2005). The chick: A great model system becomes even greater. *Dev. Cell* **8**, 9–17.

Stoeckli, E. T. and Landmesser, L. T. (1995). Axonin-1, Nr-CAM, and Ng-CAM Play Different Roles in the In Vivo Guidance of Chick Commissural Neurons. *Neuron* **14**, 1165–1179.

Strasser, G. a, Rahim, N. A., VanderWaal, K. E., Gertler, F. B. and Lanier, L. M. (2004). Arp2/3 is a negative regulator of growth cone translocation. *Neuron* **43**, 81–94.

Suter, D. M. and Forscher, P. (2001). Transmission of growth cone traction force through apCAM – cytoskeletal linkages is regulated by Src family tyrosine kinase activity. *J. Cell Biol.* **155**, 427–438.

Suter, D. M. and Miller, K. E. (2011). The emerging role of forces in axonal elongation. *Prog. Neurobiol.* **94**, 91–101.

Tomar, A., Lim, S., Lim, Y., Schlaepfer, D. D., Tomar, A., Lim, S., Lim, Y. and Schlaepfer, D. D. (2009). A FAK-p120RasGAP-p190RhoGAP complex regulates polarity in migrating cells A FAK-p120RasGAP-p190RhoGAP complex regulates polarity in migrating cells. *J. Cell Sci.* 1852–1862.

Wallar, B. J., Stropich, B. N., Schoenherr, J. a., Holman, H. a., Kitchen, S. M. and Alberts, A. S. (2006). The basic region of the diaphanous-autoregulatory domain (DAD) is required for autoregulatory interactions with the diaphanous-related formin inhibitory domain. *J. Biol. Chem.* **281**, 4300–4307.

Watanabe, S., Ando, Y., Yasuda, S., Hosoya, H., Watanabe, N., Ishizaki, T. and Narumiya, and S. (2008). mDia2 Induces the Actin Scaffold for the Contractile Ring and Stabilizes Its Position during Cytokinesis in NIH 3T3 Cells. *Mol. Biol. Cell* **19**, 2328–2338.

Weston, L., Coutts, A. S. and Thangue, N. B. La (2012). Actin nucleators in the nucleus : an emerging theme.

Winckler, B. and Mellman, I. (2010). Trafficking guidance receptors. *Cold Spring Harb. Perspect. Biol.* **2**, 1–19.

Wolfenson, H., Bershadsky, A., Henis, Y. I. and Geiger, B. (2011). Actomyosin-generated tension controls the molecular kinetics of focal adhesions. *J. Cell Sci.* **124**, 1425–32.

Woo, S., Rowan, D. J. and Gomez, T. M. (2009). Retinotopic mapping requires focal adhesion kinase-mediated regulation of growth cone adhesion. *J. Neurosci.* **29**, 13981–13991.

Xu, Y., Moseley, J. B., Sagot, I., Poy, F., Pellman, D., Goode, B. L. and Eck, M. J. (2004). Crystal structures of a formin homology-2 domain reveal a tethered dimer architecture. *Cell* **116**, 711–723.

Yamada, H., Abe, T., Satoh, a., Okazaki, N., Tago, S., Kobayashi, K., Yoshida, Y., Oda, Y., Watanabe, M., Tomizawa, K., et al. (2013). Stabilization of Actin Bundles by a Dynamin

1/Cortactin Ring Complex Is Necessary for Growth Cone Filopodia. *J. Neurosci.* **33**, 4514–4526.

Yang, C., Czech, L., Gerboth, S., Kojima, S., Scita, G. and Svitkina, T. (2007). Novel roles of formin mDia2 in lamellipodia and filopodia formation in motile cells. *PLoS Biol.* **5**, e317.

Zamir, E., Geiger, B. and Kam, Z. (2008). Quantitative multicolor compositional imaging resolves molecular domains in cell-matrix adhesions. *PLoS One* **3**, e1901.

Zhang, X.-F., Schaefer, A. W., Burnette, D. T., Schoonderwoert, V. T. and Forscher, P. (2003). Rho-Dependent Contractile Responses in the Neuronal Growth Cone Are Independent of Classical Peripheral Retrograde Actin Flow. *Neuron* **40**, 931–944.

Zheng, J. Q., Wan, J. J. and Poo, M. M. (1996). Essential role of filopodia in chemotropic turning of nerve growth cone induced by a glutamate gradient. *J. Neurosci.* **16**, 1140–1149.

Zimerman, B., Volberg, T. and Geiger, B. (2004). Early molecular events in the assembly of the focal adhesion-stress fiber complex during fibroblast spreading. *Cell Motil. Cytoskeleton* **58**, 143–59.